Fall 12-14-2018

Regulation of Canonical and Non-Canonical Hippo Pathway Components in Mitosis and Cancer

Seth Stauffer
University of Nebraska Medical Center

REGULATION OF CANONICAL AND NON-CANONICAL HIPPO PATHWAY COMPONENTS IN MITOSIS AND CANCER

by

Seth D. Stauffer

A DISSERTATION

Presented to the Faculty of
the University of Nebraska Graduate College
in Partial Fulfillment of the Requirements
for the Degree of Doctor of Philosophy

Pathology & Microbiology Graduate Program

Under the Supervision of Professor Jixin Dong

University of Nebraska Medical Center
Omaha, Nebraska

November, 2018

Supervisory Committee:

Kaustubh Datta, Ph.D.	Pankaj Singh, Ph.D.
Rakesh Singh, Ph.D.	Robert Lewis, Ph.D.

ACKNOWLEDGMENTS

First and foremost I would like to thank my incredible advisor, Dr. Jixin Dong, without whom this thesis would not be possible. I consider myself tremendously fortunate to be working with an advisor that mentors his students by attaining the perfect equilibrium between providing structured guidance and allowing us absolute independence. His supportive mentorship and indefatigable passion for science have aided me immensely during the course of my Ph.D. studies.

Thank you to my friends and second family in the Dong Lab past and present, Lin Zhang, Xingcheng Chen, Jiuli Zhou, Yongji Zeng, Renya Zeng, Zhan Wang, Ling Yin, and Yuanhong Chen. Thank you so much for helping train me and for being there when I needed to bounce scientific theories off someone in order to improve my ideas. Special thanks to Yuanhong for her research support and for her attentive management of the lab.

I would also like to thank my Ph.D. committee members, Dr. Kaustubh Datta, Dr. Pankaj Singh, Dr. Rakesh Singh, and Dr. Robert E. Lewis, for their support and guidance over the years. You have challenged me and have taught me to be critical of my results. Each question you ask and each comment you provide is backed by years of experience and insight.

A special thanks to Dr. Kevin O'Connell and Dr. Zhisong Qiao for mentoring me during my time at Merck Animal Health, for illuminating why I needed to get my Ph.D., and for your roles in setting me on this path to "reach for the stars". I will be forever thankful.

Next, I must thank my family. Thank you to my parents Tracy and Jenda for supporting me and encouraging me along the sometimes arduous path towards this degree. Growing up, you fostered my thirst for knowledge nurtured my inner scientist by providing me with science kits, chemistry sets, and my first microscope. You have truly molded me into the man I am today, I would not be where I am today without your love and support.

To my siblings, Kayla, Mariah, and Jake, thank you for teaching me to always find and have fun in the smallest of things, for keeping our big family interesting, as well as for being there for my family and I whenever we needed you.

To my beautiful daughters Evelyn and Adalyn, thank you for the pride of fatherhood which grows with each of your accomplishments, for all the laughter from all your silly antics, and for being such a motivation to provide a better life for our family.

Finally, a huge thank you to my wonderful wife and best friend, Katie. You have been my anchor, my foundation during my pursuit of my Ph.D. You have completely supported me in this endeavor and I would never have been able to do it without you. You have always believed in me and my capabilities, and you never doubted what I could do. Thank you for making me feel like the luckiest man in the world every single day. For filling our home with love and happiness and for giving me the most beautiful children. I love you with all my heart.

REGULATION OF CANONICAL AND NON-CANONICAL HIPPO PATHWAY COMPONENTS IN MITOSIS AND CANCER

Seth D. Stauffer, Ph.D.

University of Nebraska, 2018

Supervisor: Jixin Dong, Ph.D.

The Hippo pathway is conserved regulator of organ size through control of proliferation, apoptosis, and stem-cell self-renewal. In addition to this important function, many of the canonical signaling members have also been shown to be regulated during mitosis. Importantly, Hippo pathway components are frequently dysregulated in cancers and have attracted attention as possible targets for improved cancer therapeutics. Further exploration of Hippo-YAP (yes-associated protein) signaling has revealed new regulators and effectors outside the canonical signaling network and has revealed a larger non-canonical network of signaling proteins in which canonical Hippo pathway components crosstalk with important cellular homeostasis and apoptosis signaling pathways.

KIBRA is a regulator of the Hippo-YAP pathway, which plays a critical role in tumorigenesis. In the current study, we show that KIBRA is a positive regulator in prostate cancer cell proliferation and motility. We found that KIBRA is transcriptionally upregulated in androgen-insensitive LNCaPC4-2 and LNCaP-C81 cells when compared to the parental androgen-sensitive LNCaP cells. Ectopic expression of KIBRA enhances cell proliferation, migration and invasion in both immortalized and cancerous prostate epithelial cells. Accordingly, knockdown of KIBRA reduces migration, invasion, and anchorage-independent growth in

LNCaP-C4-2/C81 cells. Moreover, KIBRA expression is induced by androgen signaling and KIBRA is partially required for androgen receptor (AR) signaling activation in prostate cancer cells. In line with these findings, we further show that KIBRA is overexpressed in human prostate tumors. Our studies uncover unexpected results and identify KIBRA as a tumor promoter in prostate cancer.

PDZ-binding kinase (PBK) has been shown to be a target gene of YAP and plays a major role in proliferation and in safeguarding mitotic fidelity in cancer cells. Frequently upregulated in many cancers, PBK drives tumorigenesis and metastasis. PBK has been shown to be phosphorylated in mitosis by cyclin-dependent kinase 1 (CDK1)/cyclin B, however, no studies have been done examining PBK mitotic phosphorylation in oncogenesis. Additionally to the previously identified Threonine-9 phosphorylation, we found that Threonine-24, Serine-32, and Serine-59 of PBK are also phosphorylated. PBK is phosphorylated *in vitro* and in cells by CDK1 during antimitotic drug-induced mitotic arrest and in normal mitosis. We demonstrated that mitotic phosphorylation of Threonine-9 is involved in cytokinesis. The non-phosphorylatable mutant PBK-T9A augments tumorigenesis to a greater extent than wild type PBK in breast cancer cells, suggesting that PBK mitotic phosphorylation inhibits its tumor promoting activity. The PBK-T9A mutant also transforms and increases the proliferation of immortalized breast epithelial cells. Collectively, this study reveals that CDK1-mediated mitotic phosphorylation of PBK is involved in cytokinesis and inhibits its oncogenic activity.

AMP-activated protein kinase (AMPK) is a heterotrimeric serine/threonine kinase consisting of a catalytic α subunit and two regulatory β and γ subunits. AMPK regulates cellular energy homeostasis and harmonizes proliferation with energy availability. AMPK can shortcut the canonical Hippo pathway to phosphorylate and inhibit YAP directly to constrain proliferation under conditions of cellular stress. Additionally, AMPK has recently been found to sit in the center of a signaling network involving bona-fide tumor suppressors and is associated with cell cycle checkpoints, as AMPK-null cells have mitotic defects. Despite AMPK's emerging association with the cell-cycle, it still has not been fully delineated how AMPK is regulated by upstream signaling pathways during mitosis. We report for the first time, direct CDK1 phosphorylation of both the catalytic α1 and α2 subunits as well as the β1 regulatory subunit of AMPK in mitosis. We found that AMPK knockout U2OS cells have reduced mitotic indexes and that CDK1 phosphorylation-null AMPK is unable to rescue, demonstrating a role for CDK1 regulation of mitotic entry through AMPK. Our results also denote a vital role for AMPK in promoting proper chromosomal alignment, as loss of AMPK activity leads to misaligned chromosomes and concomitant metaphase delay. Importantly, AMPK expression and activity was found to be critical for paclitaxel chemosensitivity in breast cancer cells and significantly positively correlated with relapse-free survival in systemically treated breast cancer patients.

TABLE OF CONTENTS

LIST OF FIGURES AND TABLES

LIST OF ABBREVIATIONS

^{32}P	Phosphorus-32
Akt	AKT Serine/Threonine Kinase 1
AMPK	AMP-Activated Protein Kinase
APC	Anaphase-Promoting Complex
AR	Androgen Receptor
AREG	Amphiregulin
ATCC	American Type Culture Collection
CAMKK	Calcium/Calmodulin-Dependent Protein Kinase Kinase
Cas9	CRISPR Associated Protein 9
CD44	Cluster of Differentiation 44
CDC25C	Cell Division Cycle 25C
CDC27	Cell Division Cycle Protein 27
CDK1	Cyclin-Dependent Kinase 1
CDK2	Cyclin-Dependent Kinase 2
CDK4	Cyclin-Dependent Kinase 4
CDK5	Cyclin-Dependent Kinase 5
CDK6	Cyclin-Dependent Kinase 6
cDNA	Complimentary Deoxyribonucleic Acid
CHX	Cycloheximide
CRISPR	Clustered Regularly Interspaced Short Palindromic Repeats
CRPC	Castration-Resistant Prostate Cancer
DAPI	4′,6-diamidino-2-phenylindole

DKO	Double-Knockout
DMSO	Dimethyl sulfoxide
EGF	Epidermal Growth Factor
EGFP	Enhanced Green Fluorescent Protein
EMT	Epithelial-Mesenchymal Transition
ER-	Estrogen Receptor Negative
ERK	Extracellular Signal-Regulated Kinase
ERSR1	Estrogen Receptor 1
EZH2	Enhancer of Zeste 2 Polycomb Repressive Complex 2
G_1	Gap 1 Phase
G_2	Gap 2 Phase
GBF1	Golgi Brefeldin A Resistant Guanine Nucleotide Exchange Factor 1
GFP	Green Fluorescent Protein
GSK3	Glycogen Synthase Kinase 3
GST	Glutathione S-Transferase
HDlg	Human Homologue of Drosophila Discs Large
ILK	Integrin-Linked Kinase
INFG	Interferon Gamma
IPA	Ingenuity Pathway Analysis
JNK1/2	C-Jun N-terminal Kinase-1/2
KIBRA	Kidney and Brain Expressed Protein
KO	Knockout
LKB1	Liver Kinase B1

M	Mitosis
MAD2	Mitotic Arrest Deficient 2
maKO	Mono-Allelic Knockout
MAPK1	Mitogen-Activated Protein Kinase 1
MCD	Mitotic Cell Death
MEF	Mouse Embryonic Fibroblast
MEK	MAP/ERK Kinase
Mps1	Monopolar Spindle 1
MRLC	Myosin Regulatory Light Chain
MTT	3-(4,5-dimethylthiazol-2-yl)-2,5-diphenyltetrazolium bromide
NEBD	Nuclear Envelope Breakdown
Neo	Neomycin
Noc	Nocodazole
p38	P38 Mitogen Activated Protein Kinase
PAK2	p21-Activated Protein Kinase
PBK	PDZ-Binding Kinase
PLK1	Polo-Like Kinase 1
PPP1R12A	Protein Phosphatase 1 Regulatory Subunit 12A
PPP1R12C	Protein Phosphatase 1 Regulatory Subunit 12C
PSA	Prostate-Specific Antigen
Puro	Puromycin
RNA-Seq	RNA Sequencing
RT-PCR	Reverse-Transcription Polymerase Chain Reaction

SAC	Spindle Assembly Checkpoint
shRNA	Short Hairpin Ribonucleic Acid
siRNA	Small Interfering Ribonucleic Acid
SMARC4	SWI/SNF-Related Matrix-Associated Actin-Dependent Regulator of
Snf1	Sucrose Non-Fermenting 1
SWI/SNF	Switch/Sucrose Non-Fermentable
SYK	Spleen Tyrosine Kinase
T2A	Thosea Asigna Virus 2A Self-Cleaving Peptide
Taxol	Paclitaxel
TGF	Transforming Growth Factor
TP73	Tumor Protein 73
TTK	Threonine and Tyrosine Kinase
WWC1–3	WW and C2 Domain Containing Protein 1–3
YAP	Yes-Associated Protein 1

Chapter 1

KIBRA PROMOTES PROSTATE CANCER CELL PROLIFERATION AND MOTILITY*

* The material presented in this chapter was previously published: S. Stauffer et al. FEBS J 2016; 283(10): 1800-11.

ABSTRACT

KIBRA is a regulator of the Hippo-YAP (yes-associated protein) pathway, which plays a critical role in tumorigenesis. In the current study, we show that KIBRA is a positive regulator in prostate cancer cell proliferation and motility. We found that KIBRA is transcriptionally upregulated in androgen-insensitive LNCaPC4-2 and LNCaP-C81 cells when compared to the parental androgen-sensitive LNCaP cells. Ectopic expression of KIBRA enhances cell proliferation, migration and invasion in both immortalized and cancerous prostate epithelial cells. Accordingly, knockdown of KIBRA reduces migration, invasion, and anchorage-independent growth in LNCaP-C4-2/C81 cells. Moreover, KIBRA expression is induced by androgen signaling and KIBRA is partially required for androgen receptor (AR) signaling activation in prostate cancer cells. In line with these findings, we further show that KIBRA is overexpressed in human prostate tumors. Our studies uncover unexpected results and identify KIBRA as a tumor promoter in prostate cancer.

1.1. INTRODUCTION

KIBRA (expressed in kidney and brain, also called WWC1) is one of the members of the WWC (WW and C2 domain containing, WWC1, 2, 3) family of proteins [1, 2]. KIBRA is a memory performance and cognition-associated protein [3-9], and the KIBRA locus has been linked to brain-related disorders such as Alzheimer's disease [10-12]. KIBRA functions as an adaptor protein to transduce its biological functions in various physiological processes via interactions with many other proteins [13]. In addition to its functions in neurons, KIBRA also has multiple roles in non-neuronal cells involving cell polarity, trafficking, mitosis, cell proliferation, and cell migration [13]. For example, KIBRA positively regulates cell migration in podocytes [14], NRK cells [15], and breast cancer cells[16], while it does the opposite in immortalized breast epithelial cells [17]. KIBRA functions as a growth suppressive regulator through the Hippo pathway in Drosophila [18-20]. KIBRA is phosphorylated by mitotic kinases cyclin-dependent kinase 1 (CDK1) and Aurora A during mitosis and is required for chromosome alignment [21-23].

KIBRA has been linked with human cancers in several reports. Weakened expression of KIBRA in Claudin-low subtypes of breast cancer specimens correlates with poor prognosis [17]. Moreover, downregulation of KIBRA was shown to be a contributing factor to the malignancy of acute lymphocytic B-cell leukemia [24, 25]. This alteration in expression in leukemia is due to epigenetic changes in the well-defined CpG island within the promoter of the KIBRA locus [24, 25]. Strikingly, in common epithelial cancers such as colorectal, kidney, lung, breast and prostate there is virtually no methylation detected [24]. Instead of a tumor suppressive function of KIBRA, as suggested by the above studies, many previous reports have validated KIBRA's role in positively regulating proliferation and motility [14-16, 26-28] and KIBRA expression has positive clinical correlation with

gastric cancer progression [29]. This duality of KIBRA's suppression or promotion of proliferation and migration may be tissue- and context-dependent, requiring further investigation before KIBRA's role can be fully deciphered. Furthermore, a role for KIBRA in prostate cancer has not been previously defined.

Prostate cancer is the most prevalent form of cancer in men in the United States and second only to lung cancer as the leading cause of cancer deaths in men [30]. Prostatectomy, usually the initial treatment, tends to be very effective for localized prostate cancer [31]. Tumor progression is initially androgen-dependent and androgen ablation therapy is at first very successful at reducing the tumor burden. Despite this early response, genetic alterations lead to the development of androgen-independent or castration-resistant prostate cancer (CRPC), which is almost always fatal [32]. This transition from androgen-dependent to androgen-independent growth is not well understood, and further insight into the mechanisms driving this process will help with developing target-driven therapeutics for the effective treatment of CRPC in the future.

We recently reported that YAP, the Hippo pathway effector, is upregulated in androgen-insensitive prostate cancer cells (LNCaP-C4-2 and C81) and confers castration-resistant growth in vivo [33]. During that study, we noticed that in addition to YAP, the protein levels of KIBRA were also significantly increased in LNCaP-C4-2 and LNCaP-C81 cells. Here we characterize the biological significance of KIBRA upregulation in androgen-insensitive prostate cancer cells. We show that KIBRA is a positive regulator in prostate cancer cell proliferation and motility. Moreover, increased expression of KIBRA was also observed in clinical prostate tumor samples. Thus, the current study reveals an unexpected role for KIBRA in regulating cell migration and proliferation in prostate cancer cells.

1.2. MATERIALS AND METHODS

1.2.1. Expression Constructs and Cell Culture

The human KIBRA cDNA and shRNA constructs have been previously described [34]. LNCaP-C4-2 cell lines with shControl or shYAP have been described in [33]. RWPE-1 and LNCaP cell lines and related media and supplements were purchased from American Type Culture Collection (ATCC, Manassas, VA, USA), and the cell lines were cultured following ATCC's instructions. LNCaP-C4-2 was provided by Dr. Kaustubh Datta (University of Nebraska Medical Center) [35]. LNCaP-C33 and LNCaP-C81 cell lines were obtained from Dr. Ming-Fong Lin (University of Nebraska Medical Center) [36, 37]. R1881 (an androgen analog) was purchased from PerkinElmer (Waltham, MA, USA). All other chemicals were either from Sigma (St. Louis, MO, USA) or Thermo Fisher (Waltham, MA, USA).

1.2.2. Generation of Cell Lines

Ectopic expression of empty vector (control) or KIBRA in the RWPE-1 and LNCaP cell lines was achieved by a retrovirus-mediated approach. ShRNA-mediated knockdown of KIBRA in LNCaP-C4-2 or LNCaP-C81 cells was achieved similarly. Virus packaging, infection, and resistance selection were done as described [34].

1.2.3. Antibodies

Mouse monoclonal antibodies against human KIBRA have been described [21] and were used for Western blot analysis throughout the study. Anti-WWC2 antibodies were purchased from Sigma. Anti-β-actin antibodies were from Santa Cruz Biotechnology (Dallas, TX, USA). Anti-YAP, anti-vimentin, and anti-E-cadherin antibodies were from Cell Signaling Technology (Danvers, MA, USA). Anti-N-cadherin antibodies were provided by

Dr. Keith Johnson [38]. Total cell lysate preparation and Western blotting assays were done as previously described [21].

1.2.4. Cell Proliferation, Migration, Invasion, and Colony Assays

Cell proliferation assays were performed as described in [39]. Cells (3,000/well) were seeded in a 24-well plate in triplicate. Colony assays (to assess anchorage-independent growth in soft agar) were done in 6-well plates as we have described [40]. *In vitro* cell migration and invasion assays were assessed using the Transwell system (Corning Inc., Corning, NY, USA) and BioCoat invasion system (BD BioSciences, San Jose, CA, USA), respectively, according to the manufacturer's instructions. Cells (50,000 or 100,000) were seeded for each Transwell/Insert in duplicate and repeated twice [33]. The migratory and invasive cells were stained with ProLong Gold Antifade Reagent with DAPI [16, 41] and counted under a 20X lens. The rates are the average of counts in five fields of view per Transwell/Insert.

1.2.5. Quantitative Real Time-PCR

Total RNA isolation, RNA reverse transcription, and PCR were done with SYBR green (Bio-Rad) as previously described [34]. Primer sequences were as follows: WWC2: 5'-tctggcctccagacattttt (forward); 5'-tctcacacaagcttattctcagg (reverse); WWC3: 5'-agttcgtccccaacacaatc (forward); 5'-cgcgtcttttacattgacca (reverse). Other primers used in this study were listed in [33, 34].

1.2.6. Prostate Tumor Samples

Normal prostate and tumor samples/proteins were obtained from Protein Biotechnologies and the Tissue Bank at the University of Nebraska Medical Center.

1.2.7. Statistical Analysis

Statistical significance was analyzed using a two-tailed, unpaired Student's t-test.

1.3. RESULTS

1.3.1. KIBRA is Upregulated in Androgen-Insensitive Prostate Cancer Cells

LNCaP and LNCaP-C33 cells rely on androgen to grow, while the LNCaP-C4-2 and LNCaP-C81 sublines are androgen-insensitive and can grow under androgen deprivation conditions [42, 43]. We recently showed that YAP is upregulated during progression from an androgen-sensitive to an androgen-insensitive state [33]. During that work, we indeed found that KIBRA/WWC1 protein levels were also significantly increased in LNCaP-C4-2 and LNCaP-C81 cells when compared to the parental cells (Figure 1-1A, B). WWC2, which is in the same protein family as KIBRA, was increased in cancer cells when compared to RWPE-1 (immortalized prostate epithelial) cells; however, no significant change was observed between LNCaP and LNCaP-C4-2 cells (Figure 1-1A). Quantitative reverse transcription-PCR (RT-PCR) showed that the levels of KIBRA mRNA were significantly elevated in LNCaP-C4-2 and LNCaP-C81 cells (Figure 1-1C). Surprisingly, WWC2 and WWC3 mRNA levels were reduced in LNCaP-C4-2 and LNCaP-C81 cells when compared to LNCaP cells (Figure 1-1C). KIBRA protein stability/half-life is similar in both LNCaP and LNCaP-C4-2 cells (Figure 1-1D). Since KIBRA is induced by YAP [34] and YAP is elevated in androgen-insensitive prostate cancer cells [33], we tested whether KIBRA expression is YAP-dependent in LNCaP-C4-2 cells. Figure 1-1E showed that KIBRA expression was partially reduced in LNCaP-C4-2 cells with YAP knockdown (Figure 1-1E). Together, these observations indicate that KIBRA expression is transcriptionally increased in androgen-insensitive prostate cancer cells compared with androgen-sensitive cells and that its expression in these cells is partially regulated by YAP.

1.3.2. KIBRA Promotes Proliferation, Migration and Invasion in RWPE-1 Cells

To determine the role of KIBRA in prostate cancer, we first established stable cell lines expressing KIBRA in RWPE-1 cells (Figure 1-2A). Overexpression of KIBRA did not alter the WWC2 protein and WWC3 mRNA levels (Figure 1-2A). Ectopic expression of KIBRA stimulated cell proliferation (Figure 1-2B). Overexpression of KIBRA also induced cell migration (Figure 1-2C, D) and invasion (Figure 1-2E, F). KIBRA expression was not sufficient to cause anchorage-independent growth (neoplastic transformation) of RWPE-1 cells (Figure 1-2G). KIBRA regulates an epithelial-mesenchymal transition (EMT) in breast epithelial cells [17]. However, KIBRA overexpression did not alter the expression of E-cadherin (an epithelial marker) and vimentin (a mesenchymal marker) (Figure 1-2H), suggesting that KIBRA regulates EMT in a cell type specific manner.

1.3.3. KIBRA Promotes Proliferation, Migration and Invasion in LNCaP Cells

Next we investigated whether KIBRA plays a similar role in prostate cancer cells. LNCaP cells with stable expression of KIBRA was established (Figure 1-3A). No changes of WWC2 and WWC3 expression were detected in KIBRA-overexpressing cells (Figure 1-3A). LNCaP-KIBRA-expressing cells proliferated significantly faster than LNCaP-vector cells (Figure 1-3B). Similarly, KIBRA overexpression also enhanced cell migration and invasiveness in LNCaP cells (Figure 1-3C–F). However, ectopic expression of KIBRA did not alter the LNCaP cells' anchorage-independent growth (Figure 1-3G, H).

We recently showed that YAP overexpression converted LNCaP cells from androgen-sensitive to androgen-insensitive growth [33], we also tested whether KIBRA plays a role in androgen sensitivity. Under androgen-deprivation conditions, both LNCaP-vector and LNCaP-KIBRA cells failed to divide, suggesting that enhanced expression of KIBRA was not sufficient to promote androgen-insensitive growth in LNCaP cells (Figure 1-3I).

1.3.4. KIBRA Knockdown Impairs Migration, Invasion and Anchorage-Independent Growth in Prostate Cancer Cells

To explore the significance of KIBRA upregulation in androgen-insensitive prostate cancer cells, we reduced KIBRA expression using a validated shRNA against KIBRA [44] in LNCaP-C4-2 and LNCaP-C81 cells (Figure 1-4A). In contrast to the gain of function phenotypes in LNCaP and RWPE-1 cells, knockdown of KIBRA did not alter the proliferation rates in LNCaP-C4-2 and LNCaP-C81 cells (Figure 1-4B). Interestingly, knockdown of KIBRA greatly reduced migration and invasion (Figure 1-4C–E) and anchorage-independent growth (Figure 1-4F) in these cells. Together, these data revealed that KIBRA is a positive regulator in prostate cancer cell proliferation and motility.

1.3.5. KIBRA is Induced by AR Signaling

Consistent with the results from RWPE-1 cells, KIBRA overexpression or knock-down did not alter the expression of E-cadherin, an epithelial marker (Figure 1-5A). N-cadherin and vimentin (both are mesenchymal markers) were not detectable in LNCaP or LNCaP-C4-2 cells. AR protein levels were not affected by KIBRA expression either (Figure 1-5A). AR signaling activity is higher in LNCaP C4-2 and LNCaP-C81 cells than in LNCaP cells [33, 45]. To analyze whether KIBRA expression is regulated by AR signaling, we treated the LNCaP cells with R1881, an analog of androgen ligand, to activate the AR signaling. Interestingly, KIBRA protein levels were dramatically increased upon R1881 treatment (Figure 1-5B). Similar findings were also observed in androgen-insensitive cells (LNCaP-C4-2 and LNCaP-C81) (Figure 1-5C). However, the levels of mRNA of KIBRA were not altered in the presence of R1881 (Figure 1-5D, E). The expression of prostate-specific antigen (PSA), a known target of AR, was induced (Figure 1-5D, E). KIBRA protein stability was not significantly affected in the presence of R1881 (Figure 1-5F). In future

studies, we will explore the underlying mechanisms through which AR signaling activation by R1881 induces KIBRA expression.

Interestingly, mRNA levels of PSA were significantly reduced in KIBRA knockdown LNCaP-C4-2 cells, suggesting that KIBRA is required for full activation of AR signaling (Figure 1-5G). However, it is not known how KIBRA regulates AR activity and the down-stream signaling. Previous reports showed that both Lats2 [46] and YAP [46] associate with AR, and that KIBRA interacts with Lats2 [34]. Therefore, KIBRA may form a complex with AR through other binding partners to regulate AR activity though KIBRA expression did not affect the Lats1 kinase activity and YAP phosphorylation in prostate cancer cells (Figure 1-5H).

1.3.6. KIBRA is Upregulated in Prostate Tumors

Having established the role of KIBRA in prostate cancer with cell culture systems, we wanted to determine the clinical relevance of KIBRA in prostate cancer. Publically available data demonstrated that mRNA levels of KIBRA were significantly higher in prostate tumors than normal prostate tissue (Figure 1-6A–D). Moreover, KIBRA protein levels were also greatly increased in prostate tumors than normal prostate tissue in another set of samples (Figure 1-6E).

In conclusion, the results show that ectopic expression of KIBRA promotes prostate cancer cell proliferation and motility. KIBRA knockdown impairs migration and invasion in androgen-insensitive prostate cancer cells. KIBRA expression is induced by AR signaling and is increased in prostate tumors. Our findings reveal a pro-tumor function for KIBRA in prostate cancer.

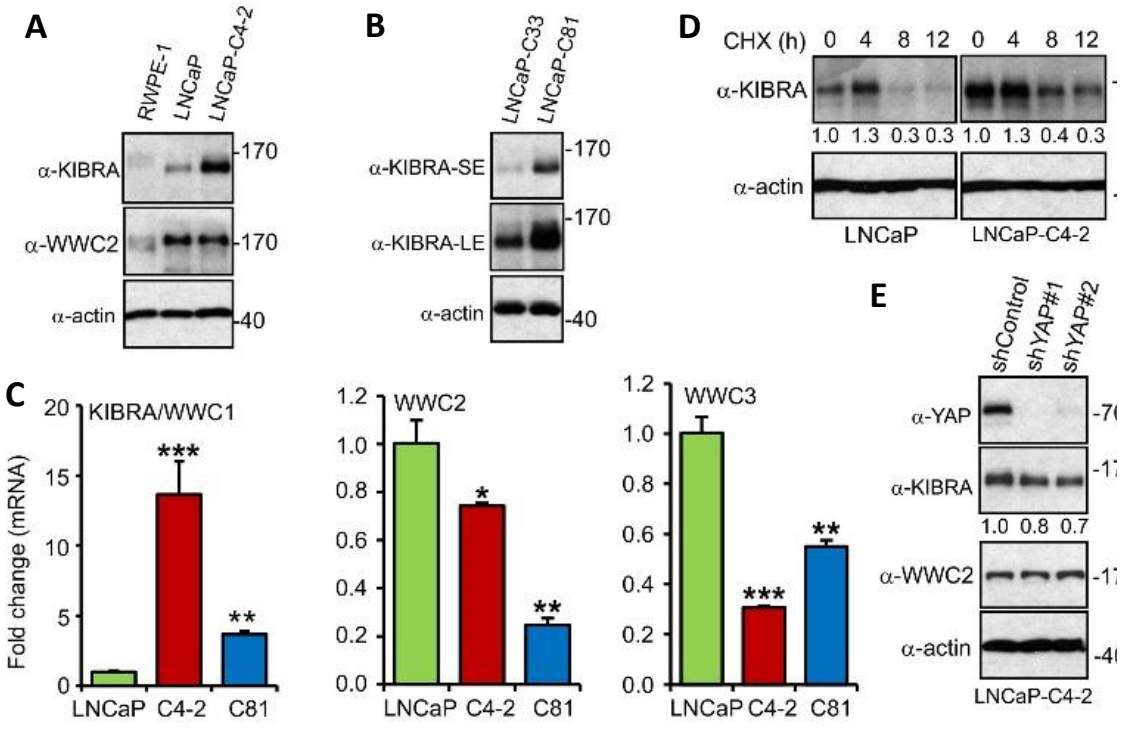

Figure 1-1. KIBRA is Transcriptionally Upregulated in Androgen-Insensitive Prostate Cancer cells

(A, B) RWPE-1, LNCaP, LNCaP-C4-2, LNCaP-C33, and LNCaP-C81 cells lines were cultured as described in 'Material and methods'. The total cell lysates were probed with the indicated antibodies. SE: short exposure; LE: long exposure. (C) Quantitative RT-PCR of WWC1/2/3 in LNCaP and its sublines. (D) LNCaP and LNCaP-C4-2 cells were treated with cycloheximide (CHX, 50 μg/ml) at the indicated time points and the total cell lysates were analyzed with the indicated antibodies. The relative intensity was shown from the average of three blots (Image J). (E) LNCaP-C4-2 cell lines expressing control shRNA or shRNA against YAP were utilized to determine the indicated protein levels by Western blotting. Data were obtained from three (n=3) independent experiments (A–E) and expressed as mean ± s.e.m (C). *: $p<0.05$; **: $p<0.01$; ***: $p<0.001$ (t-test).

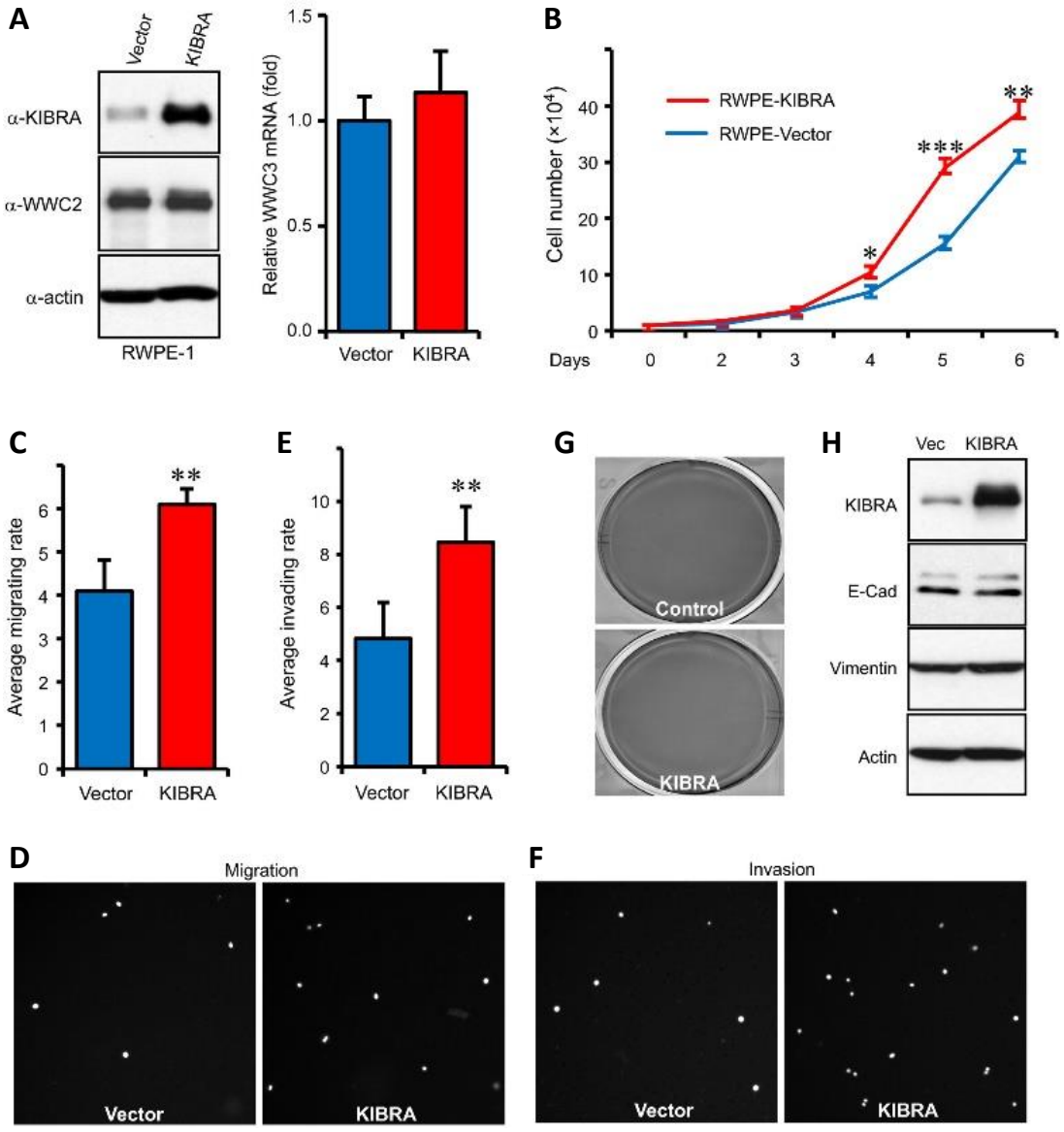
A
Vector
KIBRA
α-KIBRA
α-WWC2
α-actin
RWPE-1
Relative WWC3 mRNA (fold)
1.5
1.0
0.5
0.0
Vector
KIBRA
B
RWPE-KIBRA
RWPE-Vector
Cell number (×10⁴)
40
30
20
10
0
Days
0
2
3
4
5
6
*
***
**
C
Average migrating rate
6
5
4
3
2
1
0
**
Vector
KIBRA
E
Average invading rate
10
8
6
4
2
0
**
Vector
KIBRA
G
Control
KIBRA
H
Vec
KIBRA
KIBRA
E-Cad
Vimentin
Actin
D
Migration
Vector
KIBRA
F
Invasion
Vector
KIBRA

Figure 1-2. KIBRA Promotes Proliferation, Migration and Invasion in RWPE-1 Cells

(A) Establishment of RWPE-1 cells expressing vector (control) or KIBRA. WWC2 protein and WWC3 mRNA levels were determined in these cells. (B) The proliferation curve of the cell lines established in (A). (C, D) Cell migration effect was determined with the cell lines in (A). Representative photos for migrating cells are shown in (D). (E, F) Cell invasion effect was determined with the cell lines in (A). Representative photos for invading cells are shown in (F). (G) Anchorage-independent growth (colony assay in soft agar) was determined with the cell lines established in (A). No colony was formed in RWPE-1-vector and –KIBRA cells. (H) Total cell lysates from cell lines established in (A) were probed with the indicated antibodies. Data were obtained from three (n=3) independent experiments (A–H) and expressed as mean ± s.e.m (B, C). *:

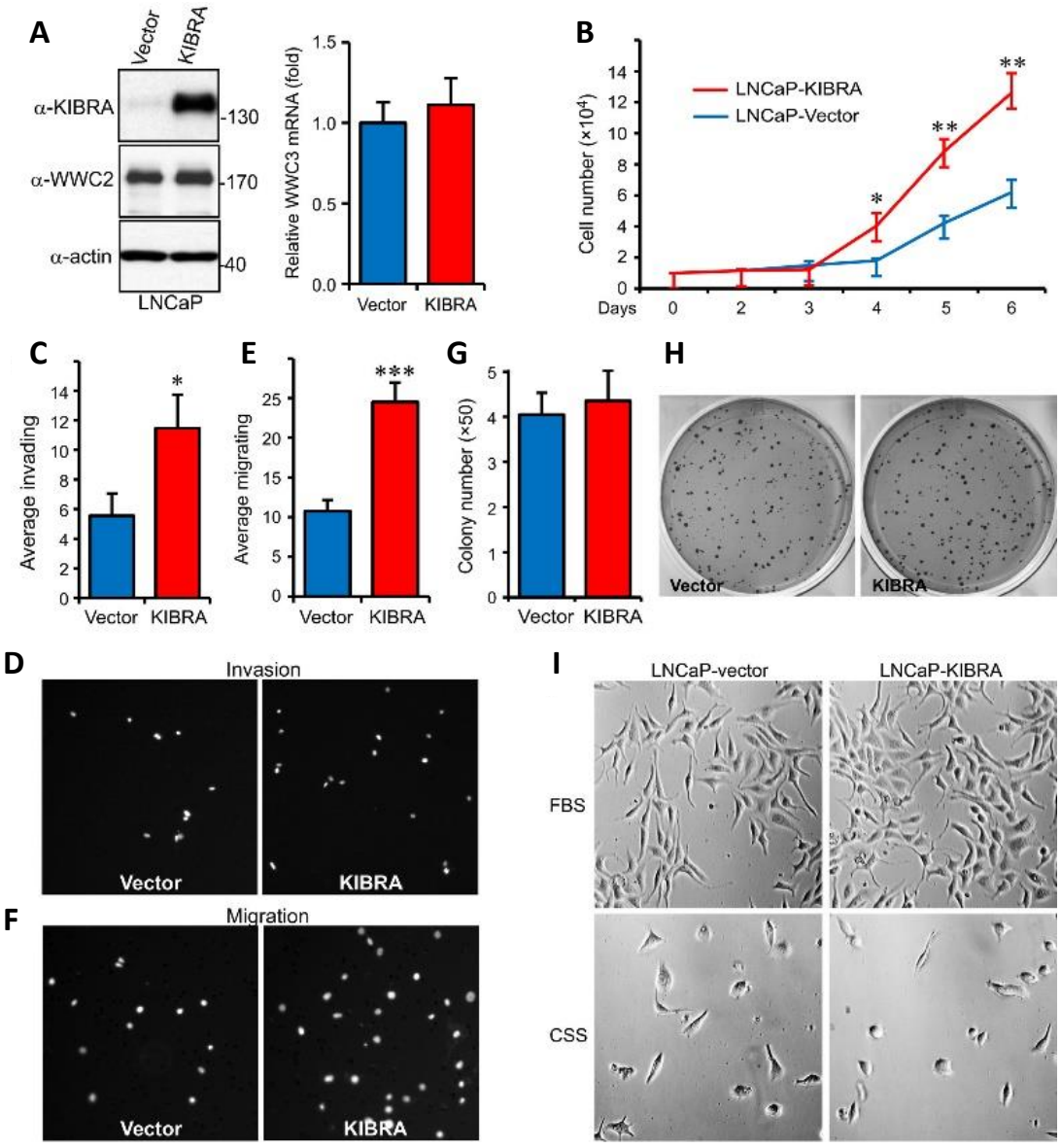
A
Vector
KIBRA
α-KIBRA
α-WWC2
α-actin
130
170
40
LNCaP
Relative WWC3 mRNA (fold)
1.5
1.0
0.5
0.0
Vector
KIBRA
B
LNCaP-KIBRA
LNCaP-Vector
Cell number (×10⁴)
Days
0
2
3
4
5
6
*
**
**
C
Average invading
*
Vector
KIBRA
E
Average migrating
***
Vector
KIBRA
G
Colony number (×50)
Vector
KIBRA
H
Vector
KIBRA
D
Invasion
Vector
KIBRA
F
Migration
Vector
KIBRA
I
LNCaP-vector
LNCaP-KIBRA
FBS
CSS

Figure 1-3. KIBRA Promotes Proliferation, Migration and Invasion in LNCaP Cells

(A) Establishment of LNCaP cells expressing vector (control) or KIBRA. WWC2 protein and WWC3 mRNA levels were determined in these cells. (B) The proliferation curve of the cell lines established in (A). (C, D) Cell invasion effect was determined with the cell lines established in (A). Representative photos for invading cells are shown in (D). (E, F) Cell migration effect was determined with the cell lines established in (A). Representative photos for invading cells are shown in (F). (G, H) Anchorage-independent growth (colony assay in soft agar) was determined with the cell lines established in (A). (I) Representative photos of LNCaP-vector or LNCaP-KIBRA cells that have been cultured in normal medium (FBS) or androgen deprivation medium (CSS) for 4 days. FBS: fetal bovine serum; CSS: charcoal striped serum. Data were obtained from three (n=3) independent experiments (A–I) and expressed as mean ± s.e.m (B, C, E, G). *: $p<0.05$; **: $p<0.01$; ***: $p<0.001$ (t-test).

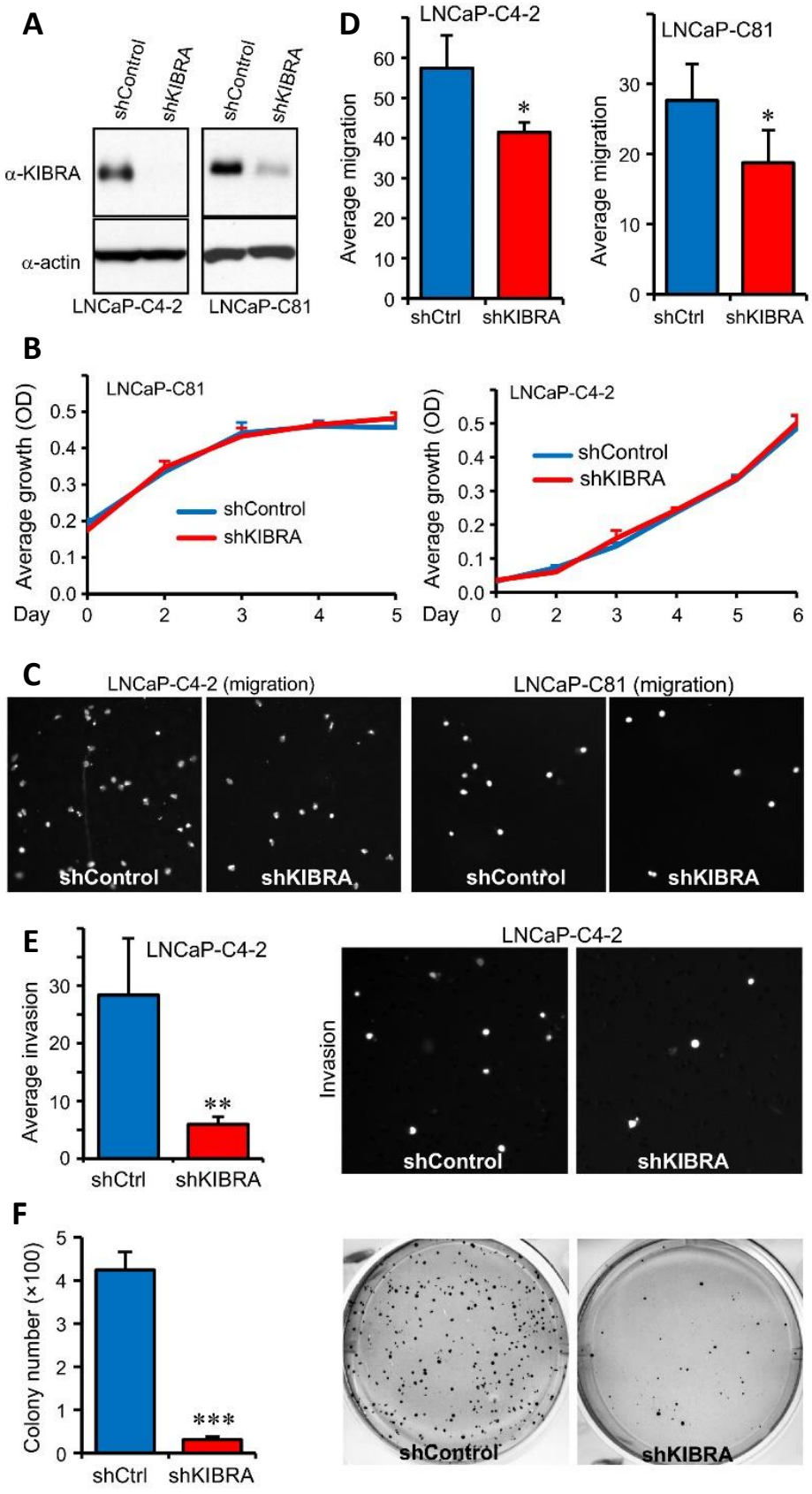
A
shControl
shKIBRA
shControl
shKIBRA
α-KIBRA
α-actin
LNCaP-C4-2
LNCaP-C81
D
LNCaP-C4-2
Average migration
shCtrl
shKIBRA
LNCaP-C81
Average migration
shCtrl
shKIBRA
B
LNCaP-C81
Average growth (OD)
Day
shControl
shKIBRA
LNCaP-C4-2
Average growth (OD)
Day
shControl
shKIBRA
C
LNCaP-C4-2 (migration)
shControl
shKIBRA
LNCaP-C81 (migration)
shControl
shKIBRA
E
LNCaP-C4-2
Average invasion
shCtrl
shKIBRA
LNCaP-C4-2
Invasion
shControl
shKIBRA
F
Colony number (×100)
shCtrl
shKIBRA
shControl
shKIBRA

Figure 1-4. KIBRA Knockdown Impairs Motility and Anchorage-Independent Growth in Prostate Cancer Cells

(A) Establishment of LNCaP-C4-2/C81 cells expressing control shRNA (shControl) or shRNA against KIBRA (shKIBRA). (B) The proliferation curves (determined by MTT assays) of the cell lines established in (A). (C, D) Cell migration effect was determined with the cell lines established in (A). Representative photos for migrating cells are shown in (C). (E) Cell invasion effect was determined with the cell lines established in (A). (F) Colony formation assays in LNCaP-C4-2 cells established in (A). Data were obtained from three (n=3) independent experiments (A–F) and expressed as mean ± s.e.m (B, D-F). *: $p<0.05$; **: $p<0.01$; ***: $p<0.001$ (t-test).

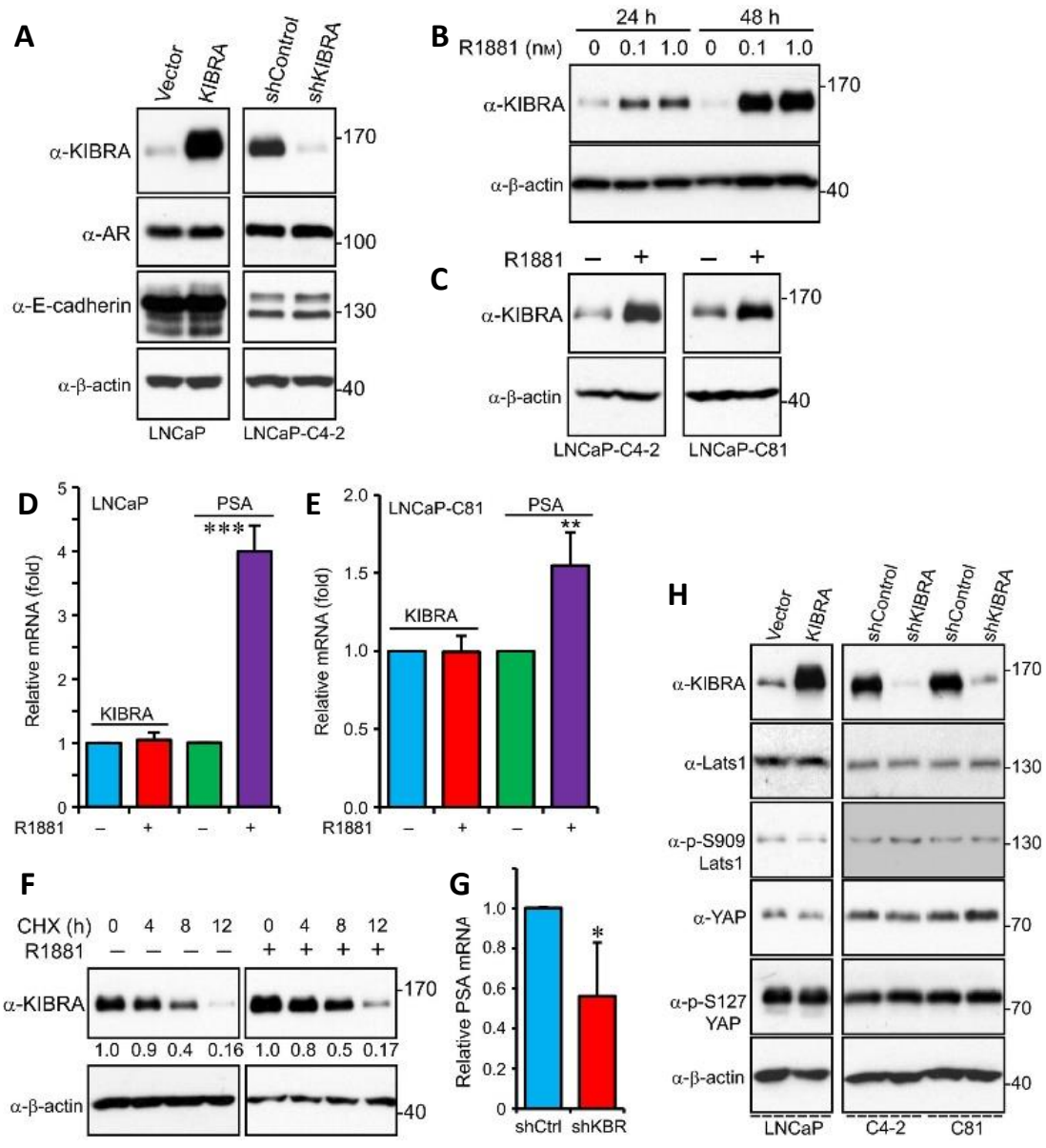
A
Vector
KIBRA
shControl
shKIBRA
α-KIBRA
α-AR
α-E-cadherin
α-β-actin
170
100
130
40
LNCaP
LNCaP-C4-2
B
24 h
48 h
R1881 (nM)
0 0.1 1.0 0 0.1 1.0
α-KIBRA
α-β-actin
170
40
C
R1881 – + – +
α-KIBRA
α-β-actin
170
40
LNCaP-C4-2
LNCaP-C81
D
LNCaP
PSA
***
KIBRA
Relative mRNA (fold)
R1881 – + – +
E
LNCaP-C81
PSA
**
KIBRA
Relative mRNA (fold)
R1881 – + – +
F
CHX (h) 0 4 8 12 0 4 8 12
R1881 – – – – + + + +
α-KIBRA
1.0 0.9 0.4 0.16 1.0 0.8 0.5 0.17
α-β-actin
170
40
G
Relative PSA mRNA
*
shCtrl
shKBR
H
Vector
KIBRA
shControl
shKIBRA
shControl
shKIBRA
α-KIBRA
α-Lats1
α-p-S909 Lats1
α-YAP
α-p-S127 YAP
α-β-actin
170
130
130
70
70
40
LNCaP
C4-2
C81

Figure 1-5. KIBRA is Induced by R1881 and is Required for AR Signaling Activation

(A) Total cell lysates from various stable cell lines were probed with the indicated antibodies. (B) LNCaP cells were treated with R1881 as indicated. Total protein lysates were subjected to Western blot analysis. (C) LNCaP-C4-2 and LNCaP-C81 cells were treated with R1881 (1 nM) for 24 h and total protein lysates were subjected to Western blot analysis with the indicated antibodies. (D, E) Quantitative RT-PCR in LNCaP or LNCaP-C81 cells treated or not treated with R1881 (1 nM) for 24 h. (F) LNCaP-C81 cells were treated with cycloheximide (CHX, 50 μg/ml) at the indicated time points and the total cell lysates were analyzed with the indicated antibodies. The relative intensity was shown from the average of three blots (Image J). (G) Quantitative RT-PCR for PSA in LNCaP-C4-2 cells with control or KIBRA knockdown. (H) Total cell lysates from various stable cell lines were probed with the indicated antibodies. Data were obtained from three (n=3) independent experiments (A–H) and expressed as mean ± s.e.m (D–G). *: $p<0.05$; ***: $p<0.001$ (t-test).

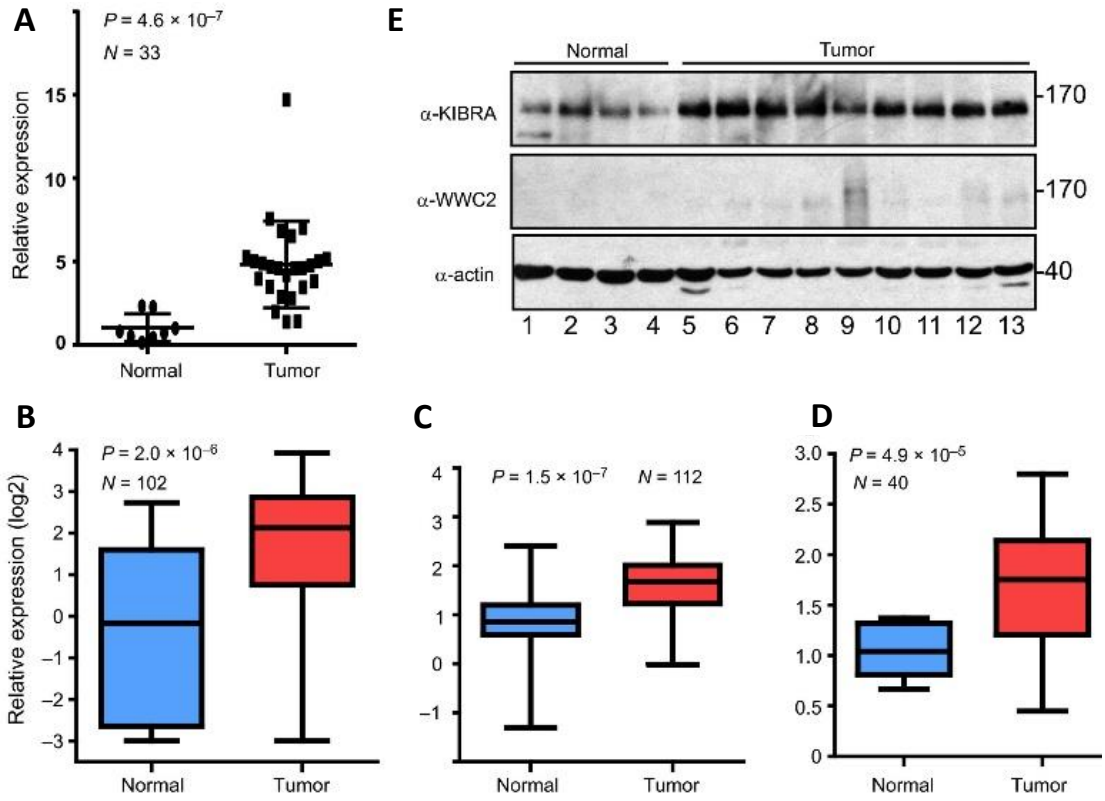

Figure 1-6. KIBRA is Overexpressed in Prostate Cancer

(A–D) KIBRA mRNA is increased in clinical samples. Data were mined from published studies through biogps.org (A) and oncomine.org (B–D). The original references are: [47] (A), [48] (B), [49] (C), and [50] (D). The box (B–D) extends from the 25th to 75th percentiles. The line is plotted at the median and the whiskers go to the smallest and the largest value for each group (B–D). (E) Total protein lysates from prostate tumors and normal prostate tissue were subjected to Western blot analysis with the indicated antibodies.

Chapter 2

CDK1-MEDIATED MITOTIC PHOSPHORYLATION OF PBK IS INVOLVED IN CYTOKINESIS AND INHIBITS ITS ONCOGENIC ACTIVITY*

* The material presented in this chapter was previously published: S. Stauffer et al. Cell Signal 2017; 39: 74-83.

ABSTRACT

PDZ-binding kinase (PBK) plays a major role in proliferation and in safeguarding mitotic fidelity in cancer cells. Frequently upregulated in many cancers, PBK drives tumorigenesis and metastasis. PBK has been shown to be phosphorylated in mitosis by cyclin-dependent kinase 1 (CDK1)/cyclin B, however, no studies have been done examining PBK mitotic phosphorylation in oncogenesis. Additionally to the previously identified Threonine-9 phosphorylation, we found that Threonine-24, Serine-32, and Serine-59 of PBK are also phosphorylated. PBK is phosphorylated *in vitro* and in cells by CDK1 during anti-mitotic drug-induced mitotic arrest and in normal mitosis. We demonstrated that mitotic phosphorylation of Threonine-9 is involved in cytokinesis. The non-phosphorylatable mutant PBK-T9A augments tumorigenesis to a greater extent than wild type PBK in breast cancer cells, suggesting that PBK mitotic phosphorylation inhibits its tumor promoting activity. The PBK-T9A mutant also transforms and increases the proliferation of immortalized breast epithelial cells. Collectively, this study reveals that CDK1-mediated mitotic phosphorylation of PBK is involved in cytokinesis and inhibits its oncogenic activity.

2.1. INTRODUCTION

PDZ-binding kinase (PBK) also named Lymphokine-Activated Killer T-Cell-Originated Protein Kinase (TOPK) is a MAPKK-like serine/threonine kinase. PBK was originally isolated due to its increased expression in IL-2 activated killer T-cells and was found to interact with the human homologue of the Drosophila discs large tumor suppressor (hDlg) [51, 52]. Normally only having detectible expression in testicular germ cells and some fetal tissues, PBK is overexpressed in a wide array of cancers including pancreatic, breast, ovarian, colorectal, lung, bladder, gastric, and oral cancer [53-61]. In addition, PBK overexpression is sufficient to transform mouse epidermal cells [61] and is strongly associated with patient survival and tumor grade [53, 59, 62]. Several studies have shown that PBK knockdown decreases cell viability and proliferation [57, 61, 63-66] as well as suppressing the cologenic potential of cancer cells [57, 60, 61, 65].

PBK has been shown to be upregulated during mitosis and that PBK binding and phosphorylation by CDK1/cyclin B is required for its mitotic activity [67]. Other studies have described a key role for PBK in mitosis, as cells treated with PBK inhibitors or siRNA targeting PBK develop cytokinetic defects [57, 68, 69]. Threonine-9 of PBK has been described previously as the principle mitotic phosphorylation target of CDK1/cyclin B and that its phosphorylation is required for proper binding of PBK to its effector proteins as well as for PBK's mitotic activity [52, 67, 70]. However, no functional studies have been carried out to examine the role of PBK mitotic phosphorylation in cytokinesis and cancer related properties. Interestingly, another study has revealed that phosphorylated bands were still present for HA-tagged PBK-T9A mutant protein in mitotically arrested cells, indicating the possibility of other phosphorylation sites [71].

A recent report uncovered that PBK expression is regulated by Yes-associated protein (YAP), a transcriptional co-activator of the Hippo pathway [72, 73], and is

responsive to geranylgeranyl signaling in ER-breast cancer cells [74]. In this report, we identified additional CDK1/cyclin B phosphorylation sites on PBK and elucidate the role of the CDK1/PBK axis in breast cancer. We found that CDK1-mediated mitotic phosphorylation of PBK is involved in cytokinesis and inhibits its oncogenic activity.

2.2. MATERIALS AND METHODS

2.2.1. Cell Culture and Transfection

HEK293T, HeLa, U2OS, MCF10A, and T47D cell lines were purchased from American Type Culture Collection (ATCC) and cultured as ATCC instructed. The cell lines were authenticated at ATCC and were used at low (< 25) passages. Attractene (Qiagen) was used for transient overexpression of proteins in HEK293T cells following the manufacturer's instructions. SiRNA transfections were done with HiPerfect (Qiagen). The MISSION siRNA for PBK was purchased from Sigma. The target sequences are: 5′-GACCATAGTTTCTTGTTAA-3′ and 5′-CTGGATGAATCATACCAGA-3′. Lentivirus packaging, infection, and subsequent selection were done as we have described previously [34]. Nocodazole (100 ng/mL for 16 h) and taxol (100 nM for 16 h) (Selleck Chemicals) were used to arrest cells in mitosis unless otherwise indicated. Kinase inhibitors were purchased from Selleck Chemicals (VX680, BI2536, Purvalanol A, SP600125, SB216736, and MK2206), ENZO life Sciences (RO3306 and Roscovitine), or LC Laboratory (U0126 and SB203580). All other chemicals were from either from Sigma or Thermo Fisher.

2.2.2. Expression Constructs

The pWZL-Neo-Myr-Flag-PBK vector was a gift from William Hahn & Jean Zhao (Addgene plasmid # 20558). To make the Lentiviral PBK expression constructs, the above vector was used to clone full-length PBK cDNA into the pSIN4-Flag-IRES-puro vector. The

pSIN4-Flag-IRES-puro vector was made by inserting an N-terminal Flag-tag with multiple-cloning-site sequences into the empty pSIN4-EF1α-IRES-Puro vector, which was originally obtained from Addgene [75]. Point mutations were generated by the QuikChange Site-Directed PCR mutagenesis kit (Stratagene) and verified by sequencing.

2.2.3. EGFP-Expressing All-In-One CRISPR Construct

To establish the CRISPR vector which expresses EGFP, we modified the pX330A_D10A-1x2 all-in-one vector, from the Takashi Yamamoto laboratory [76]. We removed the small sequence between the FseI and NotI sites and added a T2A-EGFP sequence from pSpCas9(BB)-2A-GFP (PX458) in its place [77].

To construct the all-in-one CRISPR/Cas9n plasmid targeting PBK, the sense and anti-sense oligonucleotides from Table 1 were synthesized, annealed, and Golden Gate assembled into the pX330A_D10A-1x2-EGFP and pX330S-2 vectors as described previously [76]. After the two vectors were generated, a final Golden Gate assembly was performed to generate the all-in-one vector as described previously [76]. The resulting pX330A_D10A-1x2-EGFP-PBK-AB construct was transfected into cells and GFP-positive clones were selected by flow cytometry-based cell sorting.

2.2.4. Recombinant Protein Purification and *In Vitro* Kinase Assay

GST-tagged PBK and PBK-4A were cloned in pGEX-5X-1 and proteins were bacterially expressed and purified on GSTrap FF affinity columns (GE Healthcare) following the manufacturer's instructions. GST-PBK (0.5–1 µg) was incubated with 10 U recombinant CDK1/cyclin B complex (New England Biolabs) or 100 ng CDK1/cyclin B (SignalChem) in kinase buffer (New England Biolabs) in the presence of 5 µCi γ-32P-ATP (3000 Ci/mmol, PerkinElmer). Phosphorylation (32P incorporation) was visualized by autoradiography followed by Western blotting or detected by phospho-specific antibodies.

2.2.5. Antibodies

The PBK and phospho-PBK (pT9) antibodies were purchased from Cell Signaling Technology (4942 and 4941). Rabbit polyclonal phospho-specific antibodies against PBK T24, S32, and S59 were generated and purified by AbMart. The peptides used for immunizing rabbits were SVLCS-pT-PTINI (T24), INIPA-pS-PFMQK (S32) and RGLSH-pS-PWAVK (S59). The corresponding non-phosphorylated peptides were also synthesized and used for antibody purification and blocking assays. Anti-Flag antibody was from Sigma. Anti-PLK1 was from BioLegend. Anti-β-actin, anti-Mps1/TTK, anti-cyclin E1, and anti-cyclin B antibodies were from Santa Cruz Biotechnology. Anti-aurora-A, anti-CDK2, anti-glutathione S-transferase (GST), anti-BUB1, and anti-BubR1 antibodies were from Bethyl Laboratories. Anti-phospho-S10 H3, anti-YAP, anti-phospho-S127 YAP, anti-phospho-S397 YAP, anti-vimentin, anti-E-cadherin, anti-N-cadherin, anti-CDC25C, anti-CDK4, anti-CDK5, anti-CDK6, anti-Cyclin A2, anti-Cyclin E2, anti-MAD2, anti-phospho-S795 Rb, anti-Wee1, and anti-phospho-S642 Wee1 antibodies were from Cell Signaling Technology. Anti-β-tubulin (Sigma) antibodies were used for immunofluorescence staining.

2.2.6. Phos-Tag and Western Blot Analysis

Phos-tag™ was obtained from Wako Pure Chemical Industries, Ltd. (cat#: 304-93521) and used at 10–20 μM (with 100 μM MnCl2) in 8% SDS-acrylamide gels as described [78]. Western blotting and lambda phosphatase treatment assays were done as previously described [34].

2.2.7. Immunofluorescence Staining and Confocal Microscopy

Cell fixation, permeabilization, immunofluorescence staining, and microscopy were done as previously described [79]. For peptide blocking, a protocol from the Abcam website was used, as we previously described [41].

2.2.8. Proliferation, Migration and Invasion Assays

Proliferation of cells was determined by MTT assay. Briefly, the cell lines MCF10A and T47D were seeded into 12-well plates, in triplicate, at a density of 5×10^4 and 1×10^5 cells/well respectively. Next, culture media with 0.5 µg/mL MTT were added to the cells which were incubated in the dark at 37 °C for 1 h. After incubation, the media was removed and the reduced MTT was liberated from the cells and dissolved by addition of 500 µL of DMSO. Then 150 µL of the released dye was transferred, in triplicate, to 96-well plates. The absorbance was determined at a wavelength of 570 nm. Wound healing assays were utilized for measuring migratory activity as previously described [80]. *In vitro* cell invasion assays were performed using the BioCoat invasion system (BD BioSciences) according to the manufacturer's instructions. The outer section was filled with 750 µL of a culture medium. Cell suspensions in 500 µL of serum free medium were seeded in the inner chambers. After incubation for 24 h, the cells on the upper surface of the chamber were removed with a cotton swab, and the cells that invaded to the lower surface of the chamber were fixed with methanol and stained using ProLong Gold Antifade Reagent with DAPI [41].

2.2.9. Statistical Analysis

Statistical significance was analyzed using a two-tailed, unpaired Student's t-test.

2.3. Results

2.3.1. Antimitotic Drugs Trigger PBK Phosphorylation at Mitosis of Cell Cycle and Can Be Blocked by CDK1 Inhibitors

To further explore PBK's involvement in mitosis, we treated HeLa cells with taxol or nocodazole to arrest the cells in mitosis and as shown in Figure 2-1A, PBK protein was dramatically up-shifted on a Phos-tag gel (Figure 2-1A). Lambda phosphatase treatment largely abolished the PBK mobility shift, suggesting that PBK is phosphorylated during mitotic arrest (Figure 2-1B). We used various kinase inhibitors to identify the candidate kinase for PBK phosphorylation. Inhibition of PLK1 (with BI2536), Aurora-A, -B, -C (with VX680), Akt (with MK2206), p38 kinase (with SB203580), JNK1/2 (with SP600125), MEK/ERK (with U0126), or GSK3 (with SB216763) failed to alter the phosphorylation level and resultant mobility shift of PBK during G_2/M arrest (Figure 2-1C, lanes 5–11). These inhibitors are effective under the conditions used [41, 81]. Treatments with RO3306 (CDK1-specific inhibitor) or Purvalanol A (CDK1/2/5 inhibitor) virtually blocked the PBK mobility shift/phosphorylation entirely (Figure 2-1C, lanes 3–4). These data suggest that PBK is likely phosphorylated by CDK1 during mitotic arrest induced by taxol or nocodazole treatment.

2.3.2. CDK1 Phosphorylates PBK *In Vitro*

Next, with bacterially purified PBK proteins as substrates, we performed *in vitro* kinase assays to determine whether CDK1 can directly phosphorylate PBK. Figure 2-2A shows that purified CDK1/cyclin B kinase complex strongly phosphorylated GST-PBK proteins *in vitro* and that the CDK1 inhibitor RO3306 greatly reduced the phosphorylation of GST-PBK (Figure 2-2A). There are a total of four conserved sites on the N-terminus of PBK that fit the proline-directed consensus sequence of CDK1-phosphorylation sites [82] (Figure 2-2B). Intriguingly, these four sites (Threonine-9, Threonine-24, Serine-32, and

Serine-59) have been identified as mitotic phosphorylation sites from large scale proteomic studies [83, 84]. Mutating these four sites to non-phosphorylatable alanines (PBK-4A) completely eliminated the ^{32}P incorporation onto PBK, indicating that T9, T24, S32 and S59 are the main CDK1 phosphorylation sites (Figure 2-2C). We generated phospho-specific antibodies against T24, S32 and S59. Using these antibodies, as well as a commercial phospho-specific T9 antibody, we demonstrated that CDK1 phosphorylates PBK at T9, T24, S32 and S59 *in vitro* and that addition of RO3306 abolished this phosphorylation (Figure 2-2D).

2.3.3. CDK1 Phosphorylates PBK at Multiple Sites in Cells

Next, we sought to examine if the four PBK mitotic phosphorylations occur in cells. Taxol and nocodazole treatment significantly increased the phosphorylation of T24 on endogenous PBK in HeLa cells (Figure 2-3A). Phospho-antibody incubation with phospho-peptide, but not the regular peptide, completely blocked the phospho-signal, suggesting that this antibody specifically detects the phosphorylated form of PBK (Figure 2-3A). Likewise, taxol and nocodazole treatment significantly increased the phosphorylation of T9, S32, and S59 on endogenous PBK (Figure 2-3B). The phospho-signal of PBK T9, T24, S32, and S59 during taxol treatment was considerably reduced in PBK knockdown cells, further validating the specificity of these phospho-antibodies (Figure 2-3C). Additionally, we further demonstrated that the phosphorylation of PBK is CDK1-dependent by using CDK1 inhibitors (Figure 2-3D, lanes 3 and 4). Taken together, these observations indicate that PBK is phosphorylated by CDK1 at T9, T24, S32, and S59 in cells during antimitotic drug-induced mitotic arrest.

2.3.4. CDK1 Mediates PBK Phosphorylation during Mitotic Arrest and In Normal Mitosis

We next performed immunofluorescence microscopy with these phospho-specific antibodies in HeLa cells. The antibody against p-T24 detected a strong signal in nocodazole-arrested prometaphase cells (Figure 2-4A, white arrows). The signal was scarcely detectable in interphase cells (Figure 2-4A, yellow arrows). Again, pre-incubation with the phospho-peptide, but not the control regular peptide, predominantly blocked the signal, suggesting that these antibodies specifically detect PBK only when it is phosphorylated (Figure 2-4A, middle panels). Addition of the CDK1 inhibitor RO3306 largely reduced the signal detected by the PBK p-T24 antibody in mitotically arrested cells, once again demonstrating that this phosphorylation of PBK is CDK1-dependent (Figure 2-4A, lower panels).

Subsequently, we utilized a double thymidine block and release method [80] to further investigate the spatial and temporal dynamics of PBK phosphorylation in HeLa cells during unperturbed, normal mitosis. This way, we could more accurately determine the phospho-status of PBK during the different mitotic phases. We found that the p-PBK T24 signal was readily detectable in prometaphase and peaked in metaphase. The signal deteriorated in anaphase and was further reduced in telophase and cytokinesis (Figure 2-4B, C). We observed phosphorylation patterns for p-PBK T9, S32, and S59 which were similar to p-PBK T24 when probing lysates taken at 0, 8, 9, 13, and 24 h after double thymidine block and release (Figure 2-4D). Collectively, these data strongly indicate a dynamic, mitotic phosphorylation of PBK in cells.

2.3.5. CRISPR-Induced PBK Knockout Leads to Cytokinesis Failure and Tetraploidy

To characterize the impact of PBK on mitotic processes, we generated PBK knockout (KO) U2OS cells using CRISPR/Cas9-nickase (Cas9n) (Figure 2-5A). We then performed immunofluorescence staining, so as to observe which types of mitotic defects

may appear. We found that the PBK KO U2OS displayed a marked increase in cells that did not fully complete cytokinesis when compared to parental U2OS (Figure 2-5B, C).

We next sought to elucidate the roles the mitotic phosphorylation sites engage in to regulate cytokinesis. To do this, we re-expressed exogenous wild type (WT) PBK or the PBK T9A mutant in PBK KO U2OS cells (Figure 2-5D). It must be noted that we attempted multiple times to generate both a 3A (T24A/S32A/S59A) and a 4A (T9A/T24A/S32A/S59A) mutant stable cell lines but were unable to get sufficient expression of either protein, so we proceeded with characterizing the T9A mutant. As shown earlier, PBK is phosphorylated at T9, T24, S32 and S59 in parental U2OS when treated with taxol and, as expected, CRISPR-mediated PBK KO fully ablates each of these phospho-antibody signals (Figure 2-5D, lanes 1–4). Reconstitution of WT PBK in PBK-null U2OS rescues each of these taxol-induced phosphorylations (Figure 2-5D, lanes 5 and 6). In contrast, p-T9 PBK signal cannot be detected in PBK-T9A reconstitution cells, but has no significant effect on phosphorylation at the other additional three sites (Figure 2-5D, lanes 7 and 8). To examine the effects of WT and T9A PBK reconstitution on the perturbed cytokinesis seen in PBK KO cells, we again performed immunofluorescence staining. Reconstitution with WT PBK fully rescued the cytokinesis failure, whereas expression of T9A PBK mutant failed to alter this phenotype found in PBK-null U2OS cells (Figure 2-5E), suggesting that mitotic phosphorylation on T9 of PBK is involved in proper cytokinesis in U2OS cells. Since mitotic defects classically lead to genomic instability, we looked to quantify the ploidy changes resulting from knocking out PBK. Utilizing flow cytometry, we discovered that the number of tetraploid cells significantly increased in PBK KO U2OS (Figure 2-5F). Although WT PBK reconstitution cells had percent-tetraploid cells in similar levels to parental U2OS, T9A PBK reconstitution cells maintained the dramatically high ratio of tetraploid to diploid cells found in PBK-null U2OS cells (Figure 2-5F).

A previous study identified PBK as a downstream target of Hippo/YAP signaling [74], so we examined total and phospho-YAP levels in parental and PBK KO U2OS cells to determine if loss of PBK would affect the status of YAP. We found no noticeable changes to the total YAP protein level, nor did we see any changes to phosphorylation levels at S127 (Figure 2-5G). However, we observed a twofold increase of p-S397 of YAP (Figure 2-5G). Next, we screened numerous mitotic and cell-cycle regulators in parental and PBK KO U2OS cells to attempt to identify proteins with altered expression or phosphorylation levels between the two (Figure 2-5H). Of the proteins assayed, none were altered, except cyclin E1. Cyclin E1 expression was found, repeatedly, to be reduced (about 60%) (Figure 2-5H). These findings suggest that the mitotic phosphorylation of PBK at T9 is required for proper mitotic division and for maintaining genomic stability.

2.3.6. PBK Overexpression Leads to Epithelial-Mesenchymal Transition in Normal Cells

PBK has been identified as an oncogene in many types of cancer, including breast cancer [85]. Therefore, to determine the biological significance of mitotic phosphorylation of PBK, we used breast cell lines as a model system. We assessed PBK protein levels in MCF10A (an immortalized breast epithelial cell line) and various breast cancer cell lines. PBK expression was very high in most of the cancer cell lines and was barely detectible in MCF10A cells (Figure 2-6A). Next, we stably expressed PBK-WT or PBK-T9A in MCF10A cells. Neither the overexpression of PBK-WT or PBK-T9A led to changes in either total YAP protein level or p-YAP S127 (Figure 2-6B). Interestingly, PBK-WT and -T9A overexpression in MCF10A led to changes in epithelial-mesenchymal transition (EMT) markers, with E-cadherin downregulation and N-cadherin upregulation (Figure 2-6C). Accompanying this molecular change, PBK-WT and PBK-T9A overexpressed MCF10A cells displayed a spindle-shaped morphology and grew in a more loosely

arranged manner compared to the cuboidal shape of vector control MCF10A cells which grew in organized, compact islets (Figure 2-6D).

Both PBK-WT and PBK-T9A MCF10As had significantly increased rates of cell migration in wound healing assays when compared to vector control, although, no difference was observed between the two (Figure 2-6E, F). Interestingly, overexpression of PBK-WT in MCF10A led to significantly higher proliferation in comparison to vector control and surprisingly, PBK-T9A expressing MCF10A cells grew even faster than the PBK-WT expressing cells (Figure 2-6G). Since PBK-null U2OS cells which were reconstituted with PBK-T9A displayed high levels of cytokinesis failure, we examined the effect of overexpressing PBK-T9A on MCF10A mitotic division. Similarly, immunofluorescence microscopy revealed that MCF10A cells overexpressing PBK-T9A had a significantly higher percentage of mitotic cells in anaphase and telophase than did either vector control or PBK-WT overexpression (Figure 2-6H). Taken together, these findings suggest that mitotic phosphorylation of PBK T9 partially inhibits its oncogenic activity.

2.3.7. Mitotic Phosphorylation of PBK Inhibits Its Oncogenic Activity in Cells

We further determined the impact of mitotic phosphorylation of PBK in cancer cells by attempting to generate a full knockout cell line, but unfortunately were unable to do so, possibly because a complete loss of PBK activity is lethal in breast cancer; something that has been shown previously using PBK inhibitors [68]. We did however generate a PBK mono-allelic knockout (maKO) T47D cell line and used it to overexpress either WT or T9A PBK (Figure 2-7A). With these cell lines we examined PBK's role in invasion using Matrigel. Invasion of PBK maKO T47D cells was dramatically reduced when compared to parental T47D, whereas ectopic expression of PBK-WT rescued this drop in invasiveness (Figure 2-7B, C). Expression of PBK-T9A further increased the invading activity when

compared to PBK-WT (Figure 2-7B, C). T47D PBK maKO cells, having a reduced PBK expression level, possess much lower migratory activity than do parental T47D cells (Figure 2-7D, E). Overexpression of PBK-T9A increased cell migration to a greater extent when compared to PBK-WT overexpression (Figure 2-7D, E). Interestingly, overexpression of PBK-T9A significantly increased cell proliferation over that of control and PBK-WT-overexpressing cells, suggesting that mitotic phosphorylation of PBK can constrain proliferation (Figure 2-7F). As expected, cells partially lacking PBK expression (PBK maKO) proliferated at a rate significantly slower when compared to control cells (Figure 2-7F). Together, our data suggest that mitotic phosphorylation of PBK inhibits its oncogenic activity in breast cancer cells.

Several groups have described that mitotic phosphorylation at T9 on PBK is required for PBK's proper mitotic functionality [52, 67, 70]. However, little is known regarding the role of PBK mitotic phosphorylation in cancer related properties. Our studies revealed that mitotic phosphorylation on T9 is inhibitory on PBK's oncogenic activity (Figure 2-6, Figure 2-7). Here we identified three novel mitotic phosphorylation sites on PBK which are regulated by CDK1/cyclin B, extricating another layer mitotic phospho-regulation of PBK. However, the function of the other three CDK1 phosphorylation sites (T24, S32, S59) has not been defined. We discovered that the PBK-3A (T24A/S32A/S59A) and -4A (T9A/3A) mutants cannot be stably expressed. Utilizing a proteasomal inhibitor, we found that both of these proteins are being expressed, but are in fact being quickly degraded (data not shown). Further investigation using individual mutants is needed to determine if one or more of these sites are important for proper protein folding or if their phosphorylation is required to block targeting of PBK for proteasomal turnover.

Overexpression of PBK has been associated with increased tumorigenicity and clinical lethality of various cancers [53, 59, 60, 62, 86]. Future experiments are also needed to further investigate the relationship between the levels of PBK protein and PBK

mitotic phosphorylation in cancer patient samples. Equally important is to identify PBK's protein substrate(s) that are essential for cytokinesis and cancer cell survival and proliferation. Addressing these questions will not only help with understanding the cellular function of PBK in mitosis, but also provide insights into the underlying mechanisms of PBK overexpression in cancer development.

2.4. Discussion

PBK is related to the dual specific mitogen-activated protein kinase kinase (MAPKK) family. Overexpression of PBK has been associated with increased tumorigenicity and clinical lethality of various cancers [53, 59, 60, 62, 86]. Moreover, PBK has been shown previously to be upregulated during mitosis and that phosphorylation by CDK1/cyclin B is required for PBK mitotic activity (Abe 2007) [67]. Correspondingly, cells treated with PBK inhibitors or siRNA targeting PBK develop cytokinetic defects, pointing towards a key role for PBK in mitosis [57, 68, 71]. Several groups have described that mitotic phosphorylation at T9 on PBK is carried out by CDK1/cyclin B and that it is required for PBK's mitotic activity [52, 67, 70]. In addition, we also confirm that PBK is phosphorylated by CDK1/cyclin B during mitosis, but not solely at T9. Here we identified three novel mitotic phosphorylation sites on PBK which are regulated by CDK1/cyclin B, extricating another layer mitotic phospho-regulation of PBK. Helping to confirm this, a recent study has shown that the loss of phosphorylation of PBK at T9, alone, cannot block tumorigenesis, as a PBK T9A mutant transfectant in JB6 cells can still form colonies in soft agar similar to PBK WT [87] and yet another study found that PBK T9A mutant protein from mitotic cell lysates is still shifted in SDS-PAGE gel [71]. Wild-type PBK overexpression can induce epithelial-mesenchymal transition in normal breast epithelial cells but is not more oncogenic than the T9A mutant. Expression of PBK T9A mutant protein leads to increased cytokinesis failure and higher proliferation in MCF10A.

Compared with wild-type PBK, the non-phosphorylatable T9A mutant has a faster proliferating rate as well as increased cell motility and invasion breast cancer cells. These observations suggest that proper phospho-regulation of PBK is critical for suppressing its oncogenic function. Thus, our study revealed another layer of regulation for PBK during tumorigenesis via mitotic phosphorylation.

In this study, we have shown that CDK1/cyclin B1 phosphorylates PBK during mitosis *in vitro* and in cells at T9, T24, S32, and S59 (Figures 2-1 through 2-4). We also found that CRISPR-Cas9n mediated PBK knockout U2OS cells display an increase in cytokinesis failure and tetraploidy as well as that re-expression of PBK harboring the T9A mutation displays a similar defective phenotype (Figure 2-5). Furthermore, we have shown that both PBK WT and T9A can induce EMT changes to the normal, immortalized breast epithelial cell line MCF10A and confer an increase in cell motility (Figure 2-6). Similarly, another group described that both PBK WT and T9A transfected JB6 cells develop similar numbers of colonies in soft agar [87]. This alludes to the possibility that, since PBK is a mitotic kinase, other mitotic regulatory post-translational modifications outside of T9 also govern PBK's oncogenic potential. Intriguingly, the PBK T9A transformant bears a proliferative advantage and an increase in cytokinesis defects when compared to wild-type and control (Figure 2-6). These defects can lead to the development of tetraploidy which can overload the mitotic machinery, spurring chromosomal instability (CIN). Subsequently, CIN can generate a new aneuploid karyotype that stably proliferates. Occasionally, this aneuploidy may cause gene expression changes which are advantageous through alterations in gene dosage or by amplifying the rate of mutations in tumor suppressors and oncogenes [88, 89].

We have shown that PBK expression is required for breast cancer cell viability and tumorigenesis by using CRISPR-Cas9n to knock out one PBK allele in T47D breast cancer cells (Figure 2-7). We have speculated that the reason we were unable to isolate PBK-

null T47D cells may be because full loss of PBK expression in breast cancer cells is lethal. Numerous groups report that either PBK knockdown or drug-inhibition can result in decreased cell proliferation and viability as well as failure of cytokinesis [57, 60, 61, 63-66, 68, 71]. We have also demonstrated that re-expression of PBK T9A mutant in PBK maKO T47D cells increases their proliferation, invasion, and cell motility over that of the WT rescue (Figure 2-7). The differences in oncogenicity between PBK maKO/KO and T9A reconstitution, although both causing cytokinesis defects, could be explained in that PBK T9A possibly confers an advantageous level of CIN while PBK maKO/KOs high level of CIN is devastating for cell viability through processes involving metabolic stress and proteotoxicity [90, 91]. Since PBK is overexpressed in many types of cancers, future experiments are also needed to further investigate the relationship between the levels of PBK protein and PBK mitotic phosphorylation in cancer patient samples as well as to identify the PBK's protein substrates that are essential for cancer cell survival and proliferation. Addressing these questions will not only help with understanding the cellular function of PBK in mitosis, but also provide insights into its biological significance and the underlying mechanisms of PBK overexpression in cancer development.

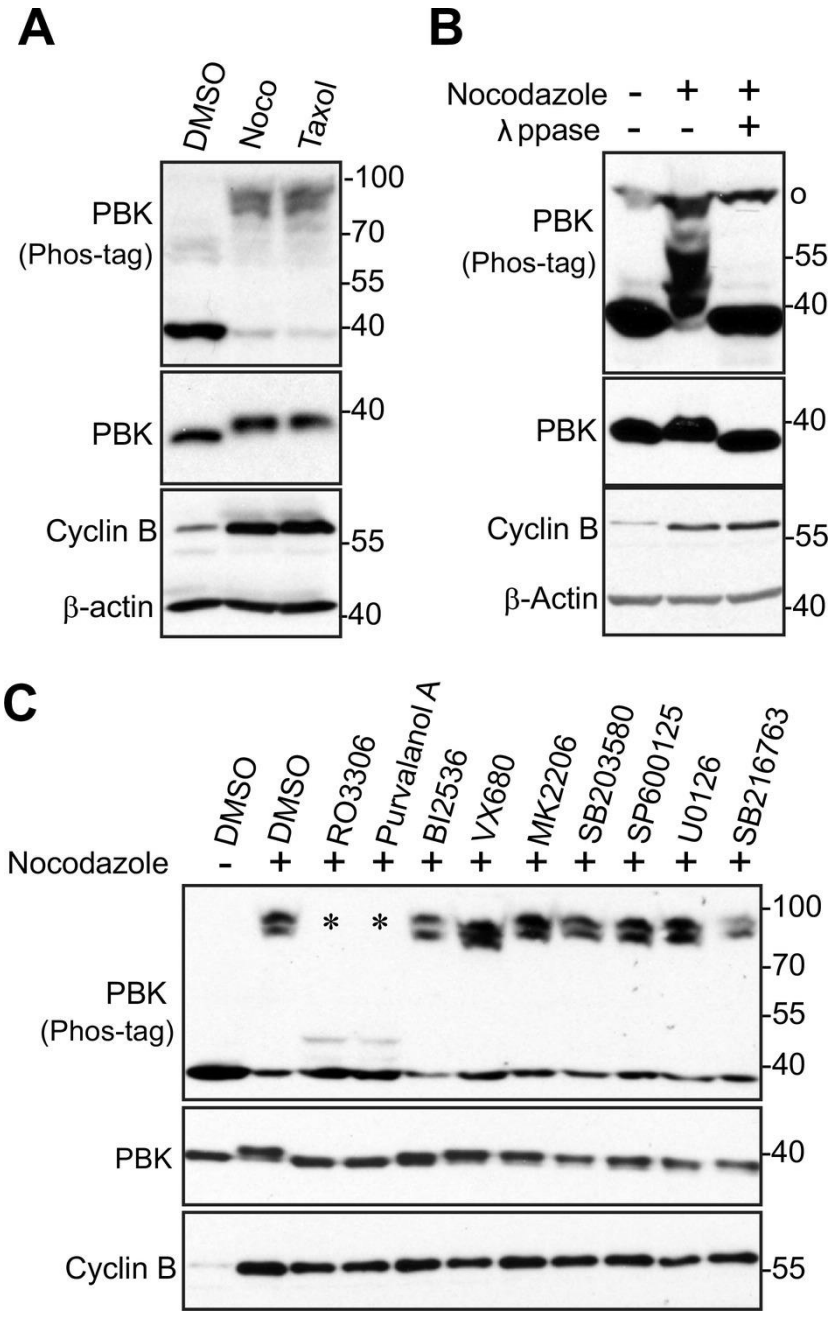
A
DMSO
Noco
Taxol
PBK
(Phos-tag)
PBK
Cyclin B
β-actin
100
70
55
40
40
55
40
B
Nocodazole - + +
λ ppase - - +
PBK
(Phos-tag)
PBK
Cyclin B
β-Actin
o
55
40
40
55
40
C
Nocodazole
- DMSO
+ DMSO
+ RO3306
+ Purvalanol A
+ BI2536
+ VX680
+ MK2206
+ SB203580
+ SP600125
+ U0126
+ SB216763
PBK
(Phos-tag)
PBK
Cyclin B
100
70
55
40
40
55

Figure 2-1. Phosphorylation of PBK by CDK1 during Mitotic Arrest

(A) HeLa cells were treated with DMSO, taxol (100 nM for 16 h) or nocodazole (100 ng/mL for 16 h). Total cell lysates were probed with the indicated antibodies on Phos-tag or regular SDS-polyacrylamide gels. (B) HeLa cells were treated with nocodazole as indicated and cell lysates were further treated with (+) or without (−) λ-phosphatase (ppase). Total cell lysates were probed with anti-PBK antibody. o marks a non-specific band. (C) HeLa cells were treated with nocodazole together with or without various kinase inhibitors as indicated. RO3306 (5 μM), Purvalanol A (10 μM), BI2536 (100 nM), VX680 (2 μM), MK2206 (10 μM), SB203580 (10 μM), SB203580 (20 μM), SP600125 (20 μM), U0126 (20 μM), and SB216763 (10 μM) were used. Inhibitors were added 1.5 h before harvesting the cells (with MG132 to prevent cyclin B degradation and consequent mitotic exit). Total cell lysates were subjected to Western blotting with the indicated antibodies. * marks the two lanes in which the PBK mobility-shift was inhibited.

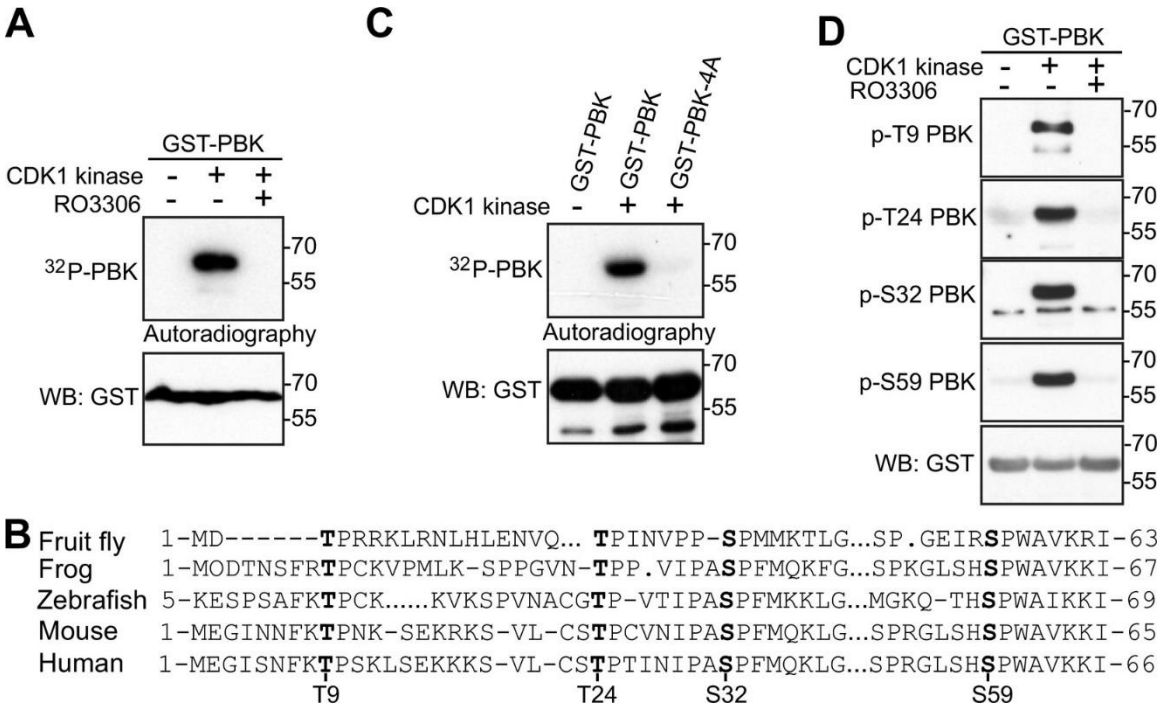

Figure 2-2. CDK1 Phosphorylates PBK *In Vitro*

(A*) In vitro* kinase assays with purified CDK1/cyclin B complex and recombinant GST-PBK. RO3306 (5 μM) was used to inhibit CDK1 kinase activity. (B) Conservation of PBK's mitotic phosphorylation sites. (C) *In vitro* kinase assays with purified CDK1/cyclin B complex to phosphorylate recombinant GST-PBK or GST-PBK-4A. D, *In vitro* kinase assays were done as in (A) except anti-phospho-PBK T9, T24, S32 and S59 antibodies were used.

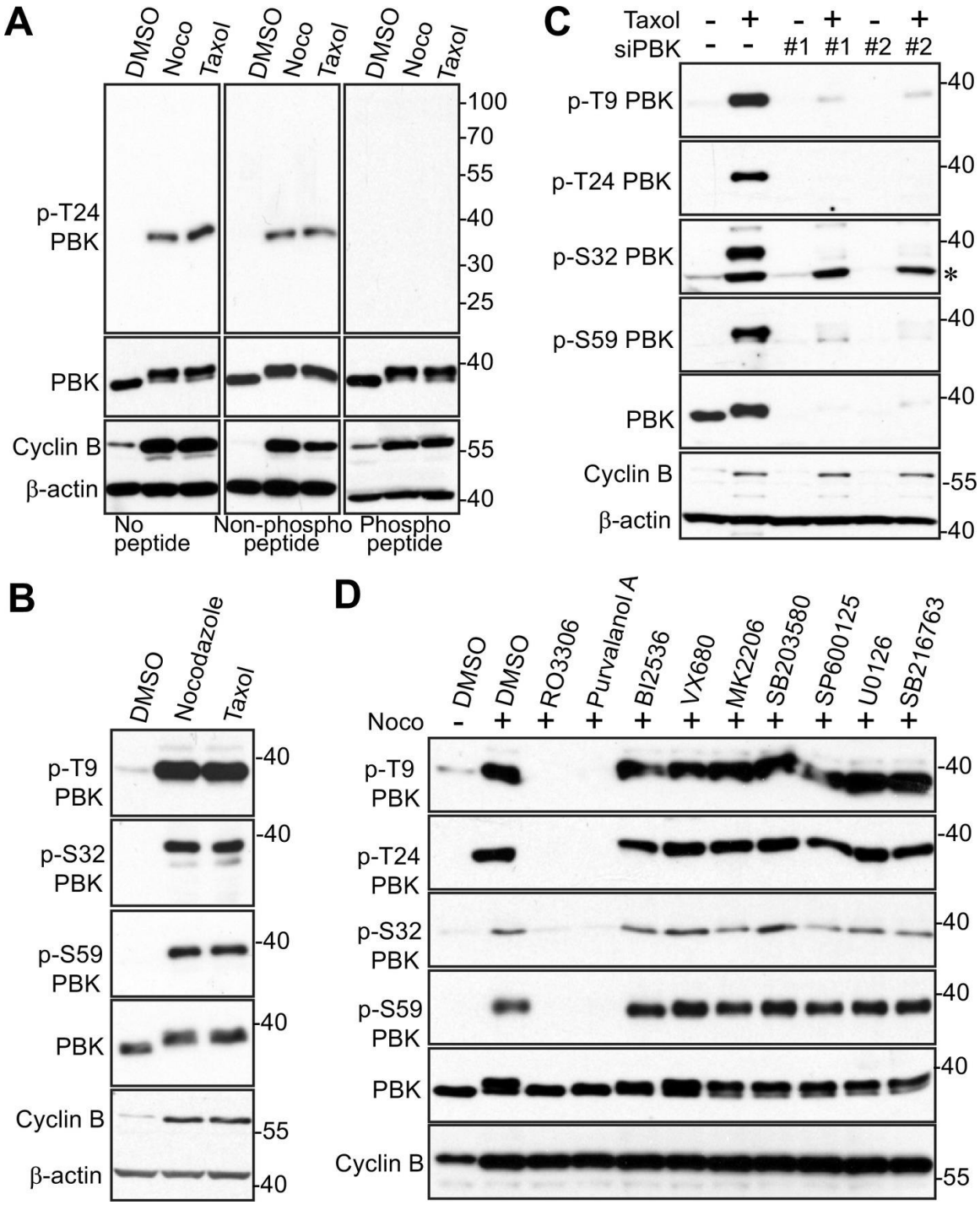
A
DMSO
Noco
Taxol
p-T24 PBK
PBK
Cyclin B
β-actin
100
70
55
40
30
25
No peptide
Non-phospho peptide
Phospho peptide
B
Nocodazole
p-T9 PBK
p-S32 PBK
p-S59 PBK
C
Taxol
siPBK
#1
#2
*
D
Noco
RO3306
Purvalanol A
BI2536
VX680
MK2206
SB203580
SP600125
U0126
SB216763

Figure 2-3. CDK1 Phosphorylates PBK in Cells

(A) HeLa cells were treated with nocodazole or taxol for 16 h. The T24 phospho-antibody was incubated for 16 h at 4 °C with either PBS (no peptide), peptide, or phospo-peptide used for immunizing rabbits, before Western blotting. (B) HeLa cells were treated with nocodazole or taxol for 16 h before Western blotting was performed with the indicated antibodies. (C) HeLa cells were transfected with scrambled siRNA (control) or siRNA against PBK for 48 h and were further treated with (+) or without (−) taxol for 16 h. The total cell lysates were subjected to Western blotting with the indicated antibodies. * marks a non-specific band. (D) HeLa cells were nocodazole together with or without various kinase inhibitors as indicated. Inhibitors were added with MG132 (to halt cyclin B degradation and prevent mitotic exit) for 1.5 h before harvesting the cells. Total cell lysates were subjected to Western blotting with the indicated antibodies.

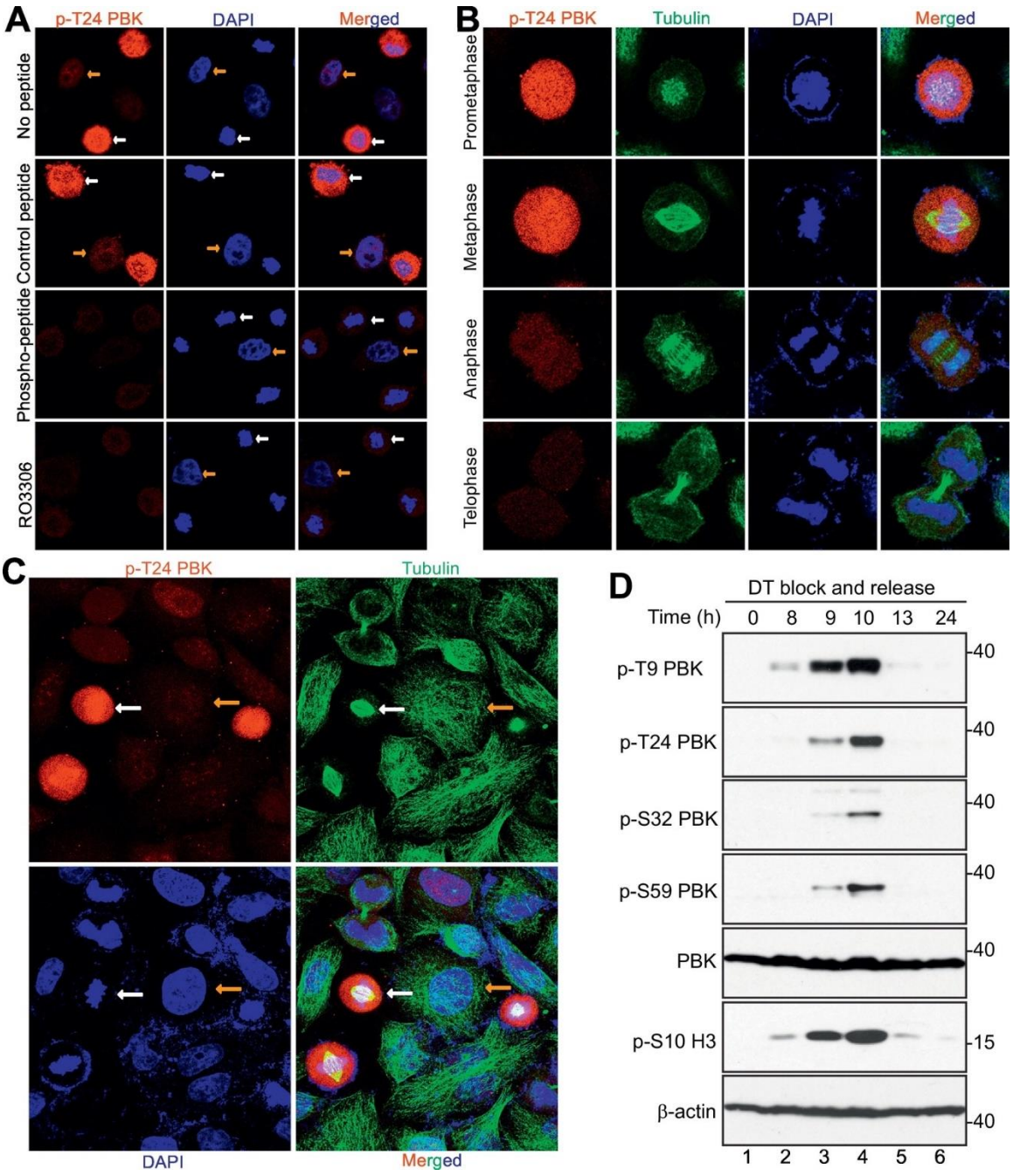
A
p-T24 PBK
DAPI
Merged
No peptide
Control peptide
Phospho-peptide
RO3306
B
p-T24 PBK
Tubulin
DAPI
Merged
Prometaphase
Metaphase
Anaphase
Telophase
C
p-T24 PBK
Tubulin
DAPI
Merged
D
DT block and release
Time (h) 0 8 9 10 13 24
p-T9 PBK
p-T24 PBK
p-S32 PBK
p-S59 PBK
PBK
p-S10 H3
β-actin
40
40
40
40
40
15
40
1 2 3 4 5 6

Figure 2-4. CDK1 Phosphorylates PBK in Normal Mitosis and during Mitotic Arrest

(A) HeLa cells were treated with nocodazole or taxol for 16 h and then fixed. Before the cells were immunostained with the T24 phospho-antibody, the antibody was incubated for 16 h at 4 °C with either PBS (no peptide), peptide, or phospho-peptide. White and yellow arrows mark some of the metaphase cells and the interphase cells, respectively. (B) HeLa cells were synchronized by the double thymidine block and release method. Cells were stained with antibodies against p-PBK T24, β-tubulin, and with DAPI. C, A low power (40 × objective) lens was used to view various phases of the cells in a field from (B). (D) HeLa cells were synchronized by a double thymidine block and release method. Total cell lysates were harvested at the specified time points after release and subjected to Western blotting analysis with the indicated antibodies.

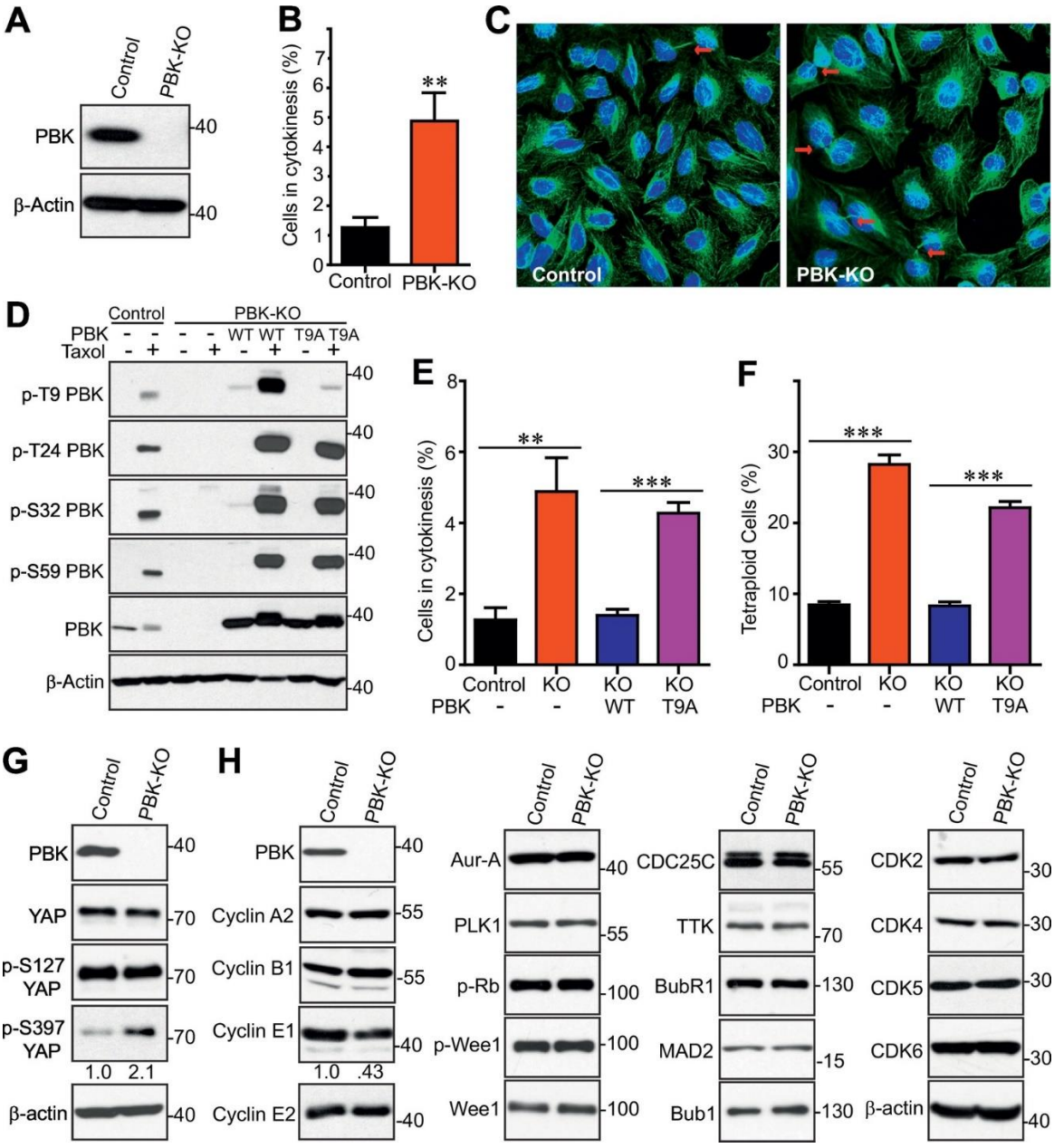
A
Control
PBK-KO
PBK
β-Actin
40
40
B
Cells in cytokinesis (%)
**
Control
PBK-KO
C
Control
PBK-KO
D
Control
PBK-KO
PBK - - - - WT WT T9A T9A
Taxol - + - + - + - +
p-T9 PBK
p-T24 PBK
p-S32 PBK
p-S59 PBK
PBK
β-Actin
E
Cells in cytokinesis (%)
**
***
Control KO KO KO
PBK - - WT T9A
F
Tetraploid Cells (%)
***
***
Control KO KO KO
PBK - - WT T9A
G
Control
PBK-KO
PBK
YAP
p-S127 YAP
p-S397 YAP
1.0 2.1
β-actin
H
Control
PBK-KO
PBK
Cyclin A2
Cyclin B1
Cyclin E1
1.0 .43
Cyclin E2
Aur-A
PLK1
p-Rb
p-Wee1
Wee1
CDC25C
TTK
BubR1
MAD2
Bub1
CDK2
CDK4
CDK5
CDK6
β-actin

Figure 2-5. Generation and Characterization of PBK Knockout (KO) U2OS Cell Line

(A) Western blot of parental and PBK knockout U2OS cell lines. Equal amount of U2OS control and PBK knockout cell lysates were probed with anti-PBK antibody. (B) U2OS control and PBK knockout cells were used to quantify the percentage of cells in cytokinesis. (C) Immunofluorescence confocal images showing the difference in the amount of cytokinesis between the U2OS control and PBK knockout cell lines. β-Tubulin is shown in green and nuclei is stained with DAPI (blue). The arrows point to cytokinetic bridges. (D) U2OS KO cells were stably transduced with vector, PBK, or PBK-T9A. Total cell lysates from U2OS cell lines which were treated with taxol and probed with the indicated antibodies. (E) The indicated U2OS cell lines were used to quantify the percentage of cells in cytokinesis as in (B). (F) The specified U2OS cell lines were labeled with PI and flow cytometry analysis was performed to determine the percentage of tetra-ploidy cells in the whole population. (G) U2OS control and PBK knockout cell whole lysates were probed with the indicated YAP antibodies. Numbers below the p-S397 YAP blot indicate the quantification of relative band intensity from three independent experiments. (H) U2OS control and PBK knockout cell whole lysates were probed with the indicated cell cycle-related antibodies. Numbers below the Cyclin E1 blot indicate the quantification of relative band intensity from three independent experiments. **: $p < 0.01$; ***: $p < 0.001$ (t-test).

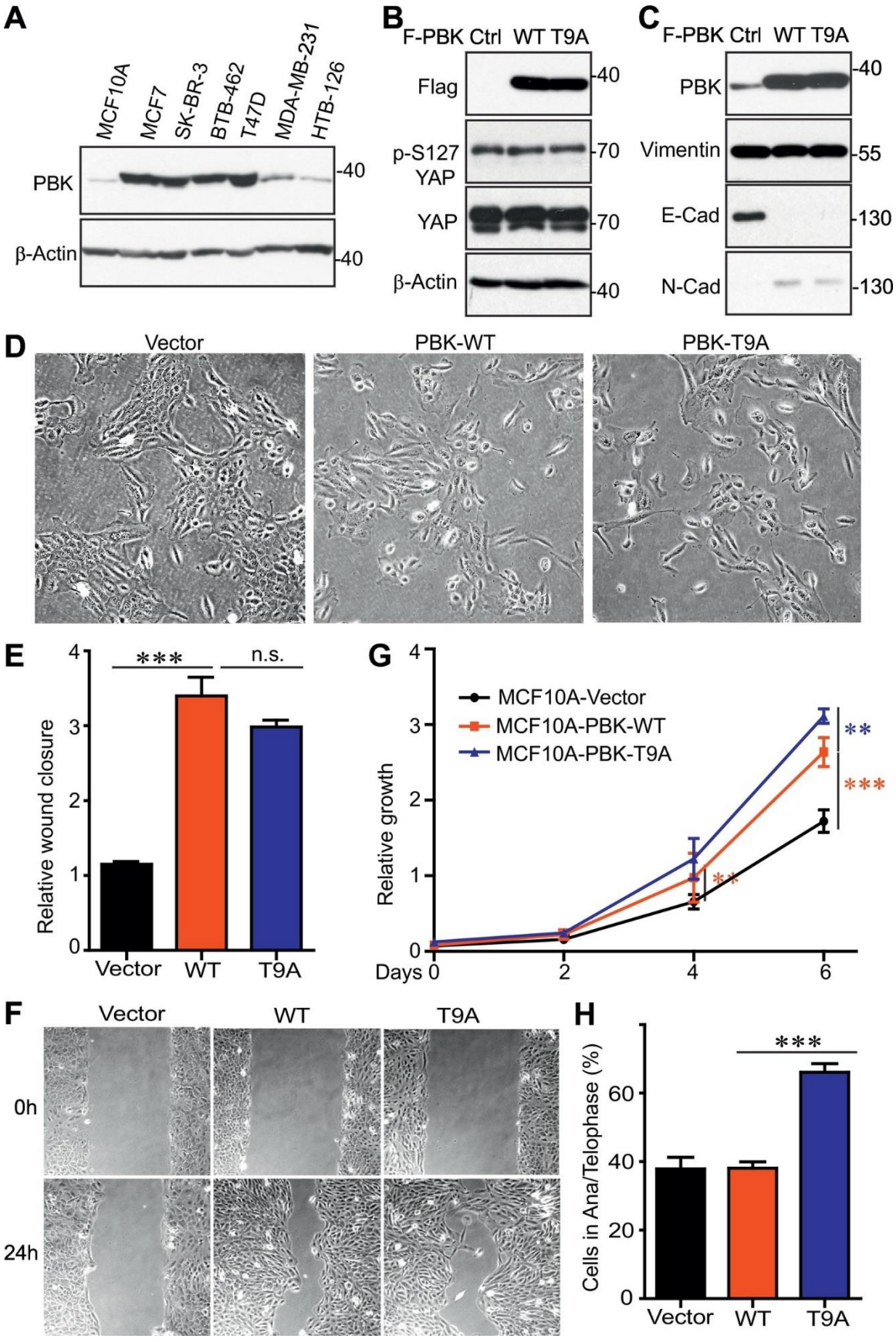
A
MCF10A
MCF7
SK-BR-3
BTB-462
T47D
MDA-MB-231
HTB-126
PBK
β-Actin
40
40
B
F-PBK Ctrl WT T9A
Flag
p-S127 YAP
YAP
β-Actin
40
70
70
40
C
F-PBK Ctrl WT T9A
PBK
Vimentin
E-Cad
N-Cad
40
55
130
130
D
Vector
PBK-WT
PBK-T9A
E
***
n.s.
Relative wound closure
Vector
WT
T9A
G
MCF10A-Vector
MCF10A-PBK-WT
MCF10A-PBK-T9A
Relative growth
Days 0
2
4
6
**
**
***
F
Vector
WT
T9A
0h
24h
H
***
Cells in Ana/Telophase (%)
Vector
WT
T9A

Figure 2-6. Overexpression of PBK Elicits EMT in Normal Cells

(A) PBK protein expression in various normal and breast cancer cell lines. (B) MCF10A (an immortalized breast epithelial cell line) cells transduced with vector control, PBK, or PBK-T9A and probed with the indicated YAP antibodies. (C) MCF10A cells transduced with vector control, PBK, or PBK-T9A and probed with the indicated EMT marker antibodies. (D) 10× microscope images displaying the morphology differences between MCF10A vector control, PBK, and PBK-T9A. (E, F) Cell migration (wound healing) assays with cell lines established in (B). (G) Cell proliferation assays with cell lines established in (B). (H) The cell lines established in (B) were used to quantify the percentage of cells in anaphase/telophase. **: $p < 0.01$; ***: $p < 0.001$ (t-test).

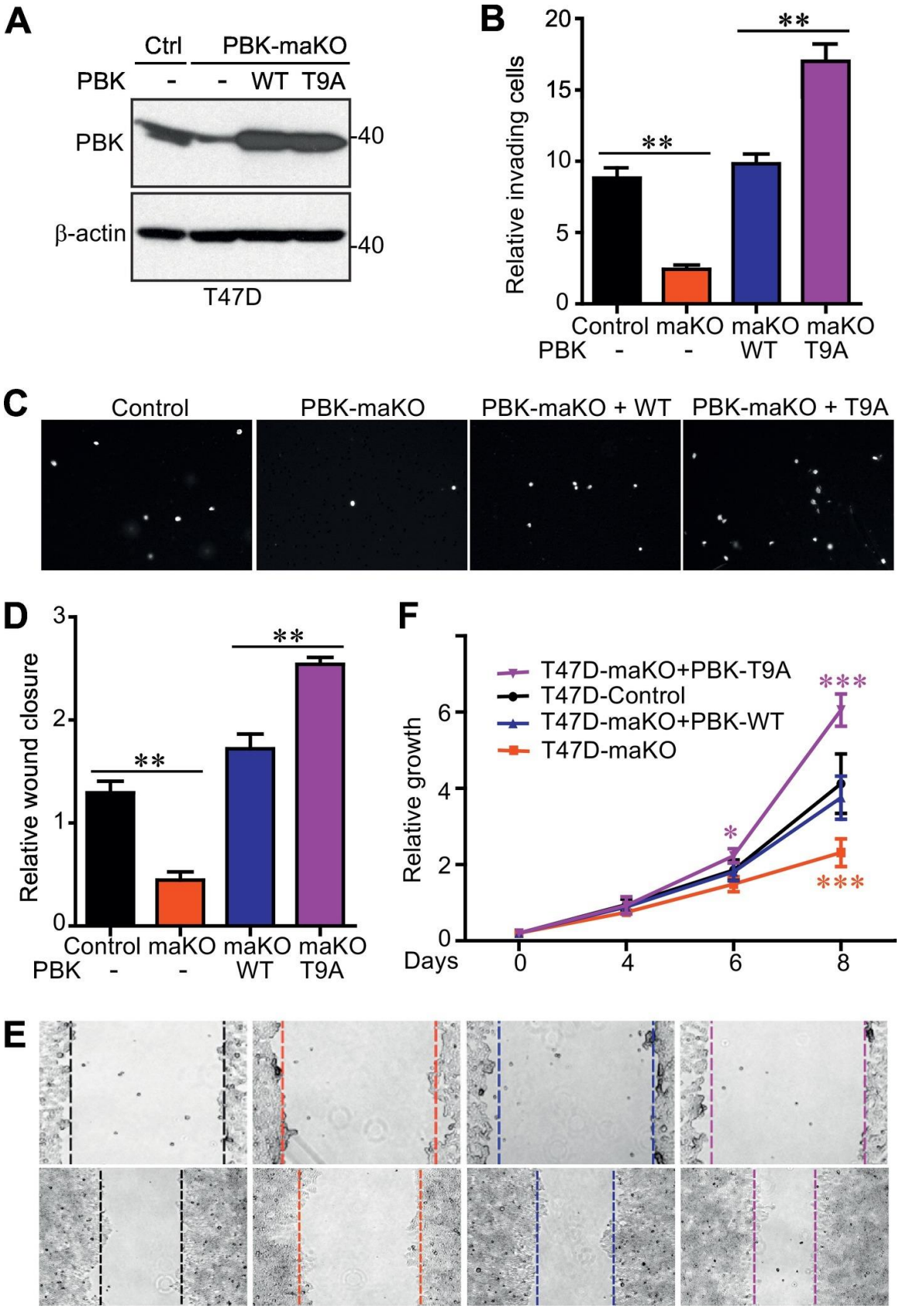
A
Ctrl
PBK-maKO
PBK - - WT T9A
PBK
β-actin
40
40
T47D
B
Relative invading cells
20
15
10
5
0
**
**
Control maKO maKO maKO
PBK - - WT T9A
C
Control
PBK-maKO
PBK-maKO + WT
PBK-maKO + T9A
D
Relative wound closure
3
2
1
0
**
**
Control maKO maKO maKO
PBK - - WT T9A
F
Relative growth
T47D-maKO+PBK-T9A
T47D-Control
T47D-maKO+PBK-WT
T47D-maKO
***
*
***
6
4
2
0
Days
0
4
6
8
E

Figure 2-7. Mitotic Phosphorylation of PBK Inhibits Its Oncogenic Activity in Cells

(A) Western blot of PBK mono-allelic knockout T47D cell line and transduced PBK and PBK-T9A cell lines. (B, C) Invasion assays with cell lines established in (A). (D, E) Cell migration (wound healing) assays with cell lines established in (A). (F) Cell proliferation assays with cell lines established in (A). *: $p < 0.05$; **: $p < 0.01$; ***: $p < 0.001$ (t-test).

Table 1.

PBK-A-Fwd	caccGAGGCCGGGATATTTATAGT
PBK-A-Rev	aaacACTATAAATATCCCGGCCTC
PBK-B-Fwd	caccGCAGAAGCTTGGCTTTGGTAC
PBK-B-Rev	aaacGTACCAAAGCCAAGCTTCTGC

Chapter 3

CYCLIN-DEPENDENT KINASE 1-MEDIATED AMPK PHOSPHORYLATION REGULATES MITOTIC PROGRESSION AND LINKS TO ANTITUBULIN CYTOTOXICITY

ABSTRACT

AMP-activated protein kinase (AMPK), a heterotrimeric serine/threonine kinase and cellular metabolic sensor, has been found to regulate cell cycle checkpoints in cancer cells in response to energetic stress to harmonize proliferation with energy availability. Despite AMPK's emergent association with the cell cycle, it still has not been fully delineated how AMPK is regulated by upstream signaling pathways during mitosis. We report, for the first time, direct CDK1 phosphorylation of both the catalytic α1 and α2 subunits as well as the β1 regulatory subunit of AMPK in mitosis. We found that AMPK-knockout U2OS osteosarcoma cells have reduced mitotic indexes and that CDK1 phosphorylation-null AMPK is unable to rescue the phenotype, demonstrating a role for CDK1 regulation of mitotic entry through AMPK. Our results also denote a vital role for AMPK in promoting proper chromosomal alignment, as loss of AMPK activity leads to misaligned chromosomes and concomitant metaphase delay. Importantly, AMPK expression and activity was found to be critical for paclitaxel chemosensitivity in breast cancer cells and positively correlated with relapse-free survival in systemically treated breast cancer patients.

3.1. INTRODUCTION

Mitosis is a dynamic and vitally important process for separating identical copies of genomic material into two daughter cells. It is thought that failure in the mitotic processes can lead to tumor initiation [92-94]. One of the hallmarks of cancer is mitotic defects, frequently seen as flaws in chromosomal adhesion, spindle attachment, chromosomal segregation, cytokinesis, and centrosomal duplication [95-97]. Another important path to cellular transformation is a change in the fidelity of mitotic checkpoints. Mutations or aberrations in the regulation of cell cycle checkpoints often result in what is known as mitotic cell death (MCD) [98] or lead to cancer [99, 100], indicating the importance of these checkpoints.

Dramatic changes to major organelles and cellular organization happen swiftly during this relatively short period of the cell cycle. This window is considered the most vulnerable period of the cell cycle and, subsequently, has become the target of multiple anticancer drugs. Many aim to activate the spindle assembly checkpoint (SAC) or to target components of the anaphase-promoting complex (APC), leading to prolonged mitotic arrest, and eventual activation of pathways promoting MCD [101]. Thus, identifying additional molecular regulation in mitosis may lead to the identification of potentially druggable targets and development of novel chemotherapeutics for combatting cancer.

AMPK is a heterotrimeric serine/threonine kinase consisting of a catalytic α subunit and two regulatory β and γ subunits. Known to be phosphorylated by kinases LKB1 and CAMKK, AMPK regulates cellular energy homeostasis and harmonizes proliferation with energy availability. Additionally, proliferation is adjusted through metabolic signals which have been shown previously to be coupled to cell cycle progression [102]. Of importance, AMPK has been found to sit in the center of a signaling network involving bona fide tumor suppressors [103] and found to be associated with cell cycle checkpoints, as AMPK-null

Drosophila cells have mitotic defects [104]. AMPK has also been found to be activated during mitosis with increased p-T172 phosphorylation seen during mitosis [105-110]. Likewise, a screen of AMPK substrates revealed multiple downstream mitotic proteins as targets of its kinase activity [111]. A chemical genetic screen of downstream AMPK substrates in human cells identified several which were involved in mitosis including protein phosphatase 1 regulatory subunit 12A and 12C (PPP1R12A/2C), cell division cycle protein 27 (CDC27), and p21-activated protein kinase (PAK2) [111]. AMPK phosphorylation of PPP1R12C blocks its inhibition of myosin regulatory light chain (MRLC) which is a regulator of cytokinesis [112], CDC27 is a member of the APC connecting AMPK to the spindle checkpoint during metaphase [113], and AMPK activation of PAK2 leads to phosphorylation of MRLC and mitotic progression [114]. MRLC has also been shown to be phosphorylated directly by AMPK at its regulatory site *in vitro* and in vivo, both in Drosophila and mammals [115]. AMPK has been connected to mitosis in other studies as well. AMPK-null Drosophila embryos display severe abnormalities in cytoskeletal apical-basal polarity as well as defective mitotic divisions which lead to polyploidy [104]. Loss of AMPK activity, through either inhibition of AMPK in cancer cells [116] or with full AMPK knockout (KO) in mouse embryonic fibroblasts (MEFs) [117], is enough to weaken the cell cycle arrest at G_2/M caused by ionizing radiation. AMPK is also active in the mitotic regulation of neural stem cells. Abolishing normal AMPK activity in the developing mouse brain leads to flawed mitosis in neural progenitor cells and abnormal brain development [118]. Recently, it has been discovered that AMPK and its ortholog Snf1 in S. cerevisiae are required for proper metaphase spindle alignment [106, 119]. Together, these studies point to a role for AMPK outside of its canonical signaling network, acting as a master regulator not only of cellular metabolism, but also cell cycle progression. Despite AMPK's connection to mitosis, how AMPK is regulated during mitotic progression remains unclear. In this report, we identify a novel layer of regulation involving CDK1-mediated phosphorylation for AMPK.

3.2. MATERIALS AND METHODS

3.2.1. Cell Culture and Transfection

HEK293T, HeLa, U2OS, MCF7, and SKBR3 cell lines were purchased from American Type Culture Collection (ATCC) and cultured as ATCC instructed. The cell lines were authenticated at ATCC and were used at low (< 25) passages. Attractene (Qiagen) was used for transient overexpression of proteins in HEK293T cells following the manufacturer's instructions. Lentivirus packaging, infection, and subsequent selection were done as we have described previously [120]. Nocodazole (100 ng/mL for 16 h) and taxol (100 nM for 16 h) (Selleck Chemicals) were used to arrest cells in mitosis unless otherwise indicated. Kinase inhibitors were purchased from Selleck Chemicals (VX680, BI2536, Purvalanol A, SP600125, SB216736, and MK-2206), ENZO life Sciences (RO3306), or LC Laboratory (U0126 and SB203580). All other chemicals were from either from Sigma or Thermo Fisher.

3.2.2. Expression Constructs

Human pcDNA3-HA-AMPKα1-WT and Myc-AMPKγ1-WT constructs were a gift from Dr. Ken Inoki [121]. Human pECE-HA-AMPKβ1-WT and pECE-HA-AMPKα2-WT were gifts from Anne Brunet (Addgene plasmid # 31666 and 31654) [111]. pLKO.1-H2B-RFP was a gift from Elaine Fuchs (Addgene plasmid # 26001) [122]. Point mutations were generated by the QuikChange Site-directed PCR mutagenesis kit (Stratagene) and verified by sequencing. Retroviral expression constructs were made by cloning full-length AMPKβ1 or AMPKα2 cDNA into MaRX^{TM}IV [34]. Lentiviral expression constructs were generated by cloning full length AMPKα2 cDNAs into pSIN4-Flag-IRES-Puro or AMPKα1 into pSIN4-Flag-IRES-Neo [123].

3.2.3. EGFP-Expressing All-In-One CRISPR Construct

To construct the all-in-one CRISPR/Cas9n plasmid targeting AMPKβ1, the sense and anti-sense oligonucleotides from Table 1A were synthesized, annealed, and Golden Gate assembled into the pX330A_D10A-1x2-EGFP and pX330S-2 vectors as described previously [123]. After the two vectors were generated, a final Golden Gate assembly was performed to generate the all-in-one vector as described previously [76]. The resulting pX330A_D10A-1x2-EGFP-PRKAB1-AB construct was transfected into cells and GFP-positive clones were selected by flow cytometry-based cell sorting.

To construct the all-in-one CRISPR/Cas9n plasmid targeting both AMPKα1 and α2, the sense and anti-sense oligonucleotides from Table 1B were synthesized, annealed, and Golden Gate assembled into the pX330A_D10A-1x2-EGFP, pX330S-2, pX330S-3, and pX330S-4. After the four vectors were generated, a final Golden Gate assembly was performed to generate the all-in-one vector. The resulting pX330A_D10A-1x2-EGFP-PRKAA1/2-ABCD construct was transfected into cells and GFP-positive clones were selected by flow cytometry-based cell sorting.

3.2.4. Recombinant Protein Purification and *In Vitro* Kinase Assay

GST-tagged AMPKα2-WT and 2A, as well as GST-tagged AMPKβ1-WT, T19A, S40A, and 2A were cloned in pGEX-5X-1. Proteins were bacterially expressed and purified on GSTrap FF affinity columns (GE Healthcare) following the manufacturer's instructions. GST-AMPKα2 or GST-AMPKβ1 (0.5–1 μg) was incubated with 10 U recombinant CDK1/cyclin B complex (New England Biolabs) or 100 ng CDK1/cyclin B (SignalChem) in kinase buffer (New England Biolabs) in the presence of 5 μCi γ-^{32}P-ATP (3000

Ci/mmol, PerkinElmer). PLK1 kinase was also obtained from SignalChem. Phosphorylation was visualized by autoradiography (^{32}P incorporation) followed by Western blotting or detected by phospho-specific antibodies.

3.2.5. Antibodies

Rabbit polyclonal antibody against p-T485/T490 AMPKα1/2 was a gift from Dr. Ken Inoki [124]. AMPKα1, AMPKα2, AMPKβ1, AMPKβ2, AMPKγ1, AMPKγ2, AMPKγ3, AMPKα1/α2, p-AMPKα (T172), p-AMPKβ1 (S182), p-AMPKβ1 (S108), p-Aurora A/B/C (T288/T232/T198), CDC25C, p-Histone H3 (S10) Alexa Fluor® 488, and cleaved PARP antibodies were from Cell Signaling Technology. Anti-β-Actin, Cyclin B1 and CDC27 antibodies were from Santa Cruz Biotechnology. Flag, HA, and Myc antibodies were from Sigma. α-Tubulin antibody was from Abcam. γ-Tubulin antibody was from Biolegend. p-AMPKα (S356/S377) and p-AMPKβ1 (T19) phospho-antibodies were generated and purified by AbMart. The phospho-peptides used for immunizing rabbits were PLIAD-pS-PKARC (p-AMPKα S356/S377) and HGGHK-pT-PRRDS (p-AMPKβ1 T19). Matching non-phosphorylated peptides were also synthesized and used for antibody purification and blocking assays.

3.2.6. Immunoprecipitation, Phos-tag™, and Western Blot Analysis

Phos-tag™ was obtained from Wako Pure Chemical Industries, Ltd. (cat#: 304-93521). Phos-tag™ gels were made using 10 μM Phos-tag™ (with 100 μM $MnCl_2$) in 8% SDS-acrylamide gels as described [125]. Immunoprecipitation, western blotting, and lambda phosphatase treatment assays were done as previously described [126].

3.2.7. Immunofluorescence staining and confocal microscopy

Cell fixation, permeabilization, immunofluorescence staining, and confocal microscopy were done as previously described [78].

3.2.8. RNA extraction, construction of RNA libraries, and RNA-Seq

We extracted the RNA using the Direct-zol™ RNA Miniprep Plus Kit (Zymo Research) and evaluated the purity and concentration of the RNA by ultraviolet spectroscopy (NanoDrop). RNA integrity numbers (RIN) were evaluated using the Agilent 2100 Bioanalyzer. RNA sequencing libraries were constructed using 1000 ng of total RNA from each sample and the TruSeqV2 kit from Illumina following manufacturer's protocol. Illumina NextSeq sequencing and NGS data acquisition were conducted at the UNMC Genomics Core Facility. The libraries were subjected to 75 bp paired-end high-output sequencing using a NextSeq500 sequencer to generate approximately 33.3 to 41.6 million reads per sample. Fastq files were generated using the bc12fastq software, version 1.8.4 and provided to the UNMC Bioinformatics Core facility for further analysis. The original fastq format reads were trimmed and filtered using the fqtirm tool (https://ccb.jhu.edu/software/fqtrim) to remove adapters, terminal unknown bases (Ns) and low quality 3' regions (Phred score < 30). The trimmed fastq files were processed by our facility's newly developed standard pipeline utilizing STAR [127] as the aligner and RSEM [128] as the tool for annotation and quantification at both gene and isoform levels. TPM values were used for comparison results (student's t-test) for all the available genes. The Benjamini-Hochberg (BH) adjusted p values [129] were also provided to adjust for multiple testing-caused false discovery rate (FDR) with significant level of adjusted p value of ≤ 0.05.

3.2.9. Live-Cell Imaging

U2OS and lentiviral-transduced U2OS were plated on black 96-well optical bottom plates (Thermo Fisher). Live-cell imaging was performed in a Cellomics Arrayscan VTI HCS Reader with 37 °C, 5% CO_2 incubation using FluroBrite DMEM (Thermo Fisher) supplemented with 4 mM L-glutamine, 10% FBS, 1% Pen/Strep. Cells were monitored for 24 h and pictures were taken every 5 min using an RFP filter. Measurements of cell cycle durations were done using the time-lapse sequences.

3.2.10. Statistical Analysis

Statistical significance was analyzed using a two-tailed, unpaired Student's t-test or using a two-way ANOVA with the Šidák correction for multiple comparisons. A P value of < 0.05 was considered to indicate statistical significance.

3.3. RESULTS

3.3.1. AMPK is Phosphorylated During Antitubulin Drug-Induced G_2/M Arrest

To examine the phosphorylation status of the AMPK subunits, we used PhosTag gel electrophoresis which selectively separates phosphorylated from unphosphorylated proteins through specific binding of phosphate ions (see [29, 30]). The mobility shifts of AMPKα1, α2, and β1 were seen to be increased during G_2/M arrest induced by antimitotic drugs (Figure 3-1A), suggesting that AMPK is phosphorylated during G_2/M arrest. The mobility of AMPKβ2, AMPKγ1, AMPKγ2 and AMPKγ3 were not altered under these conditions (Figure 3-1A). We found that the phosphorylation levels of AMPKα1/α2 at the main T172 activation site and the autophosphorylation site on β1 at S108 were not changed under these conditions, suggesting that the mobility shift of AMPK was not likely due to phosphorylation at T172 or S108 respectively, indicating the possibility of novel post-translational modification sites (Figure 3-1B). Treatment of arrested cells with λ-

phosphatase completely reversed the mobility shift of AMPKα and β1 (Figure 3-1C), indicating that the mobility shifts of AMPK subunits during G_2/M were due to phosphorylation events. In order to determine which upstream kinases could be phosphorylating AMPK, we took cells that were cultured overnight with taxol and then treated for two hours with various kinase inhibitors. Interestingly, only the CDK1 inhibitors RO-3306 and Purvalanol A were able to block the mobility shift for AMPKα (Figure 3-1D) and β1 (Figure 3-1E), signifying that possibly CDK1 is phosphorylating AMPK directly or may be acting further upstream. Taken together, these data strongly suggest that mitotic arrest-induced AMPK phosphorylation is CDK1 dependent.

3.3.2. CDK1 Phosphorylates AMPK *In Vitro*

In vitro kinase assays were performed to determine whether CDK1 can directly phosphorylate AMPKα, with GST-tagged AMPKα as substrate. Lysates of taxol-treated mitotic cells strongly phosphorylated AMPKα, and RO-3306 inhibition of CDK1 significantly reduced phosphorylation of GST-AMPKα (Figure 3-2A). Database analysis revealed multiple sites in AMPK α1, α2, and β1 as mitotic phosphorylation sites from large-scale phosphoproteomic studies [84, 130, 131]. Scanning the amino acid sequences of the AMPK α1 and α2 subunits for CDK1 consensus motifs identified two potential phosphorylated sites: S356 and T490 on α1 and S377 and T485 on α2 which are located in the AMPKα ST-stretch (Figure 3-2B). Cross-species alignment of AMPKα subunits (Figure 3-2B) and of β1 (data not shown) show a conservation of the regions flanking these sites, indicating that, possibly, these phosphorylation sites have functional roles. Interestingly, T490 was recently found to be an inhibitory phosphorylation site regulated by GSK3 that is involved in metabolic flexibility [124]. We next examined whether mutating these sites to alanine would affect CDK1 phosphorylation of AMPKα2 during taxol treatment. AMPKα-mutants S377A and T485A combined (AMPKα2-2A) completely

blocked ^{32}P labeling on AMPKα when compared with wild type (WT) AMPKα (Figure 3-2C). After identifying these sites, we generated a phospho-specific antibody for detecting p-S377 and utilized another for detecting p-T490. As expected, GST-AMPKα2 WT incubated with activated CDK1 displayed high levels of phosphorylation detected with p-S377 and p-T485 antibodies, whereas mutating the two sites to alanine completely abrogated the phospho-signal, confirming the specificity of the phospho-antibodies (Figure 3-2D). We also examined if PLK1 is able to phosphorylate AMPK, as one study described regulation of AMPK by PLK1 at T172 during mitosis [132]. We found that PLK1 fails to phosphorylate either of our mitotic sites and, as expected, both CDK1 and PLK1 were unable to phosphorylate T172 directly (Figure 3-2D). Similarly, *in vitro* kinase assays were performed to determine whether CDK1 can directly phosphorylate AMPKβ1, with GST-tagged AMPKβ1 as substrate. Lysates of mitotically arrested cells robustly phosphorylated AMPKβ1, with RO-3306 inhibition of CDK1 significantly reducing phosphorylation of GST-AMPKβ1 (Figure 3-2E). Next, the phosphorylation sites of T19 and S40 were identified on AMPKβ1 that matched the CDK1 consensus motif and likewise were hits in large-scale phosphoproteomic studies [84, 130, 131]. Interestingly, in line with our observations in Figure 3-1A, indicating that AMPKβ1, but not AMPKβ2, is phosphorylated, both T19 and S40 do not exist in AMPKβ2. *In vitro* kinase assays with activated CDK1/Cyclin B1 complex displayed clear phosphorylation of WT GST-AMPKβ1. Interestingly, the AMPKβ1 T19A and 2A mutations blocked all ^{32}P incorporation at both T19 and S40, possibly indicating lack of T19 phosphorylation precludes S40 phosphorylation, but not vice versa (Figure 3-2F). Next, we generated a phospho-specific antibody towards pT19 and found that both AMPKβ1 WT and S40A were clearly phosphorylated at T19 compared to the T19A and 2A mutants (Figure 3-2G), once again showing that T19A could be considered identical to 2A.

3.3.3. AMPK is Phosphorylated in Cells in a CDK1-Dependent Manner

After confirming AMPK phosphorylation by CDK1 *in vitro*, we next examined this phosphorylation in cells. Immunoprecipitation of endogenous AMPKα2 from HeLa cells treated with nocodazole or with nocodazole plus RO-3306 showed an increase and a loss of S377 phosphorylation respectively (Figure 3-3A). Over expressed Flag-AMPKα2 WT, S377A, and T485A constructs transfected into 293T cells treated with or without nocodazole, when Flag-immunoprecipitated, revealed increased S377 phosphorylation for WT α2 under nocodazole treatment and, unsurprisingly, a complete loss in the S377A mutant. Of note, mutating T485 to alanine does not perturb the phosphorylation at S377 (Figure 3-3B). These data indicate that AMPKα is phosphorylated at S377 in cells during nocodazole-induced G_2/M arrest in a CDK1-dependent manner. Next, to determine if the β1 subunit was also phosphorylated in cells, we performed Flag-immunoprecipitation of WT and T19A mutant AMPKβ1 from nocodazole-arrested cell lysates and probed them using the phospho-specific AMPKβ1 T19 antibody. Indeed, the phosphorylation signal was potently increased for WT AMPKβ1 in cells arrested in mitosis, but completely absent in the T19A mutant (Figure 3-3C). Subsequently, we transfected HA-AMPKα1 WT and 2A into 293T cells and immunoprecipitated HA-AMPKα1 from cells treated with either DMSO, taxol, or nocodazole. The phosphorylation of WT HA-AMPKα1 was found to be increased under taxol and nocodazole arrest, but entirely lost in the 2A mutant (Figure 3-3D). To further confirm this as a CDK1-mediated phosphorylation in cells, we immunoprecipitated HA-AMPKα1 WT and 2A from cells treated with nocodazole or with nocodazole plus RO-3306. We detected an increase of T490 phosphorylation with nocodazole treatment which could be largely abolished with the CDK1 inhibitor, RO3306, as well as a complete block of this phosphorylation in the HA-AMPKα1 2A mutant (Figure 3-3E). AMPK has several autophosphorylation sites [133-135], so we wanted to determine if AMPK mitotic

phosphorylation at S377 was either due to autophosphorylation or if AMPK kinase activity was required via feedback mechanisms for the S377 mitotic phosphorylation to occur. To do this, we transfected WT and kinase-dead (K45R) HA-AMPKα2 in 293T cells, which were treated with or without nocodazole, and then examined the levels of p-S377 (Figure 3-3F). We found there was no difference between the WT and K45R mutant for AMPKα2 S377 mitotic phosphorylation, indicating that this is not an autophosphorylation site and that AMPK kinase activity is not a precondition for S377 mitotic phosphorylation. Next, we wanted to ascertain if any of the mitotic phosphorylations were essential for AMPK subunit molecular interaction. For this, we co-expressed Myc-AMPKγ1 with either WT or 2A HA-AMPKα1 and WT or T19A Flag-AMPKβ1 in 293T cells, then treated with or without nocodazole and co-immunoprecipitated by pulling down HA-AMPKα1. Our results showed that neither of the phospho-null mutations in α1 or β1 had any deleterious effect on subunit interaction (Figure 3-3G). Overall, these data provide a strong argument that CDK1 phosphorylates multiple AMPK subunits in cells during mitosis.

3.3.4. AMPK Regulates Mitotic Progression

After we had ascertained AMPK mitotic phosphorylation is mediated by CDK1, we wanted to explore AMPK's possible role in regulating mitotic processes through gene knockout phenotypic analysis. We generated an AMPKα1/α2 double knockout (AMPKα-KO) and as well as an AMPKβ1 knockout in U2OS cells using a CRISPR-Cas9 approach. In the AMPKα-KO, not only was AMPKα1 and α2 expression completely absent, but also both the AMPKβ subunit protein levels were severely diminished, indicating a need for AMPKα subunits for stability of the other complex members (Figure 3-4A). In the AMPKβ1-KO cell line, aside from AMPKβ1 protein expression being completely lost, AMPKβ2 and AMPKα1/α2 expression remained unchanged (Figure 3-4B). Next, we took U2OS and U2OS AMPKα-KO cells, arrested them at metaphase with nocodazole, and then released

the rounded-up mitotic cells in fresh media. Upon release, we harvested cells at the indicated time points and probed with Cyclin B1, CDC25C, and CDC27 to detect the rate of mitotic exit of each cell line. No noticeable differences were seen in the rates of degradation of Cyclin B1 or dephosphorylation of CDC25C and CDC27 between U2OS AMPKα-KO and controls (Figure 3-4C). Subsequently, by way of fluorescent live-cell imaging, we examined mitotic entry and progression of parental and AMPKα-KO U2OS cells stably expressing RFP-H2B. The parental U2OS cells quickly condensed their chromatin and aligned their chromosomes in a tightly packed metaphase plate within 15 minutes. Anaphase onset occurred 35 minutes after nuclear-envelope break down (NEBD), with chromatin decondensation occurring at 50 minutes post-NEBD (Figure 3-4D upper). AMPKα-KO cells, in contrast, have a marked delay in aligning their chromosomes at metaphase, approximately 115 minutes after NEBD, and a postponement of anaphase onset to 120 minutes post-NEBD (Figure 3-4E lower). Quantification of mitotic phase-lengths revealed that AMPKα-KO cells, fascinatingly, had 77% longer prometaphase to anaphase transitions than controls (Figure 3-4F). Unsurprisingly, AMPKα-KO cells had a significantly longer mitotic length, which concurs with a previous live-cell study using bright field microscopy that specified a significantly increased mitotic length for AMPK siRNA-treated HeLa cells [106]. Of note, similar anaphase to telophase timing in U2OS control and AMPKα-KO reinforces our earlier observation of unhindered mitotic exit in these cells (Figure 3-4D-F). We noticed fewer rounded-up cells in the AMPKα-KO and AMPKβ1-KOs when treated with taxol or nocodazole, so we performed cell cycle analysis using propidium iodide and found that there was no significant difference in the percentages of G_2/M arrested cells between the knockouts and the controls (data not shown). Next we stained U2OS control, AMPKα-KO and AMPKβ1-KOs cells (treated with or without nocodazole for 0, 8, 16, or 24 hours) with fluorescently labeled phospho-Histone H3 (S10) antibody to measure the mitotic index. Surprisingly, the number of mitotic cells in AMPKα-

KO and AMPKβ1-KO U2OS, when treated for 16 or 24 hours with nocodazole, was significantly lower than that of parental U2OS, indicating these cells may not be entering mitosis, but, having completed S-phase, have 4N DNA content (Figure 3-4G).

Pharmacological abrogation of AMPK activity through use of small molecule inhibitors has been used widely for the study of AMPK function [106, 108, 109, 136]. We utilized the Compound C and a newly identified AMPK-specific inhibitor SBI-0206965, which has been demonstrated to have an entirely different set of potential off-target kinases inhibited compared to Compound C [137]. Abrupt inhibition of AMPK in RFP-H2B-expressing U2OS cells was accomplished with treatment with 5 μM SBI-0206965 or 5 μM Compound C, which were then immediately imaged for 24 hours and the timing of each mitotic phase was analyzed. Similar to AMPKα-KO cells, cells in which AMPK activity was inhibited displayed distinctly increased metaphase lengths (Figure 3-5A, B), demonstrating the importance of AMPK kinase activity for timely mitotic progression. From this, we wanted to further investigate why these cells were getting delayed at metaphase. Examination via confocal microscopy of U2OS cells with either genetic or pharmacological nullification of AMPK kinase function revealed that a vast majority of AMPKα-KOs or U2OS cells treated with Compound C fail to properly align their chromosomes during metaphase (Figure 3-5C). Representative images are shown in (Figure 3-5D), displaying unattached and misaligned chromosomes frequently seen as far away from the metaphase plate as the centrosomes. The observed metaphase arrest in cells lacking functioning AMPK could be due to, in part, how chromosomes with kinetochores unattached to the mitotic spindle activate the spindle assembly checkpoint (SAC), which delays anaphase sister-chromatid separation until each chromosome is properly attached to the spindle [138, 139].

3.3.5. AMPK Phosphorylation is Required for Mitotic Progression

The necessity for AMPKα expression for mitotic entry and proper prophase to anaphase progression prompted us to investigate the role of the two mitotic CDK1-mediated phosphorylations of AMPKα, S377 and T490. For this, we generated stable cell lines expressing either AMPKα1 WT or AMPKα1 2A in the AMPKα-KO U2OS cells (Figure 3-6A), with expression of AMPKα1 WT or 2A near the levels found in parental U2OS rescuing the expression of both AMPKβ subunits. Measurement of the mitotic index of U2OS AMPKα-KO cells treated with nocodazole, once again, revealed a concomitant drop in cells arrested in mitosis which lack AMPK expression. This could be fully rescued by the expression of AMPKα1 WT, but only partially by α2-WT or the mitotic phosphorylation-null α1-2A (Figure 3-6B), indicating that AMPKα1 could be the primary mitotic subunit in these cells and that mitotic phosphorylation by CDK1 may be important for proper progression into mitosis. We also created AMPKα2-WT, AMPKα1-K45R (kinase-dead), and AMPKα1-T183A (phospho-activation-null) add-backs to the AMPKα-KO background (Figure 3-6C). Expression of each form of α-subunit were sufficient for recovering the expression of both AMPKβ subunits (Figure 3-6C). Analysis of the mitotic index of the α1-K45R and α1-T183A mutants, showed the same significant decrease in mitotic cells as seen with AMPKα-KO (Figure 3-6D), demonstrating that both AMPK kinase activity and activation at T183 are required for mitotic arrest. AMPKα2-WT expression was only able to partially increase the suppressed phosphorylation of S10 on histone H3 (Figure 3-6D). We next sought to elucidate the roles played by AMPK mitotic phosphorylation, kinase activity, and phospho-activation in mitotic progression by stably expressing RFP-H2B in each AMPKα1 mutant and the AMPKβ1-KO cell lines, following unperturbed mitoses, and determining the timing of mitotic entry to anaphase onset. Interestingly, AMPKα1-WT and α1-T183A could fully rescue the prometaphase delay seen in AMPKα-KO cells (Figure 3-6E). In addition, knocking out AMPKβ1 had no effect on metaphase alignment or the interval from NEBD to anaphase. Contrastingly, α1-K45R could not rescue and AMPKα1-2A could only

partially rescue the prolonged arrest during prometa/metaphase (Figure 3-6E), indicating that AMPK kinase activity is required, and CDK1 mitotic phosphorylation is, at least in part, essential for proper early mitotic progression. Since we saw that the AMPKα-KOs, when treated for 16 hours with nocodazole, were indeed accumulating with 4N DNA content and were pH3 (S10)-negative, we then wanted to confirm whether these cells were endoreduplicating or simply never entering mitosis. To do this, we used fluorescent live-cell microscopy to follow individual cells under the treatment of taxol or nocodazole for 48 hours. Remarkably, 73-81% of AMPKα-KOs persisted in interphase and never arrested in mitosis, which was significantly higher than parental U2OS in which only 48-49% remained in interphase (Figure 3-6F). In contrast, AMPKα1-WT expression partially rescued and cleared more cells to progress into mitosis, so only 49-52% remained unarrested, whereas AMPKα1-2A was more like AMPKα-KO with 68-77% lingering in interphase (Figure 3-6F). These data confirmed that CDK1-mediated phosphorylation of, and the kinase activity by, AMPK is not only important for faithful mitotic entry, but also for proper progression to DNA segregation at anaphase.

3.3.6. AMPK Phosphorylation Regulates Transcription of Genes Involved in Mitosis

To get insight into the downstream signaling of AMPK, we next investigated the transcriptome of U2OS cells by next generation RNA sequencing (RNA-seq). Comparative analysis of parental U2OS (control) vs. AMPKα-KO and control vs. AMPKα1-2A was performed using Ingenuity Pathway Analysis (IPA) to examine canonical pathways similarly altered in each to designate effects due to dysregulation of CDK1 phosphosites. Intriguingly, canonical pathways influencing actin dynamics such as actin cytoskeleton signaling, ILK signaling, and regulation of actin-based motility by Rho were predicted to be significantly activated (Figure 3-7A). Unsurprisingly, the expression of a multitude of genes

involved in promoting cellular movement and migration were increased and several inhibitors of cell movement were diminished in AMPKα-KO and α1-2A cells compared to controls (Figure 3-7B). By examining alterations of downstream gene expression, upstream analysis pinpointed numerous possible upstream regulators. Most of the highest-scoring upstream effectors were analogously modulated between AMPKα-KO and α1-2A compared to controls (Figure 3-7C), indicating that loss of phosphorylation of AMPK by CDK1 is comparable to AMPK knockout for alterations seen in these particular pathways. We previously detected stark reduction of p-Histone H3 (S10) in both the AMPKα-KO and α1-2A cells, which led us to speculate that this was possibly due to either phosphatase dysregulation leading to hyper-dephosphorylation, or perturbation of kinase signaling leading to inadequate phosphorylation of Histone H3. Interestingly, there were eight significantly up- or down-regulated phosphatases found to be changed mutually between the AMPKα-KO and α1-2A cells compared to controls (Figure 3-7D). Furthermore, between the two treatments, the expression levels of ten kinases and two mitosis-associated kinases significantly changed compared to controls (Figure 3-7E).

3.3.7. AMPK Phosphorylation Potentiates Taxol Cytotoxicity

Taxanes and similar compounds rely on the disruption of microtubule dynamics in order to arrest cells in mitosis through activation of the SAC, with the prolonged arrest triggering cell death through a unique antiproliferative process called mitotic catastrophe [140] or through aberrant mitosis and eventual death in G_1 [141]. Because of this method of action, cancer cells must enter mitosis in order to suffer the effects of taxol and eventually succumb to cell death mechanisms. With this in mind, we next had to ascertain if loss of AMPK activity could indeed provide cancer cells with a means to resist cell death by taxol treatment. AMPKα-KO cells, compared to parental U2OS, had distinctly reduced levels of apoptosis revealed by cleaved PARP. Addition of AMPKα1-WT amply rescued and

resensitized the cells, whereas AMPKα1-2A had muted levels of cleaved PARP similar to AMPKα-KO (Figure 3-8A), suggesting that cells lacking AMPKα expression have a proclivity to resist taxol-mediated mitotic cell death. Similar resistance was seen in MCF7 and SKBR3 breast adenocarcinoma cells when treated concomitantly with taxol and SBI-0206965. Both cell types displayed high cleaved PARP protein levels under taxol treatment alone. Yet, when AMPK was inhibited in MCF7 and SKBR3 cells exposed to taxol for 24 hours, substantial reductions in cleaved PARP were seen (Figure 3-8B), evidencing that AMPK activity is necessary for significant levels of apoptosis elicited by taxol mitotic arrest. Both SBI-0206965 and Compound C could significantly reduce the mitotic index of HeLa cells that were treated with taxol compared to taxol treatment alone (Figure 3-8C, D), signifying that the lack of apoptosis in these cells is possibly due to AMPK inhibition blocking mitotic entry and thus protecting cancer cells from mitotic catastrophe and apoptosis triggered by paclitaxel. Survival curves for breast cancer patients who received systemic treatments and who had high AMPKα1 expression displayed significantly higher relapse-free survival (RFS) rates than survival curves for patients who had low AMPKα1 expression [142] (Figure 3-8E). Interestingly, there is no difference in RFS for patients with high or low AMPKα2 or AMPKβ2, but a moderately higher RFS rate in high AMPKβ1-expressing patients (Figure 3-8F-H). These data indicate that higher expression of the mitotically phosphorylated subunits, AMPKα1 and β1, are highly correlated with RFS of breast cancer patients undergoing systemic chemotherapies.

3.4. DISCUSSION

AMPK has previously been reported to have increased phosphorylation levels at the T172 activation site during mitosis [105, 106, 108, 111, 143]. The current study is the first to identify direct phosphorylation sites outside of T172 on the AMPK complex, targeted by a bona fide mitotic kinase. These phosphorylations by CDK1 on the AMPKα1, α2, and

β1 subunits, seen *in vitro* and in cells, adds a novel upstream kinase to the group of known AMPK phospho-regulators. CDK1 phosphorylation of AMPKα1 and α2 at S356/S377 and T490/T485, as well as of β1 at T19, was seen to be highly enriched in cells arrested in mitosis by anti-mitotic drugs, which could be abolished by addition of CDK1-specific inhibitors. The reduced mitotic index in AMPKα-KOs cells when treated with taxol or nocodazole was, interestingly, due to their lack of mitotic entry when individual cells were monitored using live-cell imaging. This could be rescued by reconstitution of α1 WT, but not α1 2A, providing evidence that AMPK activity and CDK1 phosphorylation is important for cellular entry into mitosis. It has been reported that AMPK phosphorylation of GBF1 is required for mitotic entry though regulation of mitotic Golgi fragmentation [108, 109], so it may be through this process or through other, as of yet undiscovered, means by which AMPK phosphorylation by CDK1 promotes mitotic entry.

The IPA analysis of RNA-seq data of AMPKα-KO and α1-2A cells compared to controls revealed multiple pathways, functions, and upstream effectors which are modified by loss of CDK1 phospho-regulation. From this, the predicted activation of mitogen-activated protein kinase 1 (MAPK1) could conceivably be driven through stimulation of actin cytoskeleton signaling [144]. Furthermore, the spleen tyrosine kinase (SYK) and interferon gamma (IFNG) downregulation similarly seen in both knockout and CDK1 phosphorylation-null AMPK cells is of importance due to each gene's role in suppression of tumorigenesis in breast carcinoma [145] and promotion of apoptosis [146], respectively. Stimulation of amphiregulin (AREG) signaling is of note because it promotes cancer growth through interactions with EGF/TGFα receptors [147]. Likewise, high SWI/SNF-related matrix-associated actin-dependent regulator of chromatin 4 (SMARC4) activity has been seen to promote tumor cell proliferation and is associated with poor prognosis in multiple cancers [148, 149] and has been reported to increase expression of CD44 [150], itself a promoter

of resistance to apoptosis and important in breast cancer cell migration [151, 152]. Additionally, overactive tumor protein 73 (TP73) has also been implicated in poor clinical behavior and in promotion of tumorigenesis of breast carcinomas [153]. Interestingly, estrogen receptor 1 (ERSR1) upregulation has been associated with EZH2 downregulation [154], both of which are seen to occur in AMPKα knockout and mitotic phosphorylation-null AMPKα1-2A cells. High estrogen receptor (ER) expression has been associated with increased proliferation and higher grade breast cancer [155]. Androgen receptor (AR) overexpression in triple-negative breast cancers can allow a switch from ER-dependence to AR-dependence which results in resistance to aromatase inhibitor treatments [156]. Further, phosphatases which are increased in late-stage and aggressive triple-negative breast cancers such as ALPL and PTP4A3 have been found to be indicative of poor patient survival and have been discovered as promoters of cancer cell proliferation [157, 158]. Importantly, suppression of DUSP5 expression is correlated with paclitaxel resistance and poor prognosis in basal-like breast cancer [159].

Other studies have shed some light on AMPK's role in mitosis through chemically inhibiting AMPK kinase activity. Compound C, a widely used AMPK inhibitor, has been shown to delay mitotic entry [108, 109], cause spindle misorientation and misattachment of chromosomes through actin bundling, and to increase mitotic length as measured from mitotic rounding to cytokinesis via bright field microscopy [106, 136]. Correspondingly, we found that nullification of AMPK kinase activity by Compound C or a newly described AMPK-specific inhibitor, SBI-0206965 [137], results in significantly delayed progression through mitosis from NEBD to anaphase and is marked by a profound degree of chromosomal misalignment. Our results have also shown that AMPK inhibitors can constrain the killing ability of taxol in breast cancer cells through blocking mitotic entry. This is significant because cells must proceed into mitosis in order for the mechanism of taxol microtubule

stabilization to lead to mitotic arrest and eventual cell death, indicating that in breast cancer patients, use of AMPK inhibitors is contraindicated.

Metformin, the common antidiabetic drug for treating Type 2 diabetes and activator of AMPK, has been shown to cause cell cycle arrest, suppress anchorage-depended growth, and inhibit cell proliferation in breast cancer cell lines [160-162]. Additional studies suggest that metformin may improve the efficacy of breast cancer treatments and regimens as well as selectively target and kill cancer stem cells [105, 163, 164]. Metformin has also been shown to constrain mammary tumor expansion in mice [165]. This fact has led to the dozens of clinical trials exploring the use of metformin as a neoadjuvant, in combinatorial chemotherapies or as a chemoprevention agent [166]. Indeed, several clinical Phase II and Phase III trials have recently been initiated to examine the synergistic effects of treatment with metformin and other drugs used in cytotoxic chemotherapy, such as docetaxel or paclitaxel. These were initiated after meta-analysis of retrospective studies identified the use of metformin with a significant reduction in cancer-related mortality for patients [167, 168]. Our analysis of patient data revealed that breast cancer patients who had high AMPKα1 or AMPKβ1 expression and received systemic treatments displayed significantly higher RFS rates than patients who had low AMPKα1 or AMPKβ1 expression, respectively [142]. This strongly indicates the use of metformin in breast cancer treatment regimens, especially in patients with tumors expressing low levels of the mitotically phosphorylated AMPK subunits, AMPKα1 and β1, in order to improve their survival.

In conclusion, we propose that CDK1 regulates AMPK control of mitotic entry and progression. It remains to be determined which signaling networks or processes CDK1-

phosphorylated AMPK utilizes to drive these events. Thus, future studies will need to examine whether this newly identified CDK1/AMPK axis is involved in Golgi fragmentation, mitotic spindle orientation, or some other currently unassociated mitotic process.

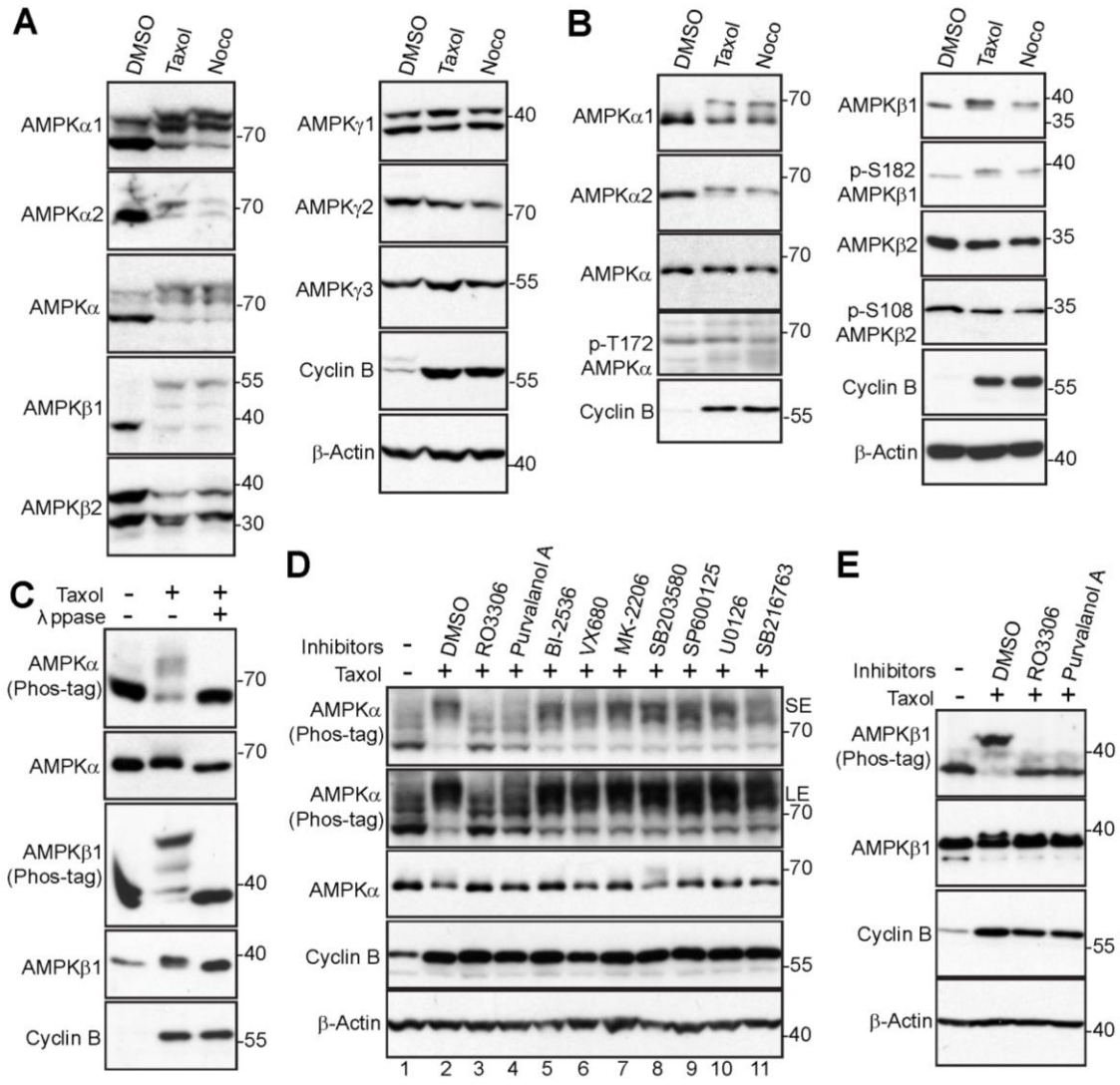
A
DMSO
Taxol
Noco
AMPKα1
AMPKα2
AMPKα
AMPKβ1
AMPKβ2
AMPKγ1
AMPKγ2
AMPKγ3
Cyclin B
β-Actin
B
AMPKα1
AMPKα2
AMPKα
p-T172 AMPKα
Cyclin B
AMPKβ1
p-S182 AMPKβ1
AMPKβ2
p-S108 AMPKβ2
C
Taxol
λ ppase
AMPKα (Phos-tag)
AMPKβ1 (Phos-tag)
D
Inhibitors
Taxol
DMSO
RO3306
Purvalanol A
BI-2536
VX680
MK-2206
SB203580
SP600125
U0126
SB216763
SE
LE
1 2 3 4 5 6 7 8 9 10 11
E
Inhibitors
Taxol
DMSO
RO3306
Purvalanol A

Figure 3-1. Phosphorylation of AMPK Subunits by CDK1 during Mitotic Arrest

(A) HeLa cells were treated with DMSO, taxol (100 nM for 16 h) or nocodazole (100 ng/mL for 16 h). Total cell lysates were probed on Phos-tag™ SDS polyacrylamide gels with the indicated antibodies. (B) Total cell lysates from A were electrophoresed on regular and Phos-tag™ SDS polyacrylamide gels and probed with the indicated antibodies. (C) HeLa cells were treated with taxol as indicated and cell lysates were further treated with (+) or without (−) λ-phosphatase (ppase). Total cell lysates were probed with the indicated antibodies. (D) HeLa cells were treated with taxol, with or without various kinase inhibitors as indicated. RO3306 (5 μM), Purvalanol A (10 μM), BI-2536 (100 nM), VX680 (2 μM), MK-2206 (10 μM), SB203580 (10 μM), SP600125 (20 μM), U0126 (20 μM), and SB216763 (10 μM) were used. Inhibitors were added 1 h before harvesting the cells (with MG132 to prevent Cyclin B degradation and subsequent mitotic exit). Total cell lysates were electrophoresed on regular and Phos-tag™ SDS polyacrylamide gels and probed with the indicated antibodies. (E) HeLa cells were treated with taxol, with or without the CDK1 inhibitors as indicated. RO3306 (5 μM), Purvalanol A (10 μM). Total cell lysates were electrophoresed on regular and Phos-tag™ SDS polyacrylamide gels and probed with the indicated antibodies.

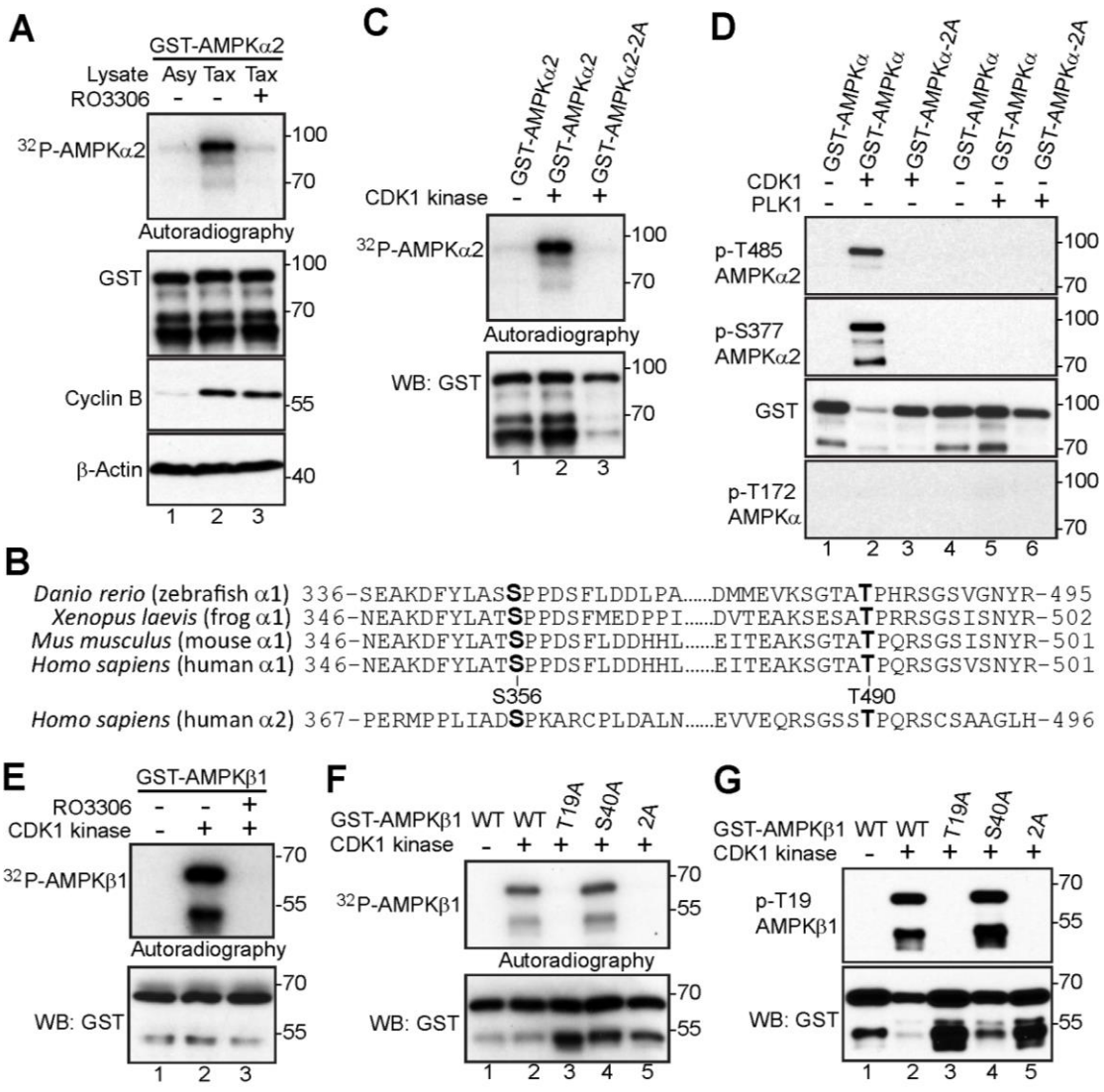
A
GST-AMPKα2
Lysate Asy Tax Tax
RO3306 - - +
32P-AMPKα2
Autoradiography
GST
Cyclin B
β-Actin
100
70
55
40
1 2 3
C
GST-AMPKα2
GST-AMPKα2
GST-AMPKα2-2A
CDK1 kinase - + +
32P-AMPKα2
Autoradiography
WB: GST
100
70
1 2 3
D
GST-AMPKα
GST-AMPKα
GST-AMPKα-2A
GST-AMPKα
GST-AMPKα
GST-AMPKα-2A
CDK1 - + + - - -
PLK1 - - - - + +
p-T485 AMPKα2
p-S377 AMPKα2
GST
p-T172 AMPKα
100
70
1 2 3 4 5 6
B
Danio rerio (zebrafish α1) 336-SEAKDFYLASSPPDSFLDDLPA.....DMMEVKSGTATPHRSGSVGNYR-495
Xenopus laevis (frog α1) 346-NEAKDFYLATSPPDSFMEDPPI.....DVTEAKSESATPRRSGSISNYR-502
Mus musculus (mouse α1) 346-NEAKDFYLATSPPDSFLDDHHL.....EITEAKSGTATPQRSGSISNYR-501
Homo sapiens (human α1) 346-NEAKDFYLATSPPDSFLDDHHL.....EITEAKSGTATPQRSGSVSNYR-501
S356
T490
Homo sapiens (human α2) 367-PERMPPLIADSPKARCPLDALN.....EVVEQRSGSSTPQRSCSAAGLH-496
E
GST-AMPKβ1
RO3306 - - +
CDK1 kinase - + +
32P-AMPKβ1
Autoradiography
WB: GST
70
55
1 2 3
F
GST-AMPKβ1 WT WT T19A S40A 2A
CDK1 kinase - + + + +
32P-AMPKβ1
Autoradiography
WB: GST
70
55
1 2 3 4 5
G
GST-AMPKβ1 WT WT T19A S40A 2A
CDK1 kinase - + + + +
p-T19 AMPKβ1
WB: GST
70
55
1 2 3 4 5

Figure 3-2. CDK1 Phosphorylates AMPK Subunits *In Vitro*

(A) *In vitro* ^{32}P kinase assays with lysates of mitotically arrested cells and recombinant GST-AMPKα2. RO3306 (5 μM) was used to inhibit CDK1 kinase activity. (B) Conservation of AMPK's mitotic phosphorylation sites. (C) *In vitro* ^{32}P kinase assays with purified CDK1/Cyclin B1 complex and recombinant GST-AMPKα2 or GST-AMPKα2-2A. (D) *In vitro* kinase assays with purified CDK1/Cyclin B1 complex or activated PLK1 and recombinant GST-AMPKα2 or GST-AMPKα2-2A and probed with phospho-antibodies. (E) *In vitro* ^{32}P kinase assays with purified CDK1/Cyclin B1 complex and recombinant GST-AMPKβ1. RO3306 (5 μM) was used to inhibit CDK1 kinase activity. (F) *In vitro* ^{32}P kinase assays with purified CDK1/Cyclin B1 complex to phosphorylate recombinant GST-AMPKβ1, GST-AMPKβ1-T19A, GST-AMPKβ1-S40A, or GST-AMPKβ1-2A. (G) *In vitro* kinase assays using purified CDK1/Cyclin B1 complex to phosphorylate recombinant GST-AMPKβ1, GST-AMPKβ1-T19A, GST-AMPKβ1-S40A, or GST-AMPKβ1-2A and probed with phospho-antibody.

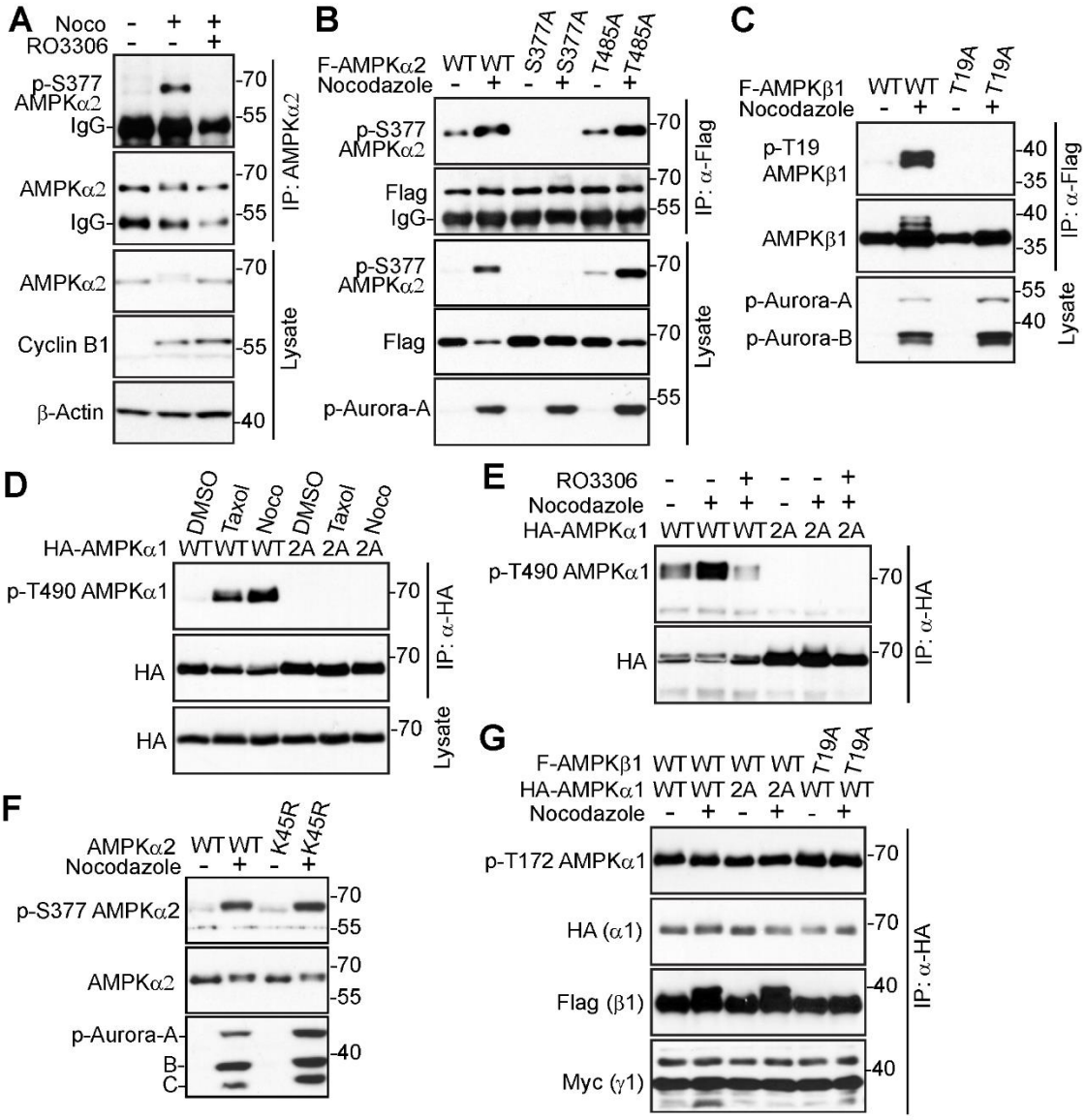
A
Noco - + +
RO3306 - - +
p-S377 AMPKα2
AMPKα2 IgG
AMPKα2
IgG
AMPKα2
Cyclin B1
β-Actin
IP: AMPKα2
Lysate
B
F-AMPKα2 WT WT S377A +S377A T485A +T485A
Nocodazole - + - + - +
p-S377 AMPKα2
Flag IgG
p-S377 AMPKα2
Flag
p-Aurora-A
IP: α-Flag
Lysate
C
F-AMPKβ1 WT WT T19A +T19A
Nocodazole - + - +
p-T19 AMPKβ1
AMPKβ1
p-Aurora-A
p-Aurora-B
IP: α-Flag
Lysate
D
DMSO Taxol Noco DMSO Taxol Noco
HA-AMPKα1 WT WT WT 2A 2A 2A
p-T490 AMPKα1
HA
HA
IP: α-HA
Lysate
E
RO3306 - - + - - +
Nocodazole - + + - + +
HA-AMPKα1 WT WT WT 2A 2A 2A
p-T490 AMPKα1
HA
IP: α-HA
F
AMPKα2 WT WT K45R +K45R
Nocodazole - + - +
p-S377 AMPKα2
AMPKα2
p-Aurora-A
B
C
G
F-AMPKβ1 WT WT WT WT T19A T19A
HA-AMPKα1 WT WT 2A 2A WT WT
Nocodazole - + - + - +
p-T172 AMPKα1
HA (α1)
Flag (β1)
Myc (γ1)
IP: α-HA

Figure 3-3. CDK1 Phosphorylates AMPK Subunits in Cells

(A) Endogenous AMPKα2 immunoprecipitation in HeLa cells treated with nocodazole (16 h) or nocodazole (16 h) with RO3306 (1 h) and probed with p-S377 antibody. (B) HEK293T cells transfected with Flag-AMPKα2-WT, Flag-AMPKα2-S377A, or Flag-AMPKα2-T485A and treated with taxol or nocodazole (16 h). Flag-tagged proteins were immunoprecipitated, then probed with p-S377 antibody. (C) HEK293T cells were transfected with Flag-AMPKβ1-WT or Flag-AMPKβ1-T19A and treated with taxol or nocodazole (16 h). Flag-tagged proteins were immunoprecipitated, then probed with p-T19 antibody. D, HEK293T cells transfected with HA-AMPKα1-WT or HA-AMPKα1-2A and treated with taxol or nocodazole (16 h). HA-tagged proteins were immunoprecipitated, then probed with p-T490 antibody. (E) HEK293T cells transfected with HA-AMPKα1-WT or HA-AMPKα1-2A and treated with nocodazole (16 h) or nocodazole (16 h) with RO3306 (1 h). HA-tagged proteins were immunoprecipitated, then probed with p-T490 antibody. (F) Total lysates of HEK293T cells transfected with Flag-AMPKα2-WT or Flag-AMPKα2-K45R and treated with nocodazole, probed with p-S377. (G) Co-immunoprecipitation of HA-tagged protein in HEK293T cells co-transfected with Myc-AMPKγ1, either HA-AMPKα1-WT or HA-AMPKα1-2A, and Flag-AMPKβ1-WT or Flag-AMPKβ1-T19A in HEK293T cells treated with nocodazole, then probed with the indicated antibodies.

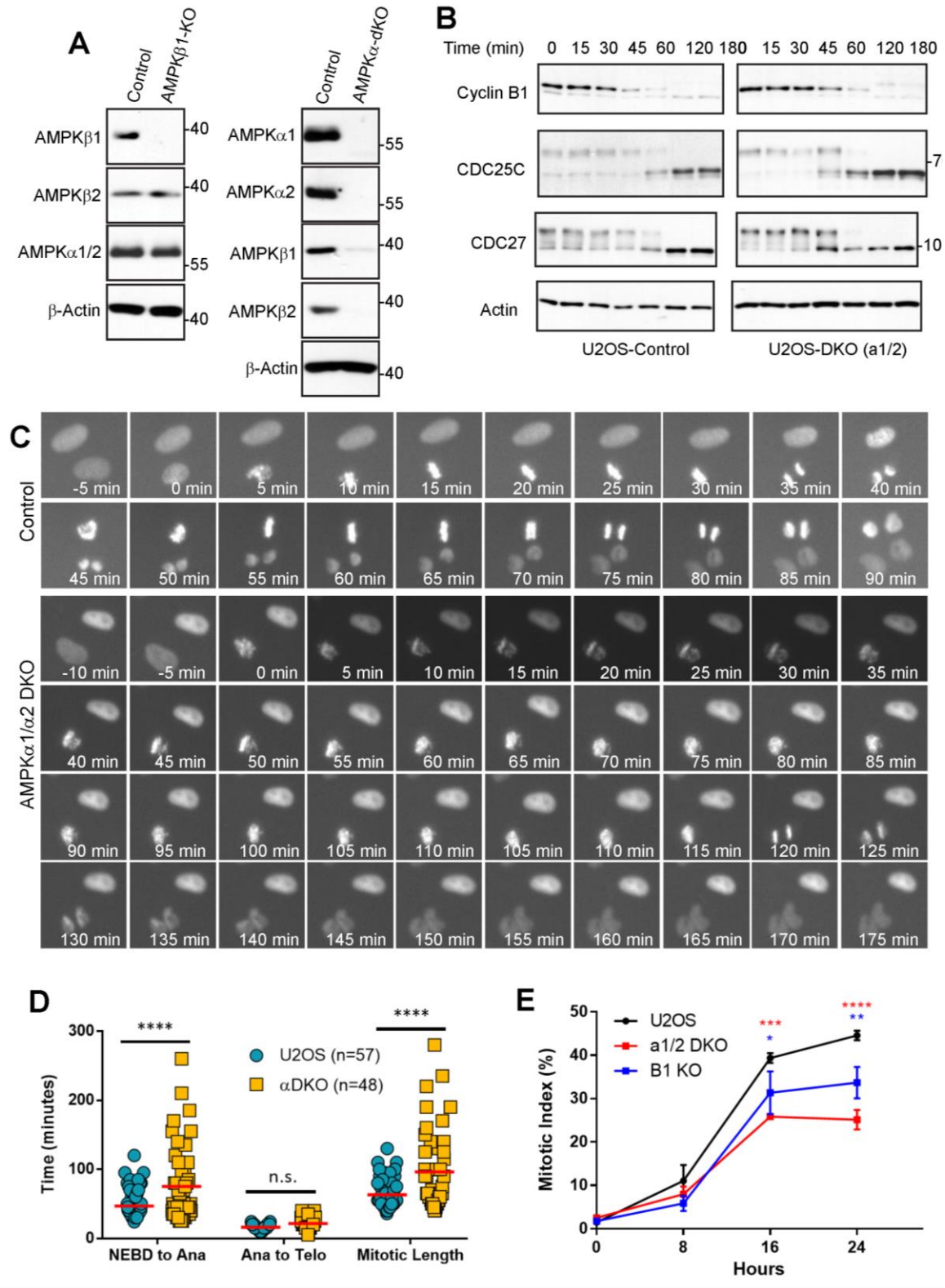
A
Control
AMPKβ1-KO
AMPKβ1
AMPKβ2
AMPKα1/2
β-Actin
40
40
55
40
Control
AMPKα-dKO
AMPKα1
AMPKα2
AMPKβ1
AMPKβ2
β-Actin
55
55
40
40
40
B
Time (min) 0 15 30 45 60 120 180 15 30 45 60 120 180
Cyclin B1
CDC25C
CDC27
Actin
7
10
U2OS-Control
U2OS-DKO (a1/2)
C
Control
AMPKα1/α2 DKO
-5 min
0 min
5 min
10 min
15 min
20 min
25 min
30 min
35 min
40 min
45 min
50 min
55 min
60 min
65 min
70 min
75 min
80 min
85 min
90 min
-10 min
-5 min
0 min
5 min
10 min
15 min
20 min
25 min
30 min
35 min
40 min
45 min
50 min
55 min
60 min
65 min
70 min
75 min
80 min
85 min
90 min
95 min
100 min
105 min
110 min
105 min
110 min
115 min
120 min
125 min
130 min
135 min
140 min
145 min
150 min
155 min
160 min
165 min
170 min
175 min
D
Time (minutes)
300
200
100
0
****
****
n.s.
U2OS (n=57)
αDKO (n=48)
NEBD to Ana
Ana to Telo
Mitotic Length
E
Mitotic Index (%)
50
40
30
20
10
0
U2OS
a1/2 DKO
B1 KO
***
*
****
**
0
8
16
24
Hours

Figure 3-4. AMPK is Required for Normal Mitotic Entry and Progression

(A, B) Western blots of U2OS, U2OS AMPK β1-KO, and U2OS AMPKα-KO (AMPKα1/α2 double KO) cells probed for various AMPK subunits. (C) HeLa cells arrested in mitosis with nocodazole (16 h) which were subsequently washed and released into fresh medium for collection at the specified time points and then probed with the indicated antibodies. (D, E) Live-cell imaging of RFP-H2B expressing U2OS or U2OS AMPKα-KO cells entering and exiting mitosis. (F) Quantification of mitotic phase timing from live-cell data. ***: $p<0.001$ (Two-way ANOVA). N.S.: not significant.

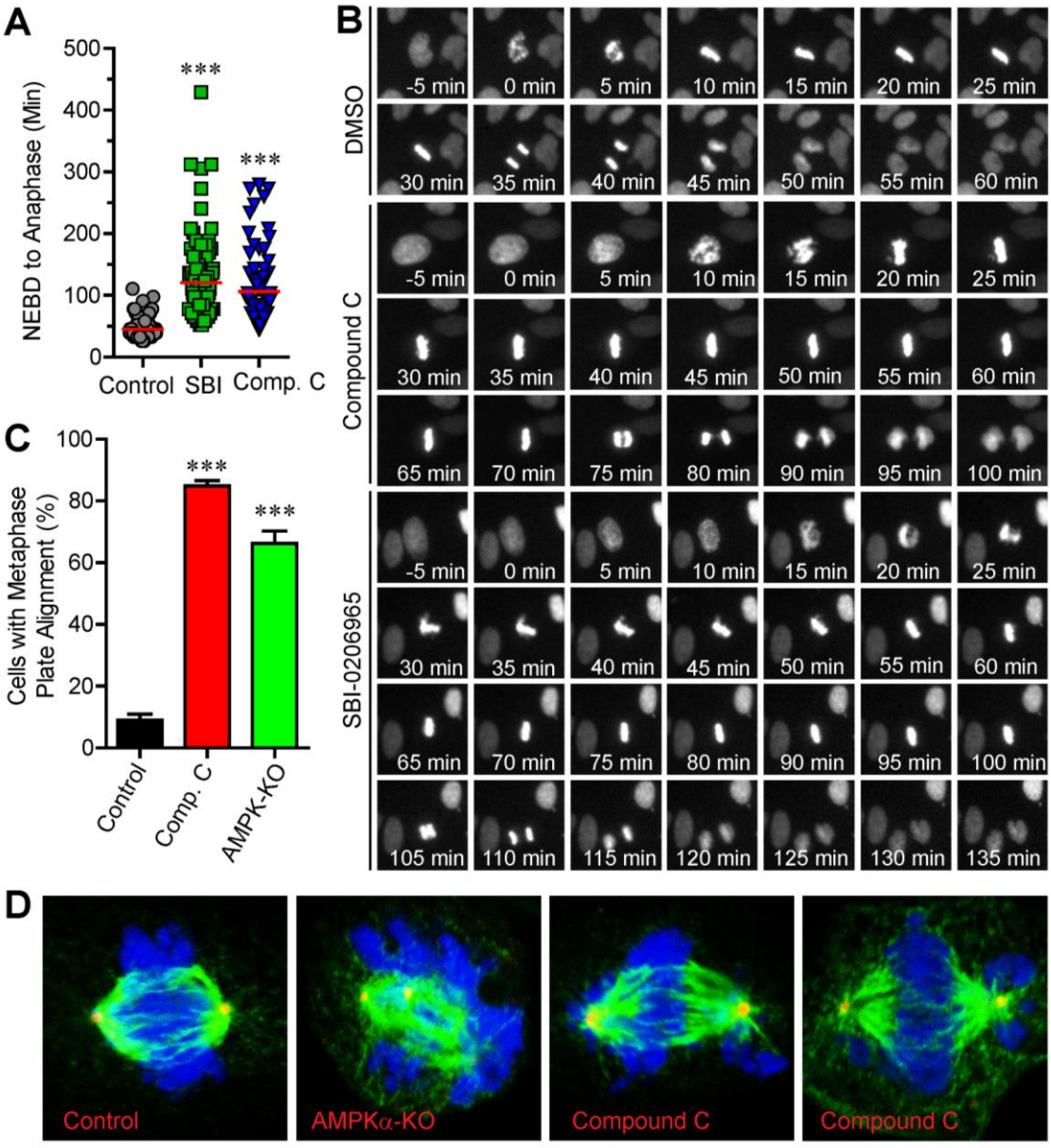
A
NEBD to Anaphase (Min)
500
400
300
200
100
0
***
***
Control
SBI
Comp. C
B
DMSO
Compound C
SBI-0206965
-5 min
0 min
5 min
10 min
15 min
20 min
25 min
30 min
35 min
40 min
45 min
50 min
55 min
60 min
65 min
70 min
75 min
80 min
90 min
95 min
100 min
105 min
110 min
115 min
120 min
125 min
130 min
135 min
C
Cells with Metaphase Plate Alignment (%)
100
80
60
40
20
0
***
***
Control
Comp. C
AMPK-KO
D
Control
AMPKα-KO
Compound C
Compound C

Figure 3-5. Small-Molecule Inhibition of AMPK Kinase Activity Phenocopies AMPK αDKO

(A) Live-cell image quantification of nuclear envelope breakdown (NEBD) to anaphase length in RFP-H2B-expressing U2OS cells treated with 5 μM SBI-0206965 (SBI) or 5 μM Compound C (Comp C) for 24h. ***: $p<0.001$ (t-test). 100 cells were analyzed for each group in 4 separate experiments. (B) Representative live-cell images demonstrating mitotic length of cells quantified in (A). (C) Confocal microscopy of fixed AMPKα-KO U2OS or U2OS cells treated with Comp C were used for quantification of abnormal metaphase plate alignment. ***: $p<0.001$ (t-test). Total cells analyzed: Control=102, Comp. C=103, AMPKα-KO=122 in 4 separate experiments. (D) Representative confocal images of cells analyzed in (C). DAPI is blue, α-tubulin is green, and γ-tubulin is red.

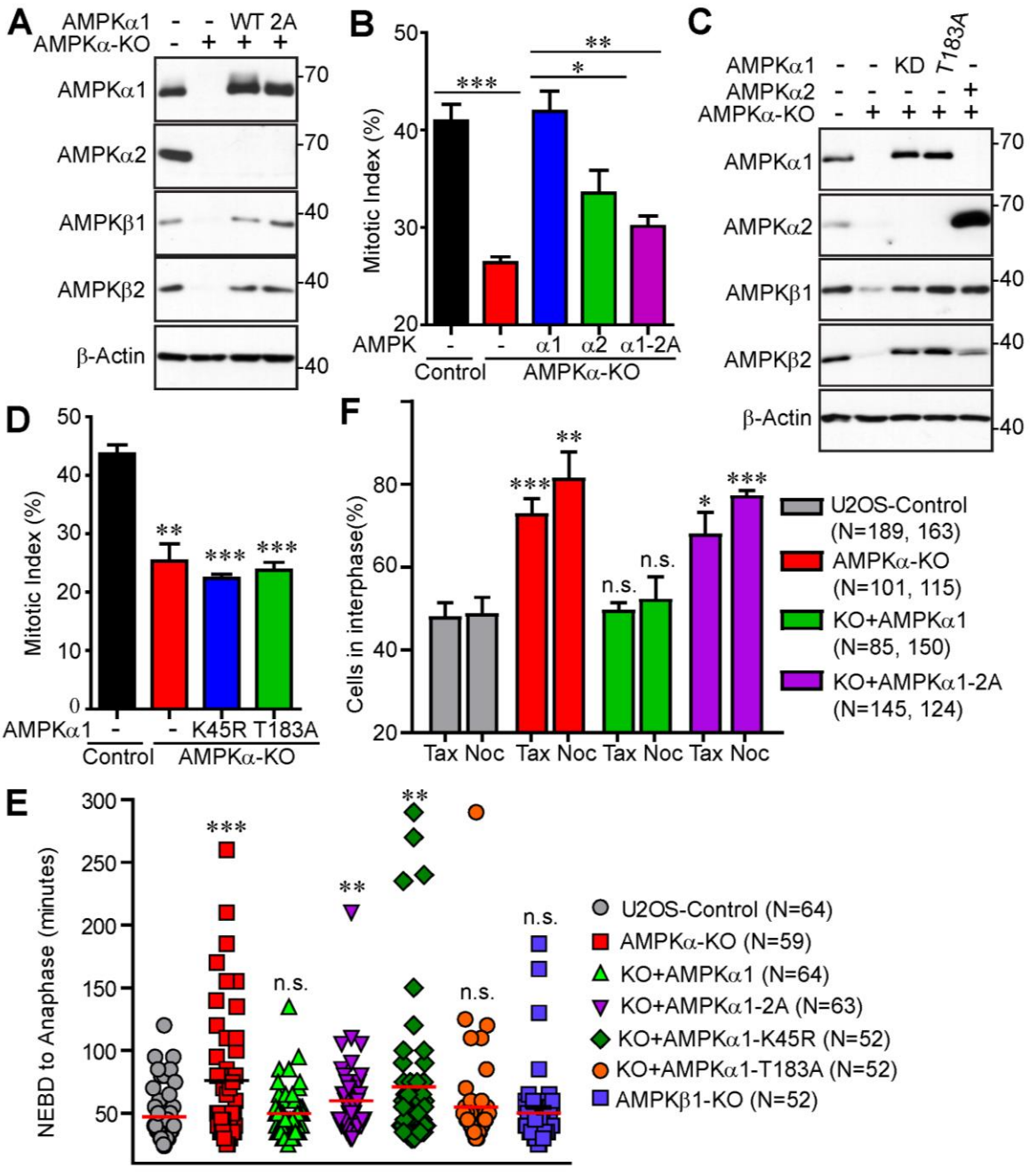
A
AMPKα1 - - WT 2A
AMPKα-KO - + + +
AMPKα1
AMPKα2
AMPKβ1
AMPKβ2
β-Actin
70
70
40
40
40
B
Mitotic Index (%)
50
40
30
20
***
**
*
AMPK - - α1 α2 α1-2A
Control
AMPKα-KO
C
AMPKα1 - - KD T183A -
AMPKα2 - - - - +
AMPKα-KO - + + + +
AMPKα1
AMPKα2
AMPKβ1
AMPKβ2
β-Actin
70
70
40
40
40
D
Mitotic Index (%)
50
40
30
20
10
0
**
***
***
AMPKα1 - - K45R T183A
Control
AMPKα-KO
F
Cells in interphase(%)
80
60
40
20
***
**
n.s.
n.s.
*
***
Tax Noc Tax Noc Tax Noc Tax Noc
U2OS-Control (N=189, 163)
AMPKα-KO (N=101, 115)
KO+AMPKα1 (N=85, 150)
KO+AMPKα1-2A (N=145, 124)
E
NEBD to Anaphase (minutes)
300
250
200
150
100
50
***
n.s.
**
**
n.s.
n.s.
U2OS-Control (N=64)
AMPKα-KO (N=59)
KO+AMPKα1 (N=64)
KO+AMPKα1-2A (N=63)
KO+AMPKα1-K45R (N=52)
KO+AMPKα1-T183A (N=52)
AMPKβ1-KO (N=52)

Figure 3-6. AMPKα1 Re-Expression Can Rescue AMPK αDKO Mitotic Phenotypes

(A) Western blots of U2OS AMPKα-KO cells stably expressing AMPKα1-WT or AMPKα1-2A, probed for various AMPK subunits. (B) Mitotic index of cells treated with nocodazole (16 h). Data were expressed as mean ± SEM from three independent experiments. *: $p<0.05$, **: $p<0.01$, ***: $p<0.001$ (t-test). (C) Western blots of U2OS AMPKα-KO cells stably expressing AMPKα1-K45R, AMPKα1-T183A, or AMPKα2-WT, probed for various AMPK subunits. (D) Mitotic index of cells treated with nocodazole (16 h). Data were expressed as mean ± SEM from three independent experiments. **: $p<0.01$, ***: $p<0.001$ (t-test). (E) Quantification of mitotic phase timing from live-cell imaging of RFP-H2B-expressing cells entering and exiting mitosis for 24 h. **: $p<0.01$, ***: $p<0.001$ (Mann Whitney U-test). N.s.: not significant. (F) Quantification of live-cell imaging of the percentage of cells remaining in interphase when treated with nocodazole for 24 h. *: $p<0.05$, **: $p<0.01$, ***: $p<0.001$ (t-test). Data were shown as mean ± SEM from four separate experiments. N.s.: not significant.

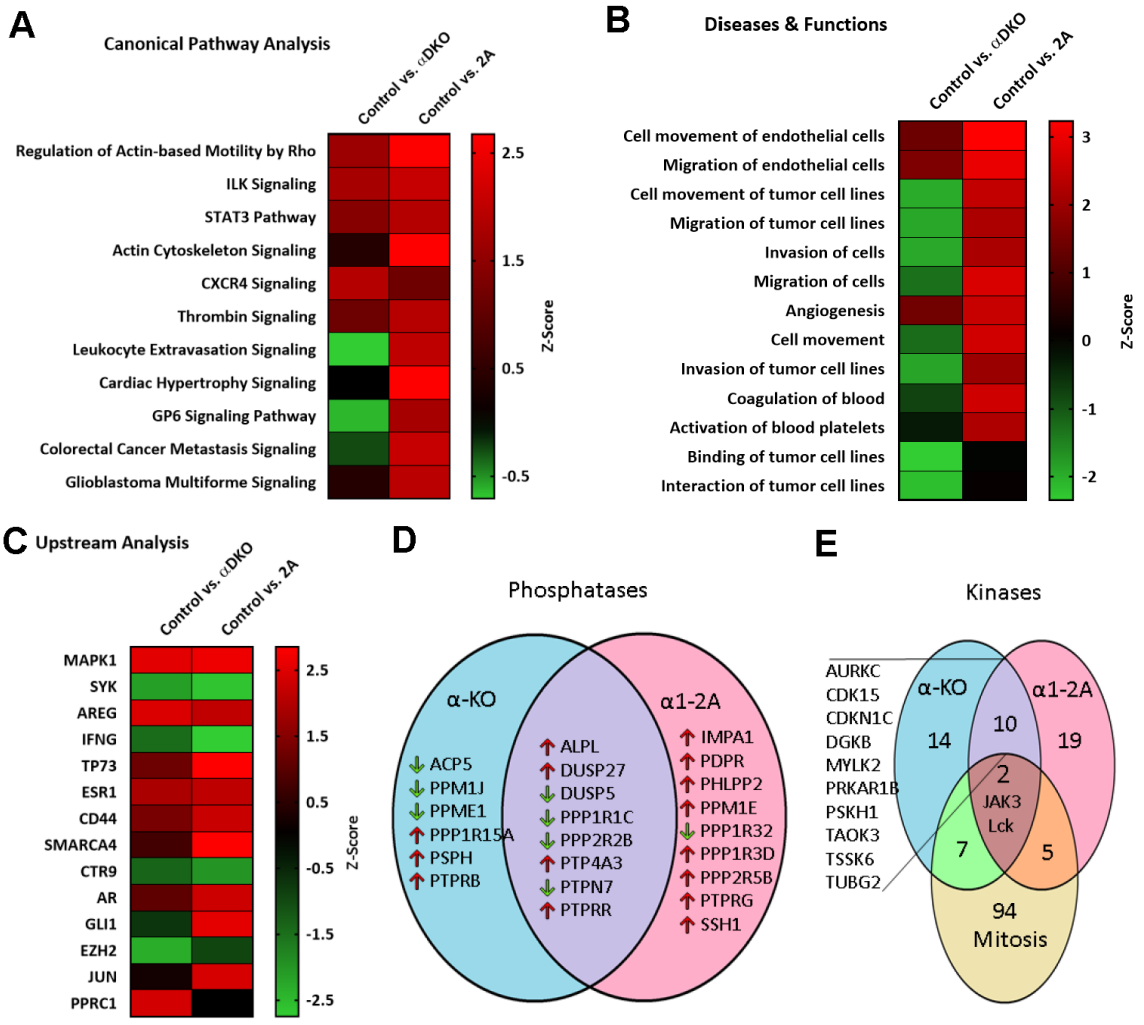
A
Canonical Pathway Analysis
Control vs. αDKO
Control vs. 2A
Regulation of Actin-based Motility by Rho
ILK Signaling
STAT3 Pathway
Actin Cytoskeleton Signaling
CXCR4 Signaling
Thrombin Signaling
Leukocyte Extravasation Signaling
Cardiac Hypertrophy Signaling
GP6 Signaling Pathway
Colorectal Cancer Metastasis Signaling
Glioblastoma Multiforme Signaling
2.5
1.5
0.5
-0.5
Z-Score
B
Diseases & Functions
Control vs. αDKO
Control vs. 2A
Cell movement of endothelial cells
Migration of endothelial cells
Cell movement of tumor cell lines
Migration of tumor cell lines
Invasion of cells
Migration of cells
Angiogenesis
Cell movement
Invasion of tumor cell lines
Coagulation of blood
Activation of blood platelets
Binding of tumor cell lines
Interaction of tumor cell lines
3
2
1
0
-1
-2
Z-Score
C
Upstream Analysis
Control vs. αDKO
Control vs. 2A
MAPK1
SYK
AREG
IFNG
TP73
ESR1
CD44
SMARCA4
CTR9
AR
GLI1
EZH2
JUN
PPRC1
2.5
1.5
0.5
-0.5
-1.5
-2.5
Z-Score
D
Phosphatases
α-KO
ACP5
PPM1J
PPME1
PPP1R15A
PSPH
PTPRB
ALPL
DUSP27
DUSP5
PPP1R1C
PPP2R2B
PTP4A3
PTPN7
PTPRR
α1-2A
IMPA1
PDPR
PHLPP2
PPM1E
PPP1R32
PPP1R3D
PPP2R5B
PTPRG
SSH1
E
Kinases
AURKC
CDK15
CDKN1C
DGKB
MYLK2
PRKAR1B
PSKH1
TAOK3
TSSK6
TUBG2
α-KO
α1-2A
14
10
19
2
JAK3
Lck
7
5
94
Mitosis

Figure 3-7. RNA-Seq Analysis of AMPK αDKO and AMPK α1-2A U2OS Cells

(A) Top canonical pathways altered in AMPKα-KO and AMPKα-KO reconstituted with AMPKα1-2A U2OS cells derived from ingenuity pathway analysis (IPA) gene ontology algorithms. (B) Top diseases and biological functions found enriched in AMPKα-KO and α1-2A reconstituted U2OS cells. (C) Upstream regulators predicted to be activated or inhibited based on genes that were significantly different for parental U2OS and AMPKα-KO or α1-2A reconstituted U2OS cells. (D) Comparison of phosphatases more than 2-fold altered in AMPKα-KO and α1-2A reconstituted U2OS cells. Kinases identified by IPA gene ontology algorithms as mitotic kinases compared with kinases more than 2-fold altered in AMPKα-KO and α1-2A reconstituted U2OS cells.

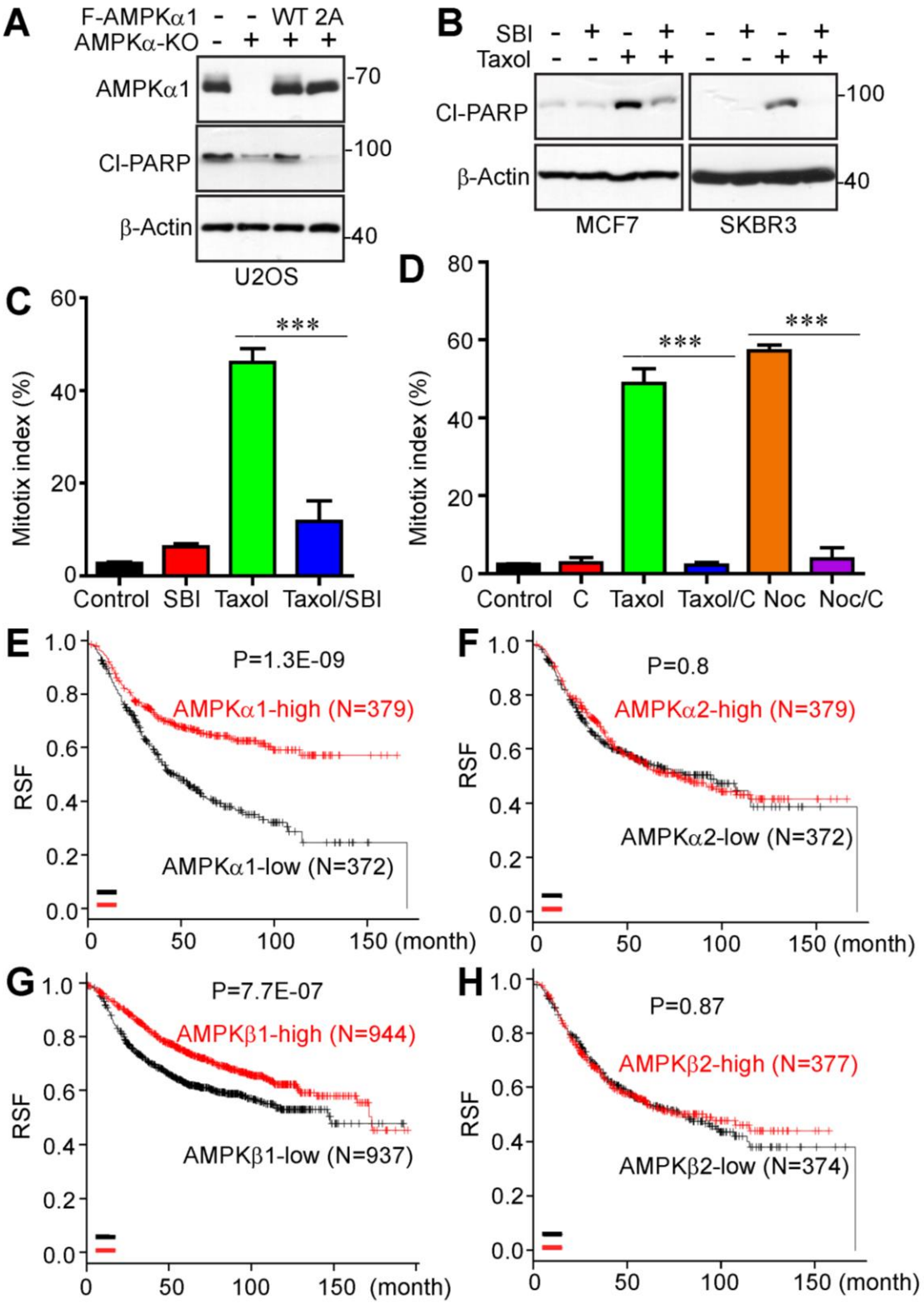
A
F-AMPKα1 - - WT 2A
AMPKα-KO - + + +
AMPKα1
Cl-PARP
β-Actin
70
100
40
U2OS
B
SBI - + - + - + - +
Taxol - - + + - - + +
Cl-PARP
β-Actin
100
40
MCF7
SKBR3
C
Mitotix index (%)
60
40
20
0
***
Control
SBI
Taxol
Taxol/SBI
D
Mitotix index (%)
80
60
40
20
0
***
***
Control
C
Taxol
Taxol/C
Noc
Noc/C
E
P=1.3E-09
AMPKα1-high (N=379)
AMPKα1-low (N=372)
RSF
1.0
0.8
0.6
0.4
0.2
0.0
0
50
100
150 (month)
F
P=0.8
AMPKα2-high (N=379)
AMPKα2-low (N=372)
RSF
1.0
0.8
0.6
0.4
0.2
0.0
0
50
100
150 (month)
G
P=7.7E-07
AMPKβ1-high (N=944)
AMPKβ1-low (N=937)
RSF
1.0
0.8
0.6
0.4
0.2
0.0
0
50
100
150 (month)
H
P=0.87
AMPKβ2-high (N=377)
AMPKβ2-low (N=374)
RSF
1.0
0.8
0.6
0.4
0.2
0.0
0
50
100
150 (month)

Figure 3-8. AMPK Expression and Kinase Activity are Crucial for Paclitaxel Drug Sensitivity and Breast Cancer Patient Relapse-Free Survival

(A) Western blot of U2OS, AMPKα-KO, AMPKα1-WT and AMPKα1-2A cells treated with taxol (100 nM) for 24 h and probed for cleaved PARP. (B) Western blot of MCF7 and SKBR3 cells treated with SBI (1 μM) and taxol (500 nM and 100 nM respectively) for 24 h and probed for cleaved PARP. (C) Mitotic indexes of HeLa cells treated with taxol alone, SBI alone, or taxol with SBI. (D) Mitotic indexes of HeLa cells treated with taxol alone, nocodazole alone, Compound C alone, taxol with Compound C, or nocodazole with Compound C. Data (C, D) were expressed as mean ± SEM from three independent experiments. ***: $p<0.001$ (t-test). (E-H) Kaplan-Meier curves of relapse-free survival vs. PRKAA1 (E), PRKAA2 (F), PRKAB1 (G), and PRKAB2 (H) expression in breast cancer patients treated systemically. Data were generated from an online survival analysis tool, KM Plotter, using microarray data of 1,809 patients [142].

BIBLIOGRAPHY

1. Kremerskothen, J., et al., *Characterization of KIBRA, a novel WW domain-containing protein.* Biochemical and Biophysical Research Communications, 2003. **300**(4): p. 862-867.

2. Yoshihama, Y., K. Chida, and S. Ohno, *The KIBRA-aPKC connection.* Communicative & Integrative Biology, 2012. **5**(2): p. 146-151.

3. Papassotiropoulos, A., et al., *Common Kibra Alleles Are Associated with Human Memory Performance.* Science, 2006. **314**(5798): p. 475-478.

4. Makuch, L., et al., *Regulation of AMPA Receptor Function by the Human Memory-Associated Gene KIBRA.* Neuron, 2011. **71**(6): p. 1022-1029.

5. Almeida, O.P., et al., *KIBRA genetic polymorphism influences episodic memory in later life, but does not increase the risk of mild cognitive impairment.* Journal of Cellular and Molecular Medicine, 2008. **12**(5a): p. 1672-1676.

6. Bates, T.C., et al., *Association of KIBRA and memory.* Neuroscience Letters, 2009. **458**(3): p. 140-143.

7. Schaper, K., et al., *KIBRA gene variants are associated with episodic memory in healthy elderly.* Neurobiology of Aging, 2008. **29**(7): p. 1123-1125.

8. Schneider, *KIBRA: a new gateway to learning and memory?* Frontiers in Aging Neuroscience, 2010.

9. Yasuda, Y., et al., *Association study ofKIBRAgene with memory performance in a Japanese population.* The World Journal of Biological Psychiatry, 2010. **11**(7): p. 852-857.

10. Corneveaux, J.J., et al., *Evidence for an association between KIBRA and late-onset Alzheimer's disease.* Neurobiology of Aging, 2010. **31**(6): p. 901-909.

11. Rodríguez-Rodríguez, E., et al., *Age-dependent association of KIBRA genetic variation and Alzheimer's disease risk.* Neurobiology of Aging, 2009. **30**(2): p. 322-324.

12. Beecham, G.W., et al., *Genome-wide Association Study Implicates a Chromosome 12 Risk Locus for Late-Onset Alzheimer Disease.* The American Journal of Human Genetics, 2009. **84**(1): p. 35-43.

13. Zhang, L., et al., *KIBRA: In the brain and beyond.* Cellular Signalling, 2014. **26**(7): p. 1392-1399.

14. Duning, K., et al., *KIBRA Modulates Directional Migration of Podocytes.* Journal of the American Society of Nephrology, 2008. **19**(10): p. 1891-1903.

15. Rosse, C., et al., *An aPKC-Exocyst Complex Controls Paxillin Phosphorylation and Migration through Localised JNK1 Activation.* PLoS Biology, 2009. **7**(11): p. e1000235.

16. Yang, S., et al., *Phosphorylation of KIBRA by the extracellular signal-regulated kinase (ERK)-ribosomal S6 kinase (RSK) cascade modulates cell proliferation and migration.* Cell Signal, 2014. **26**(2): p. 343-51.

17. Moleirinho, S., et al., *KIBRA exhibits MST-independent functional regulation of the Hippo signaling pathway in mammals.* Oncogene, 2012. **32**(14): p. 1821-1830.

18. Baumgartner, R., et al., *The WW Domain Protein Kibra Acts Upstream of Hippo in Drosophila.* Developmental Cell, 2010. **18**(2): p. 309-316.

19. Genevet, A., et al., *Kibra Is a Regulator of the Salvador/Warts/Hippo Signaling Network.* Developmental Cell, 2010. **18**(2): p. 300-308.

20. Yu, J., et al., *Kibra Functions as a Tumor Suppressor Protein that Regulates Hippo Signaling in Conjunction with Merlin and Expanded.* Developmental Cell, 2010. **18**(2): p. 288-299.

21. Xiao, L., et al., *KIBRA Protein Phosphorylation Is Regulated by Mitotic Kinase Aurora and Protein Phosphatase 1.* Journal of Biological Chemistry, 2011. **286**(42): p. 36304-36315.

22. Ji, M., et al., *Phospho-regulation of KIBRA by CDK1 and CDC14 phosphatase controls cell-cycle progression.* Biochemical Journal, 2012. **447**(1): p. 93-102.

23. Zhang, L., et al., *KIBRA Regulates Aurora Kinase Activity and Is Required for Precise Chromosome Alignment During Mitosis.* Journal of Biological Chemistry, 2012. **287**(41): p. 34069-34077.

24. Hill, V.K., et al., *Frequent epigenetic inactivation ofKIBRA,an upstream member of the Salvador/Warts/Hippo (SWH) tumor suppressor network, is associated with specific genetic event in B-cell acute lymphocytic leukemia.* Epigenetics, 2011. **6**(3): p. 326-332.

25. Shinawi, T., et al., *KIBRAgene methylation is associated with unfavorable biological prognostic parameters in chronic lymphocytic leukemia.* Epigenetics, 2012. **7**(3): p. 211-215.

26. Hilton, H.N., et al., *KIBRA interacts with discoidin domain receptor 1 to modulate collagen-induced signalling.* Biochimica et Biophysica Acta (BBA) - Molecular Cell Research, 2008. **1783**(3): p. 383-393.

27. Rayala, S.K., et al., *Essential Role of KIBRA in Co-activator Function of Dynein Light Chain 1 in Mammalian Cells.* Journal of Biological Chemistry, 2006. **281**(28): p. 19092-19099.

28. Yoshihama, Y., et al., *KIBRA Suppresses Apical Exocytosis through Inhibition of aPKC Kinase Activity in Epithelial Cells.* Current Biology, 2011. **21**(8): p. 705-711.

29. Yoshihama, Y., et al., *High expression of KIBRA in low atypical protein kinase C-expressing gastric cancer correlates with lymphatic invasion and poor prognosis.* Cancer Science, 2012. **104**(2): p. 259-265.

30. Siegel, R., et al., *Cancer statistics, 2014.* CA: A Cancer Journal for Clinicians, 2014. **64**(1): p. 9-29.

31. DeSantis, C.E., et al., *Cancer treatment and survivorship statistics, 2014.* CA: A Cancer Journal for Clinicians, 2014. **64**(4): p. 252-271.

32. Isaacs, W., A. De Marzo, and W.G. Nelson, *Focus on prostate cancer.* Cancer Cell, 2002. **2**(2): p. 113-116.

33. Zhang, L., et al., *The hippo pathway effector YAP regulates motility, invasion, and castration-resistant growth of prostate cancer cells.* Mol Cell Biol, 2015. **35**(8): p. 1350-62.

34. Xiao, L., et al., *KIBRA Regulates Hippo Signaling Activity via Interactions with Large Tumor Suppressor Kinases.* Journal of Biological Chemistry, 2011. **286**(10): p. 7788-7796.

35. Thalmann, G.N., et al., *LNCaP progression model of human prostate cancer: Androgen-independence and osseous metastasis.* The Prostate, 2000. **44**(2): p. 91-103.

36. Lin, M.-F., et al., *Expression of Human Prostatic Acid Phosphatase Correlates with Androgen-stimulated Cell Proliferation in Prostate Cancer Cell Lines.* Journal of Biological Chemistry, 1998. **273**(10): p. 5939-5947.

37. Igawa, T., et al., *Establishment and characterization of androgen-independent human prostate cancer LNCaP cell model.* The Prostate, 2002. **50**(4): p. 222.

38. Johnson, K., *P- and E-Cadherin Are in Separate Complexes in Cells Expressing Both Cadherins.* Experimental Cell Research, 1993. **207**(2): p. 252-260.

39. Zhou, Z., et al., *TAZ is a novel oncogene in non-small cell lung cancer.* Oncogene, 2011. **30**(18): p. 2181-2186.

40. Dong, J., et al., *Elucidation of a universal size-control mechanism in Drosophila and mammals.* Cell, 2007. **130**(6): p. 1120-33.

41. Yang, S., et al., *CDK1 phosphorylation of YAP promotes mitotic defects and cell motility and is essential for neoplastic transformation.* Cancer Res, 2013. **73**(22): p. 6722-33.

42. Karan, D., et al., *Expression profile of differentially-regulated genes during progression of androgen-independent growth in human prostate cancer cells.* Carcinogenesis, 2002. **23**(6): p. 967-976.

43. Karan, D., et al., *Decreased androgen-responsive growth of human prostate cancer is associated with increased genetic alterations.* Clin Cancer Res, 2001. **7**(11): p. 3472-80.

44. Xiao, L., et al., *KIBRA protein phosphorylation is regulated by mitotic kinase aurora and protein phosphatase 1.* J Biol Chem, 2011. **286**(42): p. 36304-15.

45. Qin, J., et al., *Upregulation of PIP3-dependent Rac exchanger 1 (P-Rex1) promotes prostate cancer metastasis.* Oncogene, 2009. **28**(16): p. 1853-1863.

46. Powzaniuk, M., et al., *The LATS2/KPM Tumor Suppressor Is a Negative Regulator of the Androgen Receptor.* Molecular Endocrinology, 2004. **18**(8): p. 2011-2023.

47. Su, A.I., et al., *Molecular classification of human carcinomas by use of gene expression signatures.* Cancer Res, 2001. **61**(20): p. 7388-93.

48. Singh, D., et al., *Gene expression correlates of clinical prostate cancer behavior.* Cancer Cell, 2002. **1**(2): p. 203-209.

49. Lapointe, J., et al., *Gene expression profiling identifies clinically relevant subtypes of prostate cancer.* Proceedings of the National Academy of Sciences, 2004. **101**(3): p. 811-816.

50. Henshall, S.M., et al., *Survival analysis of genome-wide gene expression profiles of prostate cancers identifies new prognostic targets of disease relapse.* Cancer Res, 2003. **63**(14): p. 4196-203.

51. Abe, Y., et al., *Cloning and expression of a novel MAPKK-like protein kinase, lymphokine-activated killer T-cell-originated protein kinase, specifically expressed in the testis and activated lymphoid cells.* J Biol Chem, 2000. **275**(28): p. 21525-31.

52. Gaudet, S., D. Branton, and R.A. Lue, *Characterization of PDZ-binding kinase, a mitotic kinase.* Proc Natl Acad Sci U S A, 2000. **97**(10): p. 5167-72.

53. Chang, C.F., et al., *PBK/TOPK Expression Predicts Prognosis in Oral Cancer.* Int J Mol Sci, 2016. **17**(7).

54. Fujibuchi, T., et al., *Expression and phosphorylation of TOPK during spermatogenesis.* Dev Growth Differ, 2005. **47**(9): p. 637-44.

55. Ikeda, Y., et al., *T-LAK Cell-Originated Protein Kinase (TOPK) as a Prognostic Factor and a Potential Therapeutic Target in Ovarian Cancer.* Clin Cancer Res, 2016. **22**(24): p. 6110-6117.

56. Long, J.I.N., et al., *Gene expression profile analysis of pancreatic cancer based on microarray data.* Molecular Medicine Reports, 2016. **13**(5): p. 3913-3919.

57. Park, J.H., et al., *PDZ-binding kinase/T-LAK cell-originated protein kinase, a putative cancer/testis antigen with an oncogenic activity in breast cancer.* Cancer Res, 2006. **66**(18): p. 9186-95.

58. Ohashi, T., et al., *Overexpression of PBK/TOPK relates to tumour malignant potential and poor outcome of gastric carcinoma.* Br J Cancer, 2017. **116**(2): p. 218-226.

59. Singh, P.K., et al., *Expression of PDZ-binding kinase/T-LAK cell-originated protein kinase (PBK/TOPK) in human urinary bladder transitional cell carcinoma.* Immunobiology, 2014. **219**(6): p. 469-74.

60. Wei, D.C., et al., *Overexpression of T-LAK cell-originated protein kinase predicts poor prognosis in patients with stage I lung adenocarcinoma.* Cancer Sci, 2012. **103**(4): p. 731-8.

61. Zhu, F., et al., *Bidirectional signals transduced by TOPK-ERK interaction increase tumorigenesis of HCT116 colorectal cancer cells.* Gastroenterology, 2007. **133**(1): p. 219-31.

62. Wang, M.Y., et al., *PDZ binding kinase (PBK) is a theranostic target for nasopharyngeal carcinoma: driving tumor growth via ROS signaling and correlating with patient survival.* Oncotarget, 2016. **7**(18): p. 26604-16.

63. Liu, Y., et al., *PBK/TOPK mediates promyelocyte proliferation via Nrf2-regulated cell cycle progression and apoptosis.* Oncol Rep, 2015. **34**(6): p. 3288-96.

64. Hu, F., et al., *PBK/TOPK interacts with the DBD domain of tumor suppressor p53 and modulates expression of transcriptional targets including p21.* Oncogene, 2010. **29**(40): p. 5464-74.

65. Ayllón, V. and R. O'connor, *PBK/TOPK promotes tumour cell proliferation through p38 MAPK activity and regulation of the DNA damage response.* Oncogene, 2007. **26**(24): p. 3451-61.

66. Rizkallah, R., et al., *Identification of the oncogenic kinase TOPK/PBK as a master mitotic regulator of C2H2 zinc finger proteins.* Oncotarget, 2015. **6**(3): p. 1446-61.

67. Abe, Y., et al., *A mitotic kinase TOPK enhances Cdk1/cyclin B1-dependent phosphorylation of PRC1 and promotes cytokinesis.* J Mol Biol, 2007. **370**(2): p. 231-45.

68. Matsuo, Y., et al., *TOPK inhibitor induces complete tumor regression in xenograft models of human cancer through inhibition of cytokinesis.* Sci Transl Med, 2014. **6**(259): p. 259ra145.

69. Park, J.H., et al., *TOPK (T-LAK cell-originated protein kinase) inhibitor exhibits growth suppressive effect on small cell lung cancer.* Cancer Sci, 2017. **108**(3): p. 488-496.

70. Matsumoto, S., et al., *Characterization of a MAPKK-like protein kinase TOPK.* Biochem Biophys Res Commun, 2004. **325**(3): p. 997-1004.

71. Park, J.H., et al., *Critical roles of T-LAK cell-originated protein kinase in cytokinesis.* Cancer Sci, 2010. **101**(2): p. 403-11.

72. Pan, D., *The hippo signaling pathway in development and cancer.* Dev Cell, 2010. **19**(4): p. 491-505.

73. Yu, F.-X., B. Zhao, and K.-L. Guan, *Hippo Pathway in Organ Size Control, Tissue Homeostasis, and Cancer.* Cell, 2015. **163**(4): p. 811-828.

74. Dou, X., et al., *PBK/TOPK mediates geranylgeranylation signaling for breast cancer cell proliferation.* Cancer Cell Int, 2015. **15**: p. 27.

75. Elcheva, I., et al., *Direct induction of haematoendothelial programs in human pluripotent stem cells by transcriptional regulators.* Nature Communications, 2014. **5**(1).

76. Sakuma, T., et al., *Multiplex genome engineering in human cells using all-in-one CRISPR/Cas9 vector system.* Scientific Reports, 2014. **4**(1).

77. Ran, F.A., et al., *Genome engineering using the CRISPR-Cas9 system.* Nature Protocols, 2013. **8**(11): p. 2281-2308.

78. Chen, X., et al., *Ajuba Phosphorylation by CDK1 Promotes Cell Proliferation and Tumorigenesis.* J Biol Chem, 2016. **291**(28): p. 14761-72.

79. Zhang, L., et al., *KIBRA regulates aurora kinase activity and is required for precise chromosome alignment during mitosis.* J Biol Chem, 2012. **287**(41): p. 34069-77.

80. Jube, S., et al., *Cancer Cell Secretion of the DAMP Protein HMGB1 Supports Progression in Malignant Mesothelioma.* Cancer Research, 2012. **72**(13): p. 3290-3301.

81. Kim, H., et al., *Wnt Signaling Translocates Lys48-Linked Polyubiquitinated Proteins to the Lysosomal Pathway.* Cell Rep, 2015. **11**(8): p. 1151-9.

82. Nigg, E.A., *Cellular substrates of p34(cdc2) and its companion cyclin-dependent kinases.* Trends Cell Biol, 1993. **3**(9): p. 296-301.

83. Olsen, J.V., et al., *Quantitative phosphoproteomics reveals widespread full phosphorylation site occupancy during mitosis.* Sci Signal, 2010. **3**(104): p. ra3.

84. Dephoure, N., et al., *A quantitative atlas of mitotic phosphorylation.* Proceedings of the National Academy of Sciences, 2008. **105**(31): p. 10762-10767.

85. Park, J.-H., et al., *PDZ-Binding Kinase/T-LAK Cell-Originated Protein Kinase, a Putative Cancer/Testis Antigen with an Oncogenic Activity in Breast Cancer.* Cancer Research, 2006. **66**(18): p. 9186-9195.

86. O Leary, P.C., et al., *Systematic antibody generation and validation via tissue microarray technology leading to identification of a novel protein prognostic panel in breast cancer.* BMC Cancer, 2013. **13**: p. 175.

87. Xiao, J., et al., *Phosphorylation of TOPK at Y74, Y272 by Src increases the stability of TOPK and promotes tumorigenesis of colon.* Oncotarget, 2016. **7**(17): p. 24483-94.

88. Malumbres, M., *Oncogene-induced mitotic stress: p53 and pRb get mad too.* Cancer Cell, 2011. **19**(6): p. 691-2.

89. Schvartzman, J.M., et al., *Mad2 is a critical mediator of the chromosome instability observed upon Rb and p53 pathway inhibition.* Cancer Cell, 2011. **19**(6): p. 701-14.

90. Torres, E.M., et al., *Effects of aneuploidy on cellular physiology and cell division in haploid yeast.* Science, 2007. **317**(5840): p. 916-24.

91. Williams, B.R., et al., *Aneuploidy affects proliferation and spontaneous immortalization in mammalian cells.* Science, 2008. **322**(5902): p. 703-9.

92. Bakhoum, S.F. and C. Swanton, *Chromosomal instability, aneuploidy, and cancer.* Front Oncol, 2014. **4**: p. 161.

93. Nowak, M.A., et al., *The role of chromosomal instability in tumor initiation.* Proc Natl Acad Sci U S A, 2002. **99**(25): p. 16226-31.

94. Pino, M.S. and D.C. Chung, *The chromosomal instability pathway in colon cancer.* Gastroenterology, 2010. **138**(6): p. 2059-72.

95. Schvartzman, J.M., R. Sotillo, and R. Benezra, *Mitotic chromosomal instability and cancer: mouse modelling of the human disease.* Nat Rev Cancer, 2010. **10**(2): p. 102-15.

96. Kops, G.J., D.R. Foltz, and D.W. Cleveland, *Lethality to human cancer cells through massive chromosome loss by inhibition of the mitotic checkpoint.* Proc Natl Acad Sci U S A, 2004. **101**(23): p. 8699-704.

97. Rao, C.V. and H.Y. Yamada, *Genomic instability and colon carcinogenesis: from the perspective of genes.* Front Oncol, 2013. **3**: p. 130.

98. Kops, G.J., B.A. Weaver, and D.W. Cleveland, *On the road to cancer: aneuploidy and the mitotic checkpoint.* Nat Rev Cancer, 2005. **5**(10): p. 773-85.

99. Reiter, R., et al., *Aurora kinase A messenger RNA overexpression is correlated with tumor progression and shortened survival in head and neck squamous cell carcinoma.* Clin Cancer Res, 2006. **12**(17): p. 5136-41.

100. Shichiri, M., et al., *Genetic and epigenetic inactivation of mitotic checkpoint genes hBUB1 and hBUBR1 and their relationship to survival.* Cancer Res, 2002. **62**(1): p. 13-7.

101. Manchado, E., M. Guillamot, and M. Malumbres, *Killing cells by targeting mitosis.* Cell Death Differ, 2012. **19**(3): p. 369-77.

102. Mihaylova, M.M. and R.J. Shaw, *The AMPK signalling pathway coordinates cell growth, autophagy and metabolism.* Nat Cell Biol, 2011. **13**(9): p. 1016-23.

103. Zadra, G., J.L. Batista, and M. Loda, *Dissecting the Dual Role of AMPK in Cancer: From Experimental to Human Studies.* Mol Cancer Res, 2015. **13**(7): p. 1059-72.

104. Lee, J.H., et al., *Energy-dependent regulation of cell structure by AMP-activated protein kinase.* Nature, 2007. **447**(7147): p. 1017-20.

105. Vazquez-Martin, A., et al., *AMPK: Evidence for an energy-sensing cytokinetic tumor suppressor.* Cell Cycle, 2009. **8**(22): p. 3679-83.

106. Thaiparambil, J.T., C.M. Eggers, and A.I. Marcus, *AMPK regulates mitotic spindle orientation through phosphorylation of myosin regulatory light chain.* Mol Cell Biol, 2012. **32**(16): p. 3203-17.

107. Vazquez-Martin, A., et al., *Polo-like kinase 1 directs the AMPK-mediated activation of myosin regulatory light chain at the cytokinetic cleavage furrow independently of energy balance.* Cell Cycle, 2012. **11**(13): p. 2422-6.

108. Mao, L., et al., *AMPK phosphorylates GBF1 for mitotic Golgi disassembly.* J Cell Sci, 2013. **126**(Pt 6): p. 1498-505.

109. Lee, I.J., C.W. Lee, and J.H. Lee, *CaMKKβ-AMPKα2 signaling contributes to mitotic Golgi fragmentation and the G2/M transition in mammalian cells.* Cell Cycle, 2015. **14**(4): p. 598-611.

110. Domenech, E., et al., *AMPK and PFKFB3 mediate glycolysis and survival in response to mitophagy during mitotic arrest.* Nat Cell Biol, 2015. **17**(10): p. 1304-16.

111. Banko, M.R., et al., *Chemical genetic screen for AMPKα2 substrates uncovers a network of proteins involved in mitosis.* Mol Cell, 2011. **44**(6): p. 878-92.

112. Ito, M., et al., *Myosin phosphatase: structure, regulation and function.* Mol Cell Biochem, 2004. **259**(1-2): p. 197-209.

113. Peters, J.M., *The anaphase promoting complex/cyclosome: a machine designed to destroy.* Nat Rev Mol Cell Biol, 2006. **7**(9): p. 644-56.

114. Tuazon, P.T. and J.A. Traugh, *Activation of actin-activated ATPase in smooth muscle by phosphorylation of myosin light chain with protease-activated kinase I.* J Biol Chem, 1984. **259**(1): p. 541-6.

115. Mirouse, V., et al., *LKB1 and AMPK maintain epithelial cell polarity under energetic stress.* J Cell Biol, 2007. **177**(3): p. 387-92.

116. Sanli, T., et al., *Ionizing radiation activates AMP-activated kinase (AMPK): a target for radiosensitization of human cancer cells.* Int J Radiat Oncol Biol Phys, 2010. **78**(1): p. 221-9.

117. Sanli, T., et al., *Ionizing radiation regulates the expression of AMP-activated protein kinase (AMPK) in epithelial cancer cells.* Radiotherapy and Oncology, 2012. **102**(3): p. 459-465.

118. Dasgupta, B. and J. Milbrandt, *AMP-activated protein kinase phosphorylates retinoblastoma protein to control mammalian brain development.* Dev Cell, 2009. **16**(2): p. 256-70.

119. Tripodi, F., et al., *Snf1/AMPK is involved in the mitotic spindle alignment in Saccharomyces cerevisiae.* Sci Rep, 2018. **8**(1): p. 5853.

120. Stauffer, S., et al., *KIBRA promotes prostate cancer cell proliferation and motility.* 2016: p. n/a-n/a.

121. Inoki, K., T. Zhu, and K.L. Guan, *TSC2 mediates cellular energy response to control cell growth and survival.* Cell, 2003. **115**(5): p. 577-90.

122. Beronja, S., et al., *Rapid functional dissection of genetic networks via tissue-specific transduction and RNAi in mouse embryos.* Nat Med, 2010. **16**(7): p. 821-7.

123. Stauffer, S., et al., *CDK1-mediated mitotic phosphorylation of PBK is involved in cytokinesis and inhibits its oncogenic activity.* Cell Signal, 2017. **39**: p. 74-83.

124. Suzuki, T., et al., *Inhibition of AMPK catabolic action by GSK3.* Mol Cell, 2013. **50**(3): p. 407-19.

125. Zhou, J., et al., *Zyxin promotes colon cancer tumorigenesis in a mitotic phosphorylation-dependent manner and through CDK8-mediated YAP activation.* Proc Natl Acad Sci U S A, 2018. **115**(29): p. E6760-E6769.

126. Zeng, Y., et al., *Cyclin-dependent kinase 1 (CDK1)-mediated mitotic phosphorylation of the transcriptional co-repressor Vgll4 inhibits its tumor-suppressing activity.* J Biol Chem, 2017. **292**(36): p. 15028-15038.

127. Dobin, A., et al., *STAR: ultrafast universal RNA-seq aligner.* Bioinformatics, 2012. **29**(1): p. 15-21.

128. Li, B. and C.N. Dewey, *RSEM: accurate transcript quantification from RNA-Seq data with or without a reference genome.* BMC Bioinformatics, 2011. **12**(1): p. 323.

129. Benjamini, Y. and Y. Hochberg, *Controlling the False Discovery Rate: A Practical and Powerful Approach to Multiple Testing.* Journal of the Royal Statistical Society. Series B (Methodological), 1995. **57**(1): p. 289-300.

130. Daub, H., et al., *Kinase-selective enrichment enables quantitative phosphoproteomics of the kinome across the cell cycle.* Mol Cell, 2008. **31**(3): p. 438-48.

131. Dulla, K., et al., *Quantitative site-specific phosphorylation dynamics of human protein kinases during mitotic progression.* Mol Cell Proteomics, 2010. **9**(6): p. 1167-81.

132. Vazquez-Martin, A., et al., *Polo-like kinase 1 regulates activation of AMP-activated protein kinase (AMPK) at the mitotic apparatus.* Cell Cycle, 2011. **10**(8): p. 1295-302.

133. Oligschlaeger, Y., et al., *The recruitment of AMP-activated protein kinase to glycogen is regulated by autophosphorylation.* J Biol Chem, 2015. **290**(18): p. 11715-28.

134. Woods, A., et al., *Identification of phosphorylation sites in AMP-activated protein kinase (AMPK) for upstream AMPK kinases and study of their roles by site-directed mutagenesis.* J Biol Chem, 2003. **278**(31): p. 28434-42.

135. Mitchelhill, K.I., et al., *Posttranslational modifications of the 5'-AMP-activated protein kinase beta1 subunit.* J Biol Chem, 1997. **272**(39): p. 24475-9.

136. Wei, C., et al., *The LKB1 tumor suppressor controls spindle orientation and localization of activated AMPK in mitotic epithelial cells.* PLoS One, 2012. **7**(7): p. e41118.

137. Dite, T.A., et al., *AMP-activated protein kinase selectively inhibited by the type II inhibitor SBI-0206965.* J Biol Chem, 2018. **293**(23): p. 8874-8885.

138. Lara-Gonzalez, P., F.G. Westhorpe, and S.S. Taylor, *The spindle assembly checkpoint.* Curr Biol, 2012. **22**(22): p. R966-80.

139. Musacchio, A. and E.D. Salmon, *The spindle-assembly checkpoint in space and time.* Nat Rev Mol Cell Biol, 2007. **8**(5): p. 379-93.

140. Vitale, I., et al., *Mitotic catastrophe: a mechanism for avoiding genomic instability.* Nat Rev Mol Cell Biol, 2011. **12**(6): p. 385-92.

141. Abal, M., J.M. Andreu, and I. Barasoain, *Taxanes: microtubule and centrosome targets, and cell cycle dependent mechanisms of action.* Curr Cancer Drug Targets, 2003. **3**(3): p. 193-203.

142. Gyorffy, B., et al., *An online survival analysis tool to rapidly assess the effect of 22,277 genes on breast cancer prognosis using microarray data of 1,809 patients.* Breast Cancer Res Treat, 2010. **123**(3): p. 725-31.

143. Pinter, K., et al., *Subunit composition of AMPK trimers present in the cytokinetic apparatus: Implications for drug target identification.* Cell Cycle, 2012. **11**(5): p. 917-21.

144. Hoffman, L., et al., *Mechanical signals activate p38 MAPK pathway-dependent reinforcement of actin via mechanosensitive HspB1.* Mol Biol Cell, 2017. **28**(20): p. 2661-2675.

145. Coopman, P.J., et al., *The Syk tyrosine kinase suppresses malignant growth of human breast cancer cells.* Nature, 2000. **406**(6797): p. 742-7.

146. Ruiz-Ruiz, C., C. Munoz-Pinedo, and A. Lopez-Rivas, *Interferon-gamma treatment elevates caspase-8 expression and sensitizes human breast tumor cells to a death receptor-induced mitochondria-operated apoptotic program.* Cancer Res, 2000. **60**(20): p. 5673-80.

147. Salomon, D.S., et al., *The role of amphiregulin in breast cancer.* Breast Cancer Res Treat, 1995. **33**(2): p. 103-14.

148. Chen, Z., et al., *Hepatic SMARCA4 predicts HCC recurrence and promotes tumour cell proliferation by regulating SMAD6 expression.* Cell Death Dis, 2018. **9**(2): p. 59.

149. Guerrero-Martínez, J.A. and J.C. Reyes, *High expression of SMARCA4 or SMARCA2 is frequently associated with an opposite prognosis in cancer.* Sci Rep, 2018. **8**(1): p. 2043.

150. Banine, F., et al., *SWI/SNF chromatin-remodeling factors induce changes in DNA methylation to promote transcriptional activation.* Cancer Res, 2005. **65**(9): p. 3542-7.

151. Lakshman, M., et al., *CD44 promotes resistance to apoptosis in human colon cancer cells.* Exp Mol Pathol, 2004. **77**(1): p. 18-25.

152. Nam, K., et al., *CD44 regulates cell proliferation, migration, and invasion via modulation of c-Src transcription in human breast cancer cells.* Cell Signal, 2015. **27**(9): p. 1882-94.

153. Domínguez, G., et al., *Different expression of P14ARF defines two groups of breast carcinomas in terms of TP73 expression and TP53 mutational status.* Genes Chromosomes Cancer, 2001. **31**(2): p. 99-106.

154. Reijm, E.A., et al., *Decreased expression of EZH2 is associated with upregulation of ER and favorable outcome to tamoxifen in advanced breast cancer.* Breast Cancer Res Treat, 2011. **125**(2): p. 387-94.

155. Moelans, C.B., et al., *ESR1 amplification is rare in breast cancer and is associated with high grade and high proliferation: a multiplex ligation-dependent probe amplification study.* Cell Oncol (Dordr), 2011. **34**(5): p. 489-94.

156. Fujii, R., et al., *Increased androgen receptor activity and cell proliferation in aromatase inhibitor-resistant breast carcinoma.* J Steroid Biochem Mol Biol, 2014. **144 Pt B**: p. 513-22.

157. Singh, A.K., et al., *Advanced stage of breast cancer hoist alkaline phosphatase activity: risk factor for females in India.* 3 Biotech, 2013. **3**(6): p. 517-520.

158. den Hollander, P., et al., *Phosphatase PTP4A3 Promotes Triple-Negative Breast Cancer Growth and Predicts Poor Patient Survival.* Cancer Res, 2016. **76**(7): p. 1942-53.

159. Liu, T., et al., *The suppression of DUSP5 expression correlates with paclitaxel resistance and poor prognosis in basal-like breast cancer.* Int J Med Sci, 2018. **15**(7): p. 738-747.

160. Zakikhani, M., et al., *Metformin Is an AMP Kinase-Dependent Growth Inhibitor for Breast Cancer Cells.* Cancer Research, 2006. **66**(21): p. 10269-10273.

161. Alimova, I.N., et al., *Metformin inhibits breast cancer cell growth, colony formation and induces cell cycle arrest in vitro.* Cell Cycle, 2009. **8**(6): p. 909-915.

162. Liu, B., et al., *Metformin induces unique biological and molecular responses in triple negative breast cancer cells.* Cell Cycle, 2009. **8**(13): p. 2031-40.

163. Hirsch, H.A., et al., *Metformin selectively targets cancer stem cells, and acts together with chemotherapy to block tumor growth and prolong remission.* Cancer Res, 2009. **69**(19): p. 7507-11.

164. Oliveras-Ferraros, C., A. Vazquez-Martin, and J.A. Menendez, *Genome-wide inhibitory impact of the AMPK activator metformin on [kinesins, tubulins, histones, auroras and polo-like kinases] M-phase cell cycle genes in human breast cancer cells.* Cell Cycle, 2009. **8**(10): p. 1633-6.

165. Anisimov, V.N., et al., *Metformin decelerates aging and development of mammary tumors in HER-2/neu transgenic mice.* Bull Exp Biol Med, 2005. **139**(6): p. 721-3.

166. Kasznicki, J., A. Sliwinska, and J. Drzewoski, *Metformin in cancer prevention and therapy.* Ann Transl Med, 2014. **2**(6): p. 57.

167. Chae, Y.K., et al., *Repurposing metformin for cancer treatment: current clinical studies.* Oncotarget, 2016. **7**(26): p. 40767-40780.

168. Marrone, K.A., et al., *A Randomized Phase II Study of Metformin plus Paclitaxel/Carboplatin/Bevacizumab in Patients with Chemotherapy-Naïve Advanced or Metastatic Nonsquamous Non-Small Cell Lung Cancer.* Oncologist, 2018. **23**(7): p. 859-865.